

## General Disclaimer

### One or more of the Following Statements may affect this Document

- This document has been reproduced from the best copy furnished by the organizational source. It is being released in the interest of making available as much information as possible.
- This document may contain data, which exceeds the sheet parameters. It was furnished in this condition by the organizational source and is the best copy available.
- This document may contain tone-on-tone or color graphs, charts and/or pictures, which have been reproduced in black and white.
- This document is paginated as submitted by the original source.
- Portions of this document are not fully legible due to the historical nature of some of the material. However, it is the best reproduction available from the original submission.

# High Efficiency Solar Photovoltaic Power Module Concept

## Final Report

Prepared by I. BEKEY  
Advanced Mission Analysis Directorate  
Advanced Orbital Systems Division

March 1978

Prepared for  
OFFICE OF AERONAUTICS AND SPACE TECHNOLOGY  
NATIONAL AERONAUTICS AND SPACE ADMINISTRATION

Contract No. NASW-3078

Systems Engineering Operations

THE AEROSPACE CORPORATION



(NASA-CR-157002) HIGH EFFICIENCY SOLAR  
PHOTOVOLTAIC POWER MODULE CONCEPT Final  
Report (Aerospace Corp., El Segundo, Calif.)  
151 p HC A08/MF A01 CSCL 10A

N78-23555

G3/44 | 15249  
Unclas

Aerospace Report No.  
ATR-78(7666)-1

HIGH EFFICIENCY SOLAR PHOTOVOLTAIC POWER MODULE CONCEPT  
FINAL REPORT

Prepared by  
I. Bekey  
Advanced Mission Analysis Directorate  
Advanced Orbital Systems Division

March 1978

Systems Engineering Operations  
THE AEROSPACE CORPORATION  
El Segundo, California

Prepared for  
OFFICE OF AERONAUTICS AND SPACE TECHNOLOGY  
NATIONAL AERONAUTICS AND SPACE ADMINISTRATION

Contract No. NASW-3078

Report No.  
ATR-78(7666)-1

HIGH EFFICIENCY SOLAR PHOTOVOLTAIC POWER MODULE CONCEPT  
FINAL REPORT


Prepared



---

I. Bekey  
Study Director  
Advanced Mission Analysis Directorate  
Advanced Orbital Systems Division

Approved



---

Samuel M. Tennant  
Vice President and General Manager  
Advanced Orbital Systems Division  
Systems Engineering Operations

## ACKNOWLEDGMENT

This study is the result of many minds. Their contributions are gratefully acknowledged:

The idea for the concept was originated by Dr. Wade Blocker.

Initial and final discussions on the merits of the idea were contributed by Dr. Harris Mayer and Dr. Wade Blocker.

The analysis of the solar cells and their attainable efficiency was performed primarily by Dr. N. A. Gokcen, under the guidance of Dr. H. K. A. Kan.

The optical and spectrum splitter analysis was performed by J. Redmann, J. Thompson, and J. Slattery.

The thermal analysis was performed by P. K. Chang.

The weights were estimated by F. W. Hawkins.

The layout and design were performed by D. Cooley and G. Yee.

Direction of the study and integration of the subsystems was performed by I. Bekey.

PRECEDING PAGE BLANK NOT FILLED

## CONTENTS

1.	INTRODUCTION . . . . .	1
2.	SUMMARY OF FINDINGS . . . . .	7
3.	DESCRIPTION OF CONCEPT . . . . .	13
3.1	Solar Cells . . . . .	19
3.2	Optical Elements . . . . .	39
3.3	Thermal Control . . . . .	61
3.4	Baseline Concept . . . . .	75
4.	EVALUATION . . . . .	99
5.	CONCLUSIONS . . . . .	117
6.	REFERENCES . . . . .	127
	APPENDIX . . . . .	A-1
	- Calculation of Solar Cell Efficiencies	

PRECEDING PAGE BLANK NOT FILLED

SECTION 1

INTRODUCTION

BACKGROUND - H-0495

This report comprises the final results of Task 1 of NASA Contract NASW-3078 entitled "Advanced Space Power Requirements" performed by The Aerospace Corporation in FY 78. The subject of Task 1 was the investigation of a preliminary concept for high efficiency solar photovoltaic power generation in space. This study was performed under contract to NASA Headquarters, with Mr. J. Mullin the overall program manager. Detailed technical direction was provided by Mr. W. (Larry) Crabtree at the Marshall Space Flight Center.

A new concept for generating photovoltaic power in space with potentially much higher conversion efficiencies than theoretically achieved by current design photovoltaic arrays was conceived by Dr. Wade Blocker, of The Aerospace Corporation, in mid-1975 and made public in 1976 and 77.<sup>(1,2)</sup> The concept is a synergistic combination of three elements, each individually known previously, and predicts a significant advantage in their simultaneous application to space power subsystems.

The first element of the idea was the recognition that a solar cell can only respond with its highest efficiency to photons whose energy is exactly equal to its design bandgap energy. Photons of lower energy will not promote an electron to the conduction band at all, while photons of higher energy will not promote more than a single electron and thus a portion of their energy will be wasted. The implication is that when faced with the task of converting sunlight efficiently, a single solar cell would be limited to a theoretical efficiency of about 44 percent, with practically attained efficiencies probably not exceeding about 25 percent as calculated by Wolf and others.<sup>(3, 4, 5)</sup> Splitting the solar spectrum into a number of narrow and separate spectral regions approaching monochromatic light in each region, and focusing each type of light on a type of solar cell whose bandgap is designed to convert that wavelength region with maximum efficiency was pointed out earlier by Jackson<sup>(6)</sup> as a means to increase the conversion efficiency. Calculations by Rappaport<sup>(7)</sup> and Jackson indicate a theoretical ideal efficiency of 69 percent results for three spectral bands, 86 percent for ten bands and 100 percent for an infinite number of bands. However, such spectrum splitting would obviously result in cell replication which would increase the cost of any array more rapidly than the efficiency gain, as indicated by the implementation schemes of Jackson and Spring.<sup>(8)</sup>

PRECEDING PAGE BLANK NOT FILMED



The second element of the idea is the use of optical concentrators to reduce the area of the cells required for a given output. Since solar cells are very expensive, it is likely that lightweight, low cost systems could be built. Furthermore, the reduced area could make shielding against large amounts of radiation relatively lightweight. This technique, however, results in very large heat inputs to the solar cells whose subsequent temperature rise, if not checked, limits the efficiency of the entire concept. A number of thermal control techniques are possible and have been investigated to limit such temperature rise. The use of multiple concentrators and passive heat sinks was reported by Sterzer<sup>(3)</sup>, Dean et. al.<sup>(9)</sup>, and Napoli, et. al.<sup>(10)</sup> They all involve significant weights and therefore significant costs, probably resulting in little net gain over a planar array.

Dr. Blocker's idea was to combine high concentration ratio optics with spectrum splitters illuminating a number of tailored bandgap solar cells. Since the high concentration ratio implies small solar cell areas, their replication would involve only a small growth in weight and cost, probably resulting in overall cost savings per kilowatt produced. Since each cell is only illuminated with a portion of the solar spectrum, the heat input to the cell is limited and its rise in temperature more easily controlled with a given weight radiator. The resultant concept promises to have high efficiency due to the use of multiple bandgap solar cells and low cost due to the promised low weight of the system. Furthermore, the small solar cell area makes it possible to shield the cells at a small weight penalty, obtaining radiation tolerance. The cost of the optics is likely to be small compared to the cost of the replaced solar cells due to the poor quality optics needed, since the sun is not a collimated source but subtends 8 mrad at the earth.

A contract for the purpose of determining the feasibility of this new technique and comparing a point design with a conventional but advanced array of the type designed for the Solar Electric Propulsion System was awarded by NASA to The Aerospace Corporation in April 1977. Since the contract amount was very small (\$50K), it was recognized that this study would at best be able to place bounds on the attainable performance of the technique. Furthermore, a cost projection and its comparison with SEPS could only be performed on the basis of a point design since the structure, radiator, splitter efficiency, deployment techniques, and structural devices would probably limit the minimum weight and therefore the cost attainable. Thus a point design was made as the basis for comparison.

The contract funds were augmented by about \$30K of corporate funds in order to maximize the visibility into the potential of this new technique for space power applications.

UNCLASSIFIED

BACKGROUND

- CONCEPT FIRST CONCEIVED BY W. BLOCKER, THE AEROSPACE CORPORATION IN MID 1975
- PREVIOUSLY KNOWN FACTORS AFFECTING SYSTEM EFFICIENCY
  1. SOLAR CELLS ARE MOST EFFICIENT WHEN CONVERTING LIGHT WITH PHOTON ENERGIES EQUAL TO ITS BANDGAP
  2. SPECTRUM SPLITTING ALONE RESULTS IN CELL REPLICATION, INCREASES COST MORE RAPIDLY THAN EFFICIENCY GAIN
  3. HIGH CONCENTRATION ALONE RESULTS IN VERY LARGE HEAT INPUTS TO CELLS AND TEMPERATURE RISE LIMITS EFFICIENCY
- SYNERGYSTIC COMBINATION OF ELEMENTS RESULTS IN NEW CONCEPT
  - SPLIT SPECTRUM
  - FOCUS ON TAILORED BAND-GAP CELLS
  - USE HIGH CONCENTRATION RATIOS
  - COOL CELL AREAS
- RESULTANT CONCEPT PROMISES HIGH EFFICIENCY, LOW COST, AND MANAGEABLE THERMAL PROBLEMS
  - REPLICATED SOLAR CELL AREAS ARE SMALL
  - HEAT INPUT PER AREA IS DRASTICALLY REDUCED
  - OPTICS CAN BE MEDIOCRE QUALITY DUE TO SUN SUBTENDED SIZE



PRECEDING PAGE BLANK NOT FILMED

SECTION 2

SUMMARY OF FINDINGS

## SUMMARY FINDINGS - H-1034

The overall conclusion reached in this design study is that the technique appears extremely promising, but requires considerable further design study and definition to verify its attainable potential performance. A number of major conclusions were reached in this study.

It is quite clear that practically attainable solar cell efficiencies can exceed 50 percent, approaching 60-70 percent. The concept must use innovative techniques wherever possible to minimize weight and cost, including the use of inflatable space rigidized thin-film optics, three to six tailored-bandgap cells, lightweight yet efficient spectrum splitters, and novel lightweight radiators such as the type recently identified by Astro Research Corporation which use dust particle transport to maximize the area-to-weight ratio.

The potential advantages over a conventional but advanced array such as that for the Solar Electric Propulsion System (SEPS) are dramatic, particularly at power levels in the order of 100 kW or more, and even more so for missions requiring long-term operation in the earth's radiation belts (for uses such as powering a propulsion stage to transfer payloads from low orbit to geostationary orbit). The best performance parameters are summarized below:

NEW CONCEPT	SEPS TYPE
192 W/kg	56 W/kg
52 \$/W	300 \$/W

As shown on the facing page, the new concept has a potential cost advantage of a factor of 6 for the same power capability. Part of this advantage stems from the ability to shield the solar cells in the new concept with a negligible weight penalty due to their small area, while shielding the SEPS array is prohibitively heavy, forcing an increase in its size to allow for degradation and resulting in a large weight penalty.

A \$6-15 million technology and research program would be required to bring two or three solar cell types other than the currently well established silicon cell to the same status

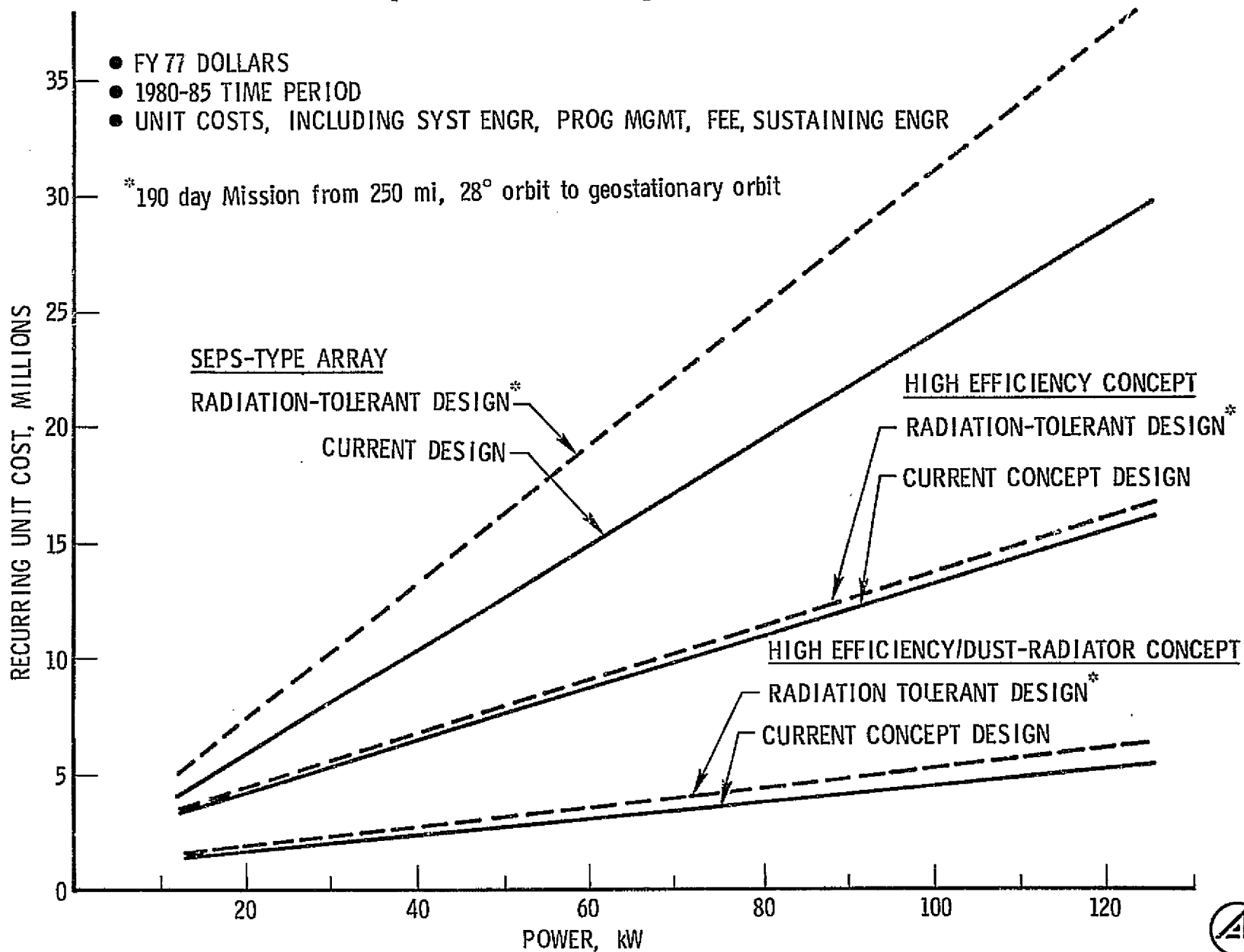
PRECEDING PAGE BLANK NOT FILMED

as that of GaAs. Typical materials which offer high promise are those with large energy gap ranging from 1.7-2.8 electron volts. Those materials could be gallium phosphide, aluminum phosphide, cadmium sulphide, mixtures of gallium and a secondary impurity such as indium, arsenic, or aluminum phosphide, and silicon carbide. Such a technology program would be a one-time investment, whose entire cost and the cost of an R&D program for the dust-radiator could both be recouped in the savings of one flight unit at 70-kW power level -- compared to the cost of a conventional array.

The advantages of this new concept are critically dependent on the weight and cost of the fairly complex non-solar cell equipment, and are thus highly design-dependent. Since the design evolved is non-optimum and utilizes extensive scaling, it will have to be refined before hard conclusions may be drawn on its potential advantages. Thus, more detailed trade-off and design studies including definition of a dust radiator or equivalent concept should be performed as a follow-on to this study. In addition, it would appear that simple laboratory experiments to verify the attainable efficiency should be performed. It is estimated that \$250K in studies and \$300-700K in laboratory experiments would suffice to attain this definition.

The closest rival technique that has the potential to attain high efficiency in solar photovoltaic systems is that of stacked multi-bandgap cells on a planar array. In principle, such cells could attain the spectrum splitting inherently by the use of tailored bandgaps without the use of separate spectral splitters and without the use of optics. Since most of the weight of planar arrays arises from the structure rather than the cells, and since the area required will probably at best be a factor of 3 smaller, it is unlikely that such an array can be significantly lighter than current projections for non-stacked planar arrays, and therefore probably will be at best competitive with the concentrated/split technique of this study. However, the inherent simplicity of the stacked bandgap cells may well offset any difference in weight and make for equivalent cost. It may eventually turn out that lightweight concentrators operating in conjunction with stacked bandgap cells offer the best promise. Such comparison studies should be included in the follow-on studies mentioned above.

# Comparative Projected Costs



ORIGINAL PAGE IS OF POOR QUALITY



SECTION 3

DESCRIPTION OF CONCEPT

PRECEDING PAGE BLANK NOT FILLED

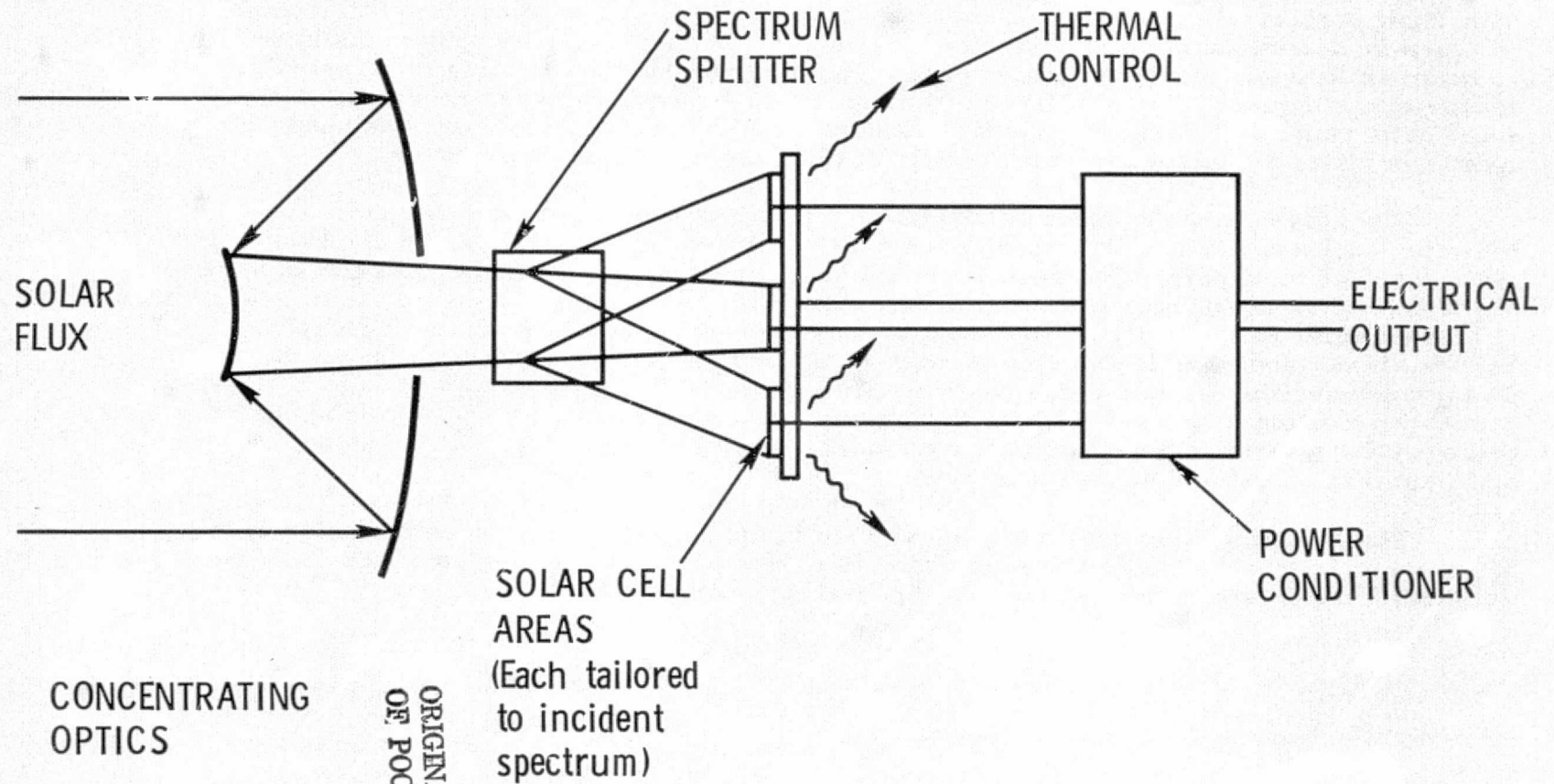
#### ELEMENTS OF CONCEPT - H-1503

The basic elements of the concept are shown in the figure on the facing page. They involve some form of optical concentrator, one or more spectrum splitting elements in the light path from the concentrator, a number of solar cell areas each receiving a narrower portion of the sun's spectrum as dictated by the characteristics of the spectrum splitter and number of solar cell types utilized, a number of the solar cells per area, each with bandgap tailored to coincide with the lower energy extreme of the wavelength region with which it is illuminated, some means for removing heat to keep the cells at or below a design temperature, and combination of the electrical outputs from each cell to result in a single electrical output.

Inasmuch as a concentrator is an inherent part of the system, the power module will require sun tracking to keep the images of the Sun on the solar cell areas. Such a tracking subsystem is implicit and not shown in the figure.



# Elements of Concept



AEROSPACE FORM NO. 4650-2

ORIGINAL PAGE IS  
OF POOR QUALITY



## MAJOR ELEMENT OPTIONS - H-0496

A number of major options exist for constructing a system of this type. These options are shown on the table on the facing page. The concentrator optics could consist of a single reflector or compound multiple reflectors, and each could be constructed as a monolithic structural device or thin inflated rigidized film. The spectrum splitter could be a prism, a transmission or reflection grating, or dichroic mirrors (otherwise known as beam splitters). In addition, a hologram could be constructed relating the single Sun source to the number of spectrally split and spatially separated images required. The solar cells could be layered in several bandgaps or could be separate, with one bandgap type illuminated by each wavelength portion issuing from the spectral splitter.

The heat rejector can use conduction to transport heat from the solar cells to a radiating surface, such as is normally the case of current planar arrays, or use heat pipes for such transport. The radiator could be a separate surface or be the back surface of the concentrating mirror if the latter is a monolithic structure. The third major class of heat rejector is one utilizing transport of mass, such as the dust radiator concept, however is not shown as it was only identified as a viable option very late in the study. The power conditioner options include operating all the cells at the same current probably resulting in some degradation in maximum power output, or optimizing each cell area for maximum power output, combining the different cell currents in some optimum fashion using a separate combiner.

The system design proceeded to evaluate the probable choices to be made for each of the major element options shown in order to arrive at a baseline design which could be weighed, costed, and compared with the SEPS -type design.

MAJOR ELEMENT OPTIONS

ELEMENT	OPTIONS	
CONCENTRATOR	SINGLE SURFACE	MONOLITHIC
		THIN FILM
	COMPOUND SURFACE	MONOLITHIC
		THIN FILM
SPECTRUM SPLITTER	PRISM	
	GRATING/HOLOGRAM	
	DICHROIC MIRRORS (BEAM SPLITTERS)	
SOLAR CELLS	LAYERED BANDGAP CELLS	
	SEPARATE CELLS	
HEAT REJECTOR	CONDUCTION TO RADIATOR	USE CONCENTRATOR
		SEPARATE
	HEAT PIPES TO RADIATOR	USE CONCENTRATOR
		SEPARATE
POWER CONDITIONER	ALL CELLS AT SAME CURRENT	
	OPTIMIZED CURRENT PER CELL TYPE	



SECTION 3.1

SOLAR CELLS

PRECEDING PAGE BLANK NOT FILMED

An analysis was made to determine the attainable efficiency of the solar cells. The detailed calculations are included in the Appendix, and are presented in summary form in the next four figures. These figures are shown as a function of the number of spectral intervals into which the spectrum is split, the temperature at which the cells are maintained, and the solar concentration factor.

Initial calculations were performed using a model of the solar cells which assumed an ideal diode except for the presence of junction current dominated by diffusion. Further calculations were then made for the case where the diode current is dominated by generation and recombination rather than diffusion, which tends to result in somewhat more pessimistic results for attainable efficiency. In practice, real life silicon cells tend to exhibit efficiencies in between the two extremes of these two models, thus probably making the results realistic assuming that other semiconductor materials behave as silicon. The calculations, while theoretical, did assume best present-day silicon technology. The efficiencies calculated therefore are not true theoretical limits but the practical limits corresponding to a technology for all the cells that is equivalent to today's best silicon technology. The results shown therefore do not attain the theoretical limiting efficiencies, which have been calculated by Jackson<sup>(6)</sup> and Rappaport<sup>(7)</sup> to reach 69 percent for 3 spectral bands, 86 percent for 10 bands, and 100 percent for an infinite number of bands. The solar cell model also assumed an infinite shunt resistance and a zero series resistance. These assumptions tend to be reasonably well approximated in practice, and should hold up to concentration factors of at least 1000, above which the collector grid area required on the cell would probably either reduce the effective cell area or introduce series resistance; and the minority carrier levels approach the majority carriers, probably invalidating the model used. The curves shown on the next four sheets were also calculated for the case where all of the junction currents were assumed equal. It was found that the efficiency obtainable compared favorably to the more ideal case in which each type of cell is allowed to operate at its own maximum power transfer current, since proper selection of the bandgap energies minimized the difference.

The following curves show efficiency data parametrically for systems from 1-20 cell types with the cells maintained at temperatures of 200, 300, 400, and 500°K. Concentration ratios of 1, 100, and 1000 are shown, with the calculations in the Appendix being performed for additional conditions. The concentration ratio applicable to each cell type is the same as that for the entire optical system, the fraction of the incident energy reaching each cell type being assumed to be determined only by the width of its illuminating spectral interval and the concentration factor.

REPRODUCING PAGE BLANK NOT FILMED

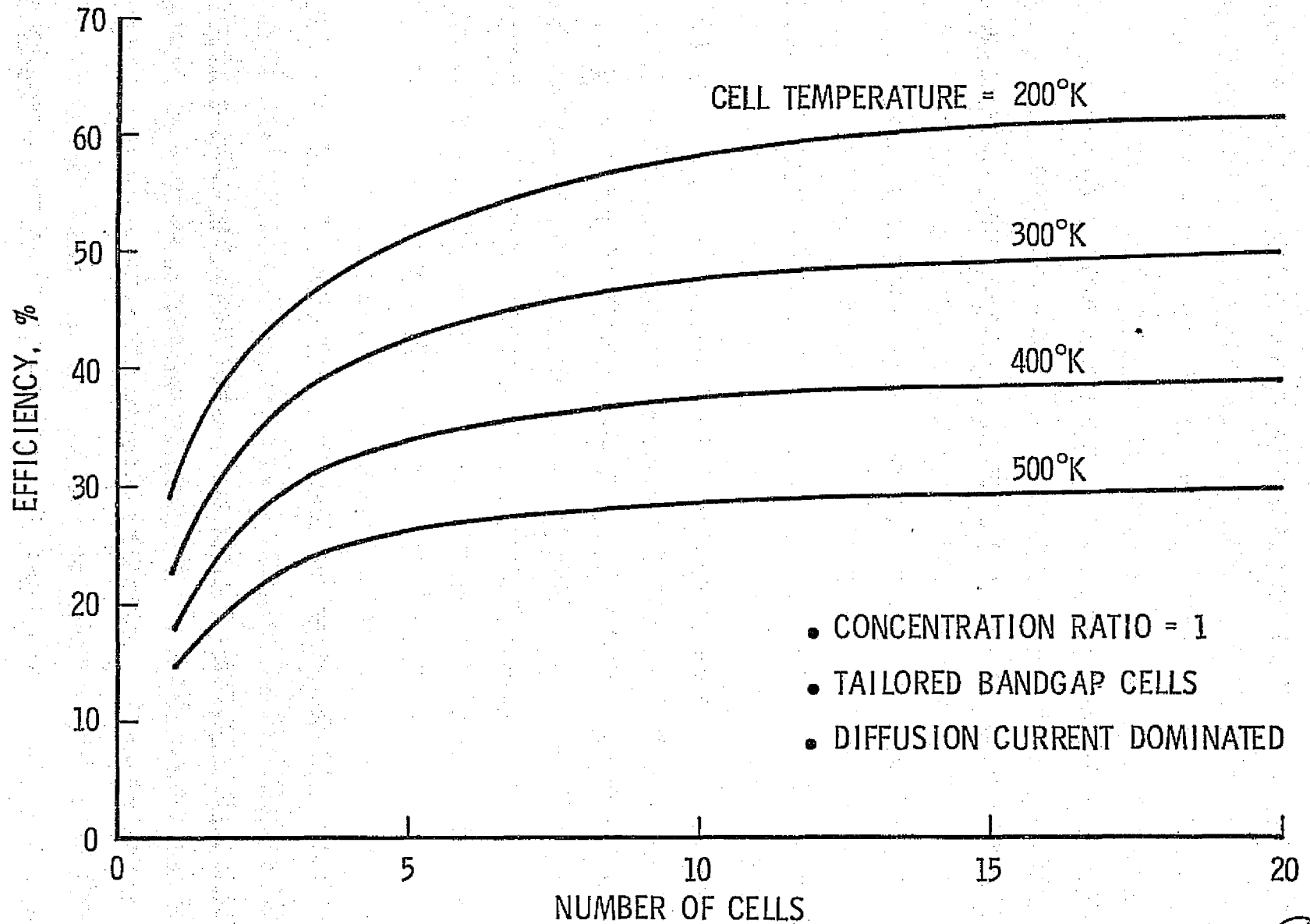
ATTAINABLE SOLAR CELL EFFICIENCY (C=1) . H-0488

The curves on the facing page show the variation in the efficiency of the solar cells for a system with no concentration, but with the number of tailored bandgap cells varying from 1-20, and cell temperature from 200-500°K.

The curves show a rapid increase from the expected 23 percent efficiency of a single cell at room temperature to efficiencies in the order of 40 percent for 10 or more cells at 400°K, 50 percent at 300°K, and 60 percent at 200°K. The knee of the curves is around 3-5 cells. The effects of reduced temperature appear to be very dramatic.

From the statements in the Introduction, it is also clear that a non-concentrated system with this many cell types will be non-competitive even though it attains very high efficiencies. For instance, a system with 10 cell types requires 10 times the area with approximately 10 times the weight and 10 times the cost of a single cell-type system. Its efficiency at 300°K is only about twice that reached in practice by single-cell planar arrays, thus making the net cost differential a factor of 3-5 in favor of single cell-type planar arrays. Similarly the added difficulty of reaching 200°K at the cells does not warrant the small (20 percent) gain in efficiency possible at such temperatures.

# Attainable Solar Cell Efficiency



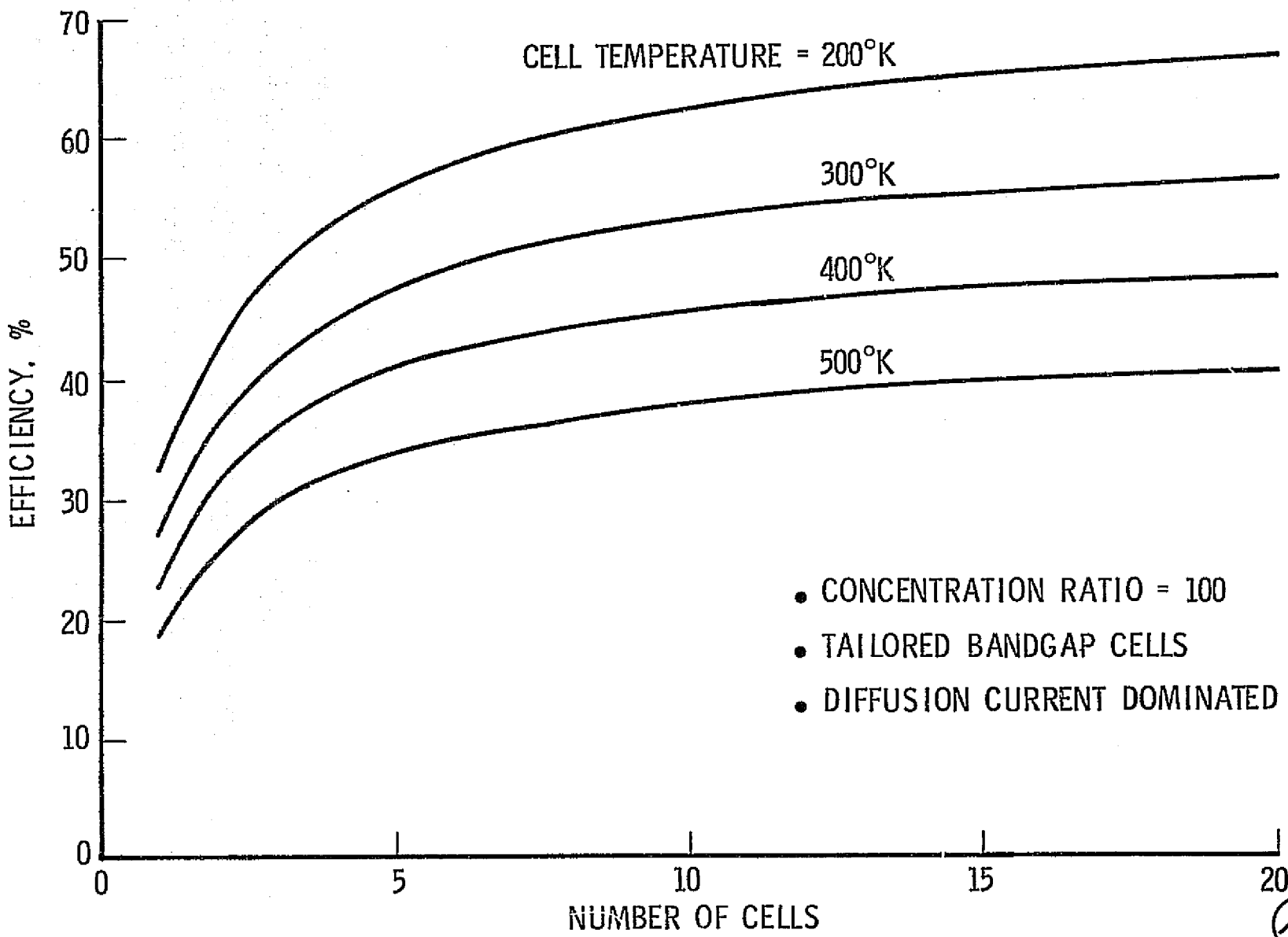
#### ATTAINABLE SOLAR CELL EFFICIENCY (C=100) - H-0489

The graph on the facing page shows the efficiency attainable as a function of the number of cell types and temperature for a concentration ratio of 100, i. e., the energy falling on every cell is the appropriate spectral interval taken from 100 times the solar flux incident on the optical system. The trends are the same as those for no concentration with 5-20 percent greater efficiency being attainable for the same conditions.

The knee of the curves is still seen to be at 3-5 cells with small increases occurring for more than 10 cells. As in the case for no concentration, the increase in efficiency from 1 cell to 10 cells at 300°K is about a factor of 2. Due to the concentration ratio, however, the total cell area required is only 0.05 times the area of an equivalent single cell-type planar array for the same power output. Thus, it is apparent that the weight and cost of the cells will be greatly reduced. The weight of the radiator, optics, and splitters will undoubtedly reduce this advantage, however, and is treated later in the report.



# Attainable Solar Cell Efficiency



AEROSPACE FORM NO. 4650-2

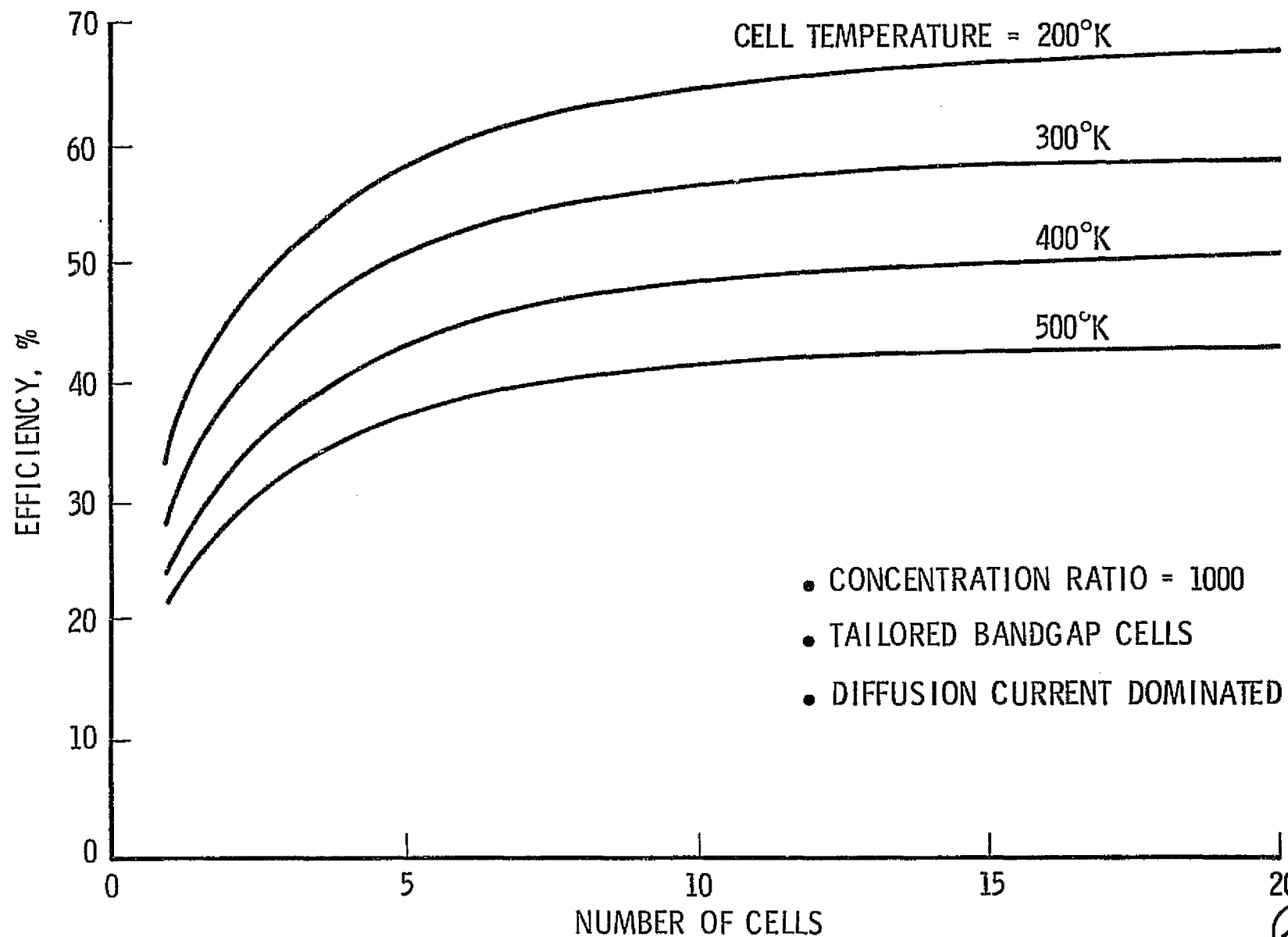


ATTAINABLE SOLAR CELL EFFICIENCY (C=1000) - H-0491

The graph on the facing page shows the efficiency calculations for a concentration ratio of 1000. The efficiencies are seen to be about 5-30 percent higher than for a concentration ratio of 1 with the knee of the curve still being around 3-5 cells. Total efficiencies attainable approach 60 percent at 300°K and 70 percent for a cell temperature of 200°K.

As in the previous case, the efficiency gain from 1-10 cells is about a factor of 2 at 300°K. Due to the large concentration ratio, the total cell area required is only 0.005 times the area of an equivalent single cell-type planar array for the same power output. This small solar cell area in turn minimizes the cell system weight, and will be shown to be particularly attractive for the case where the power system must survive for long periods of time in the earth's radiation belts in which case the penalty for shielding the small solar cell areas will be negligibly small. The weight of the optics and radiator will reduce the advantage, however. In particular, the radiator weight may well limit the lowest temperature at which the cells can be made to operate, even though efficiencies approaching 70 percent are predicted by this graph.

# Attainable Solar Cell Efficiency



## EFFECTS OF GENERATION/RECOMBINATION CURRENT - H-0502

The previous three graphs showed the efficiency attainable for solar cells whose junction current is dominated by diffusion. Such models tend to predict somewhat greater efficiencies than observed in silicon. A change in the model of the cell in which the junction current is dominated by generation-recombination currents rather than diffusion tends to predict somewhat lower efficiencies than observed in silicon. The decreases in attainable efficiency from that shown in the previous three figures is tabulated on the facing page as a function of concentration ratio, cell temperature, and number of cells.

The numbers on the facing page indicate that in general the decrease in efficiency from the previous graphs never exceeds 10 percent even for a 12-cell system at concentration ratio of 1 and 400°K. When applied to systems with concentration ratio of 500 or more, the total decrease in efficiency is less than 2 percent for 1-10 cell systems. Since real cells tend to have efficiencies in between the extremes of these models, the use of the previous graphs in the remainder of this design study appears warranted, particularly for high concentration designs.

DECREASE IN PERCENT ATTAINABLE EFFICIENCY  
DUE TO GENERATION-RECOMBINATION CURRENT

CONCENTRATION	CELL TEMPERATURE °K	NUMBER OF CELLS				
		1	2	3	6	12
1	300	4.0	5.8	6.8	8.5	9.9
	400	4.2	6.2	7.2	9.1	10.4
100	300	1.2	2.0	2.4	3.4	4.2
	400	1.3	2.1	2.6	3.5	4.6
500	300	0.4	0.3	0.5	1.3	2.2
	400	<0.1	<0.1	0.4	1.1	2.0

ORIGINAL PAGE IS  
OF POOR QUALITY

AEROSPACE FORM NO. 4650-2



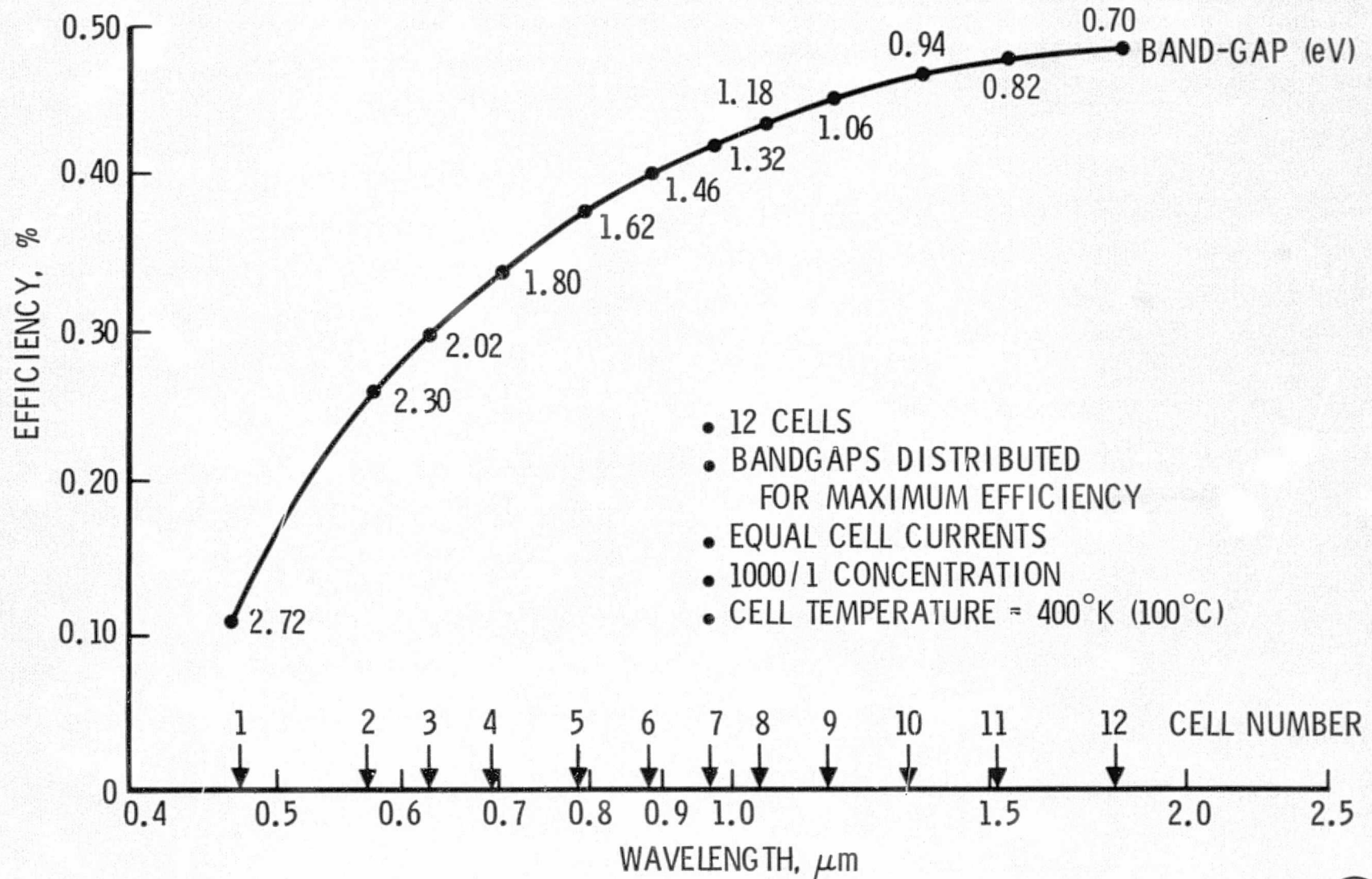
## PLACEMENT OF BANDGAP ENERGIES - H-1504

The calculations of attainable efficiency shown in the Appendix were made using a computer program which selected the bandgap energies for the components of any multi-bandgap cell system in such a way as to maximize the efficiency -- given the constraints of the number of cells, the shape of the solar spectrum, and the desire to keep the junction currents of all cell types equal to minimize the difficulty of power conditioning. A cumulative efficiency curve is shown on the facing page as an example of the many computations performed, in which the contribution of efficiency due to each type of cell is shown, and the bandgap energies and equivalent cutoff wavelengths of the cells are indicated.

The cumulative efficiency is shown for a 12-cell system in which the cell currents are equal, the cell temperature is  $400^{\circ}\text{K}$ , and the concentration ratio is 1000 solar fluxes. The computer program distributed the bandgap energies to maximize the attainable efficiency but not necessarily to coincide with the bandgap energies of available or even real materials. The effect of substitution of the bandgaps of real materials will be treated in the next table. Referring to the curve on the facing page, it is seen that 50 percent of the efficiency contribution is due to 2 cells with bandgap energies in excess of 2.3 electron volts, corresponding to wavelengths of  $0.7\ \mu\text{m}$  and shorter. Seventy percent of the efficiency is contributed by cells with bandgaps of 1.8 or more, and 90 percent by cells with bandgaps of 1.2 or more. This is an interesting result in that it calls for development of solar cells with large bandgap energies, which have received fairly little attention to date but are seen to contribute very heavily to the attainable efficiency of a solar photovoltaic system due to the solar energy distribution.

Curves for other conditions all indicate the same qualitative results, pointing out the importance of high bandgap energy solar cell development and application.

# Cumulative Efficiency of Solar Cells

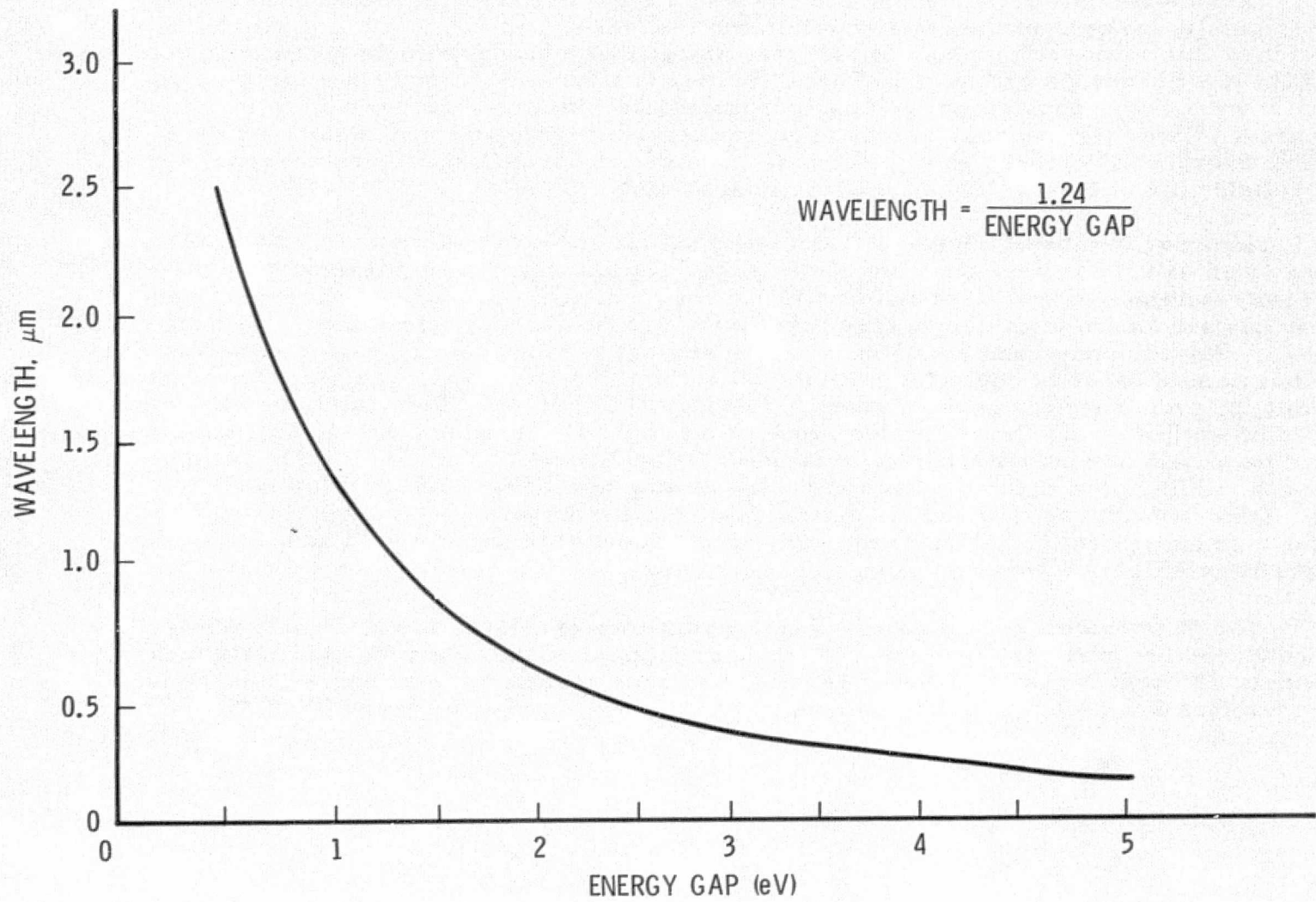


RELATION BETWEEN ENERGY GAP AND WAVELENGTH - H-0492

Some readers may not be as familiar with the characterization of cells by their energy gap (measured in electron volts) as they are with their cutoff wavelength. The relation between the two is simple and plotted on the facing page for ready use by those wishing to convert from one measure to the other.



## Relation Between Energy Gap and Wavelength



## SEMICONDUCTOR MATERIALS FOR SOLAR CELLS - H-0501

A computer program such as the one which generated the efficiencies obtained incrementally for each of the cells shown in the last graph was also used to evaluate the efficiency obtainable with the use of real materials, whose bandgap might not exactly coincide with the ideal bandgaps called for. The difference in efficiency turned out to be very small since it was always possible to identify real materials with bandgaps near those ideally required. Thus, the previous curves apply for a system with real materials. On the facing page is shown a table of the energy gaps attainable from several real cell materials, which are suitable for at least a 12-cell spectrally split system.

In order for the efficiencies of the previous charts to be attained, new types of solar cells would have to be developed and their technology brought to an equivalent state of that of GaAs, and their energy gaps tailored to the region of 1.6 - 3.0 eV. A number of cell materials are known to exhibit energy gaps in the proper regions. They are in varying degrees of development and commercial application at present. In the region 1.6 - 2.0 eV, various combinations of doping of gallium and indium, arsenic, and aluminum on phosphide exhibit the proper energy gaps. Above that energy, gallium phosphide, aluminum phosphide, cadmium sulfide, and silicon carbide are known to exhibit the proper energy gap. Some of these materials are heavily utilized in light-emitting diodes for semi-conductor readout circuits, while some such as silicon carbide are only now being developed for such applications. Cadmium sulphide is extensively used for infrared detectors. In addition to the high energy cells, gallium arsenide, silicon, and germanium would be used for the longest wavelength or smallest bandgap energy cells.

It seems evident that materials exist from which one could devise a system to satisfy the conditions required for this concept, though the state of the art of the materials technology is widely different for most of the materials, and none approach the extensive development and therefore low cost per cell of silicon.

SEMICONDUCTOR MATERIALS FOR SOLAR CELLS

ENERGY GAP (eV)	WAVELENGTH AT GAP, $\mu\text{m}$	CELL MATERIAL
2.86	0.43	SiC
2.50	0.50	AIP or CdS
2.24	0.55	GaP
2.00	0.62	} (Ga, In)P GaAsP GaAlP
1.80	0.69	
1.60	0.78	
1.40	0.89	GaAs
1.10	1.13	Si
0.70	1.77	Ge

ORIGINAL PAGE IS  
OF POOR QUALITY

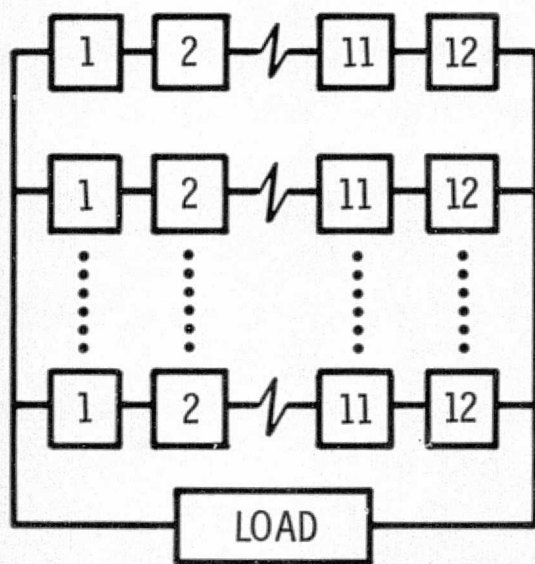
## ELECTRICAL CONSIDERATIONS - H-0487

Two major options exist for utilization of the electricity generated by these cells. One is to operate different cell types in series, thereby forcing each cell to operate off its optimum power transfer point. The other is to allow the optimization of power transfer of each cell type which requires separate inversion, combining, and conversion for each cell type. The requirements for connection are illustrated on the facing page.

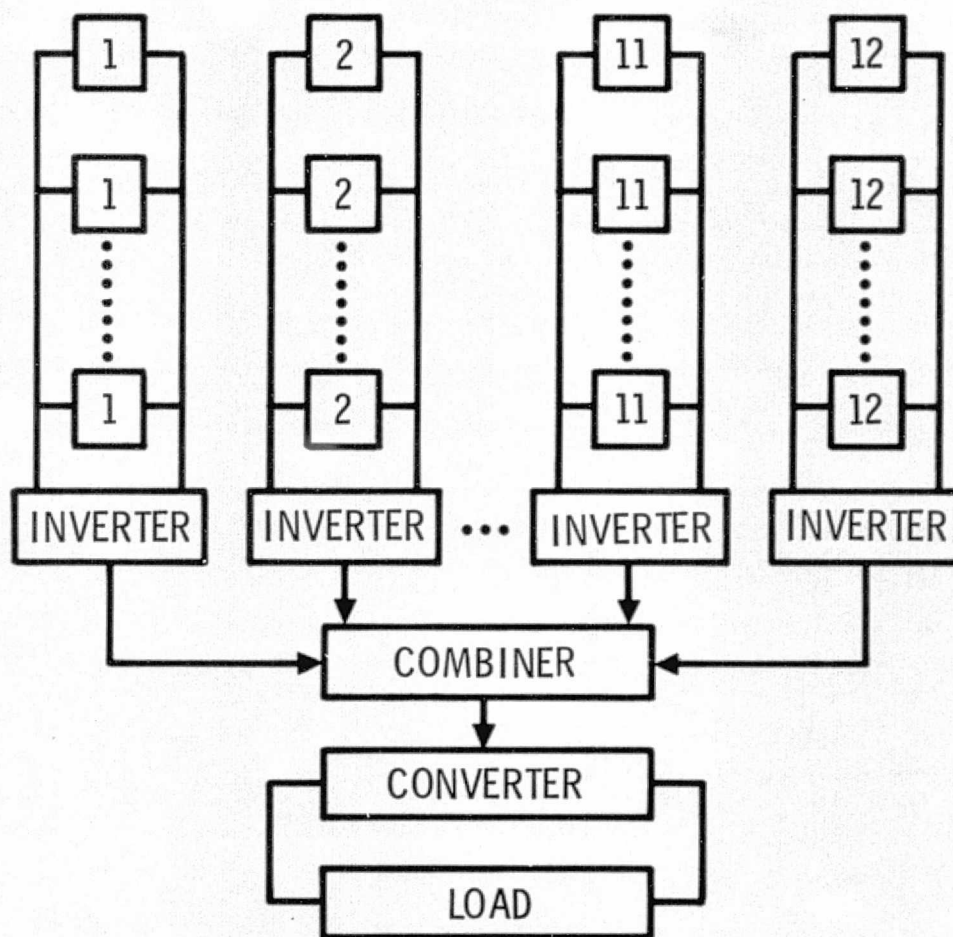
As shown in the Appendix, the loss in efficiency due to operating the different cell types at equal currents is very small and minimized by proper choice of the bandgap energies, thereby eliminating the need for heavy and expensive separate inversion, combination, and conversion operations. A further degree of freedom for the equal current constraint case is the ability to connect different numbers of cells in parallel prior to connecting them in series strings, thus adjusting the effective cell currents to be optimum without impacting the choice of bandgap energies which can then be chosen to maximize efficiency given real materials available.

# Electrical Considerations

EQUAL CURRENT CONSTRAINT



INDIVIDUAL CURRENTS (NO CONSTRAINT)



SECTION 3.2

OPTICAL ELEMENTS

PRECEDING PAGE BLANK NOT FILMED

This section treats the various design factors, options, and trade-offs affecting the design of the optical system. Fundamental considerations which limit the attainable concentration ratio are discussed, as are optics type and design and spectrum splitter options. In each case, a single optical system is presumed, followed by spectrum splitting to illuminate each of the tailored bandgap solar cell areas. The option exists of building separate small concentrating optics to illuminate each area of tailored bandgap solar cells, or for that matter carried to the ultimate to illuminate each solar cell individually. Trade-offs between the three approaches should be performed but could not be carried out in this very preliminary analysis.

PRECEDING PAGE BLANK NOT FILMED

## FUNDAMENTAL OPTICAL CONSIDERATIONS - H-1505

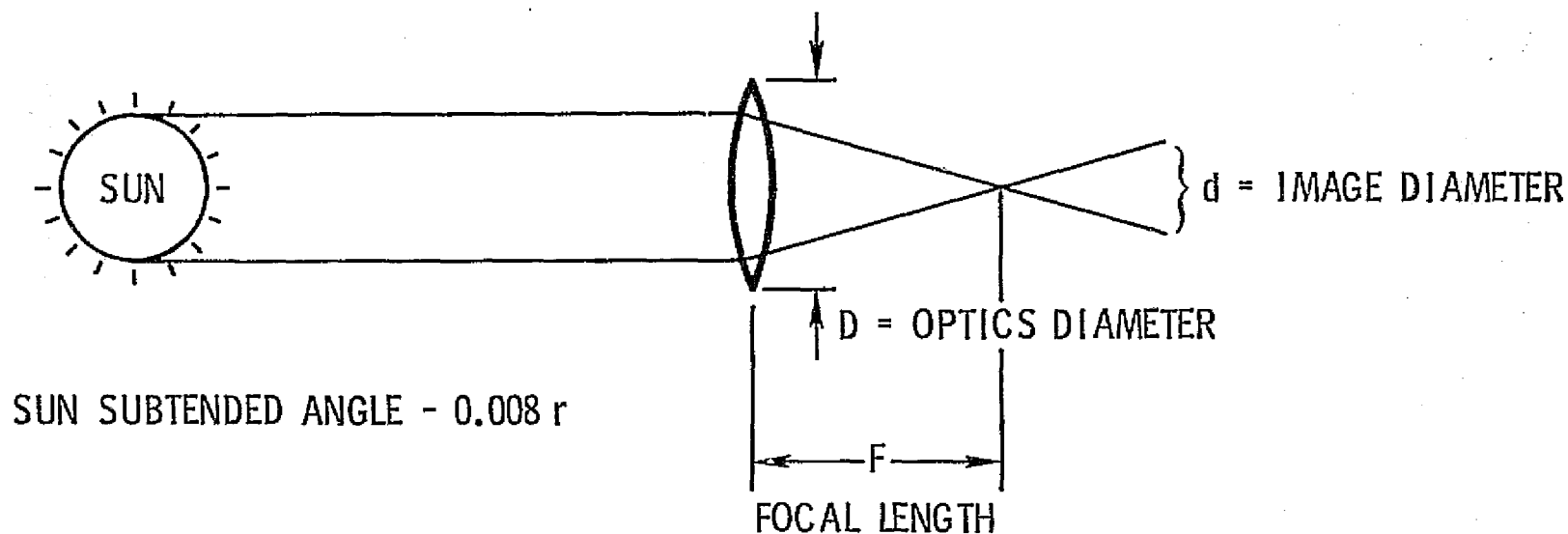
The sun is not a point source of light as seen from the Earth, but subtends about  $1/2$  deg. Thus, the optical system will be unable to focus the sun's image to a point, and at best will be able to produce an extended image of the sun with diameter dependent on the focal length-to-diameter ratio of the optical system. The figure and table on the facing page indicate the relationship between the diameter and area of the image to be occupied by each solar cell type and the F/D ratio. The table indicates that the maximum possible concentration ratio is set by the same F/D ratio, with a limit in the order of 10,000/1 concentration for practical optics. Very long focal length systems are limited to small concentration ratios, thus systems with fairly small F/D will be required to attain fairly high concentration ratios, and has implications on the optical figure required to maintain the image diameter.

Sun tracking will be required in order to maintain the sun's image on the solar cells. The required accuracy of tracking or pointing has been calculated using a criterion that the power loss due to non-overlap of the sun images and the solar cell areas result in less than 3 percent power loss. As shown on the facing page, the pointing accuracy must be in the order of 1 mrad for systems with concentration ratio in the order of 1000, requiring an F/D of about 4. While this is certainly attainable, it requires a carefully designed pointing and tracking system. The sensor for the control system to point the entire power module to the sun to these accuracies could very well consist of several solar cells at the periphery of one or more of the solar cell areas, with the control system being designed to keep the voltages equal (any deviation from equality implying an error in pointing which would be corrected by the control system). In this way, no extra sensing device need be provided for sun tracking, and it is likely that the torquers usually used for most tracking arrays will be adequate pending further design refinements.

The image diameter for an  $F/D = 4$  system with a concentration ratio of 1000 will be  $0.0316 \times \text{dia}$  of the optics. Thus, a system for 10 solar cell types would have a total solar cell area of 0.00784 times the area of the optics. This small area is likely to be far less expensive than the area of an equivalent planar array, and will require far less mass to shield from damaging radiation.



# Fundamental Optical Considerations



F/D	MAX CONCENTRATION RATIO	IMAGE DIAMETER	POINTING ACCURACY FOR 3% POWER LOSS, mr
1	$1.4 \times 10^4$	0.008D	0.26
3.16	$1.4 \times 10^3$	0.025D	0.81
10	$1.4 \times 10^2$	0.08D	2.6
31.6	$1.4 \times 10^1$	0.25D	8.1
100	1.4	0.8D	26.0

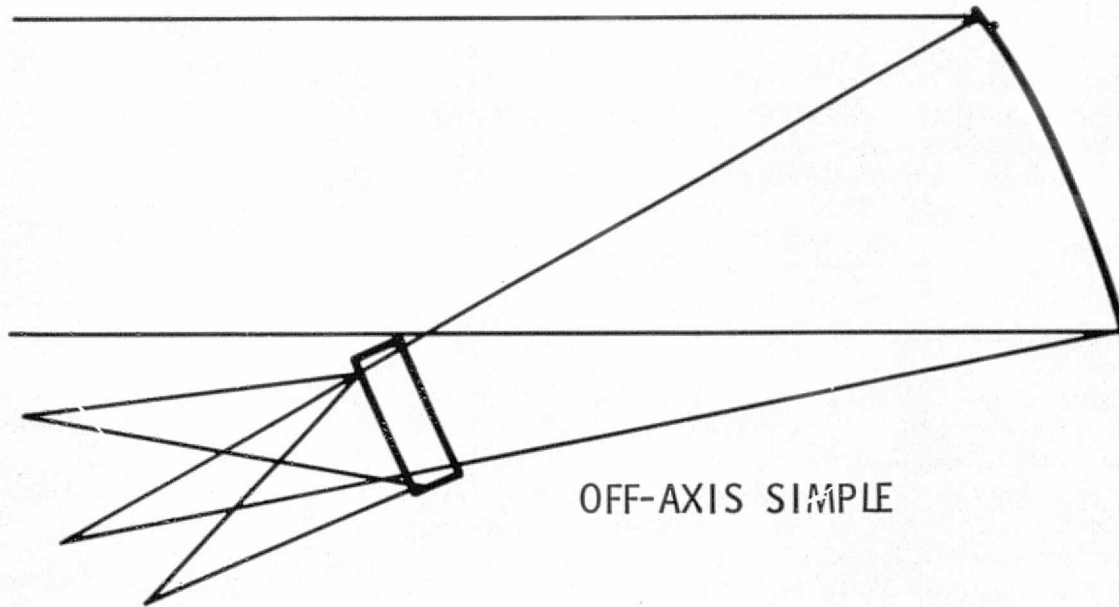
## OPTICAL ALTERNATIVES - H-1506

The primary collecting optics can be designed either as a simple or compound optical reflector with the rest of the components on-axis or off-axis. Examples of these major alternatives are shown in the diagrams on the facing page. The advantages of the off-axis simple reflector system are that only a single optical surface is required, but its disadvantages are that a rather long device results which is subject to vibration shifting of the optical image, and that a spherical surface may not be usable due to spherical off-axis aberrations. The advantages of the on-axis compound optical system are a more compact design which is less subject to vibration shifting of the image, and the possibility of using a spherical surface for the primary due to its on-axis design, which results in smaller spherical aberrations. The disadvantages are the blocking loss of the secondary reflector and the reflection losses due to the larger number of optical surfaces.

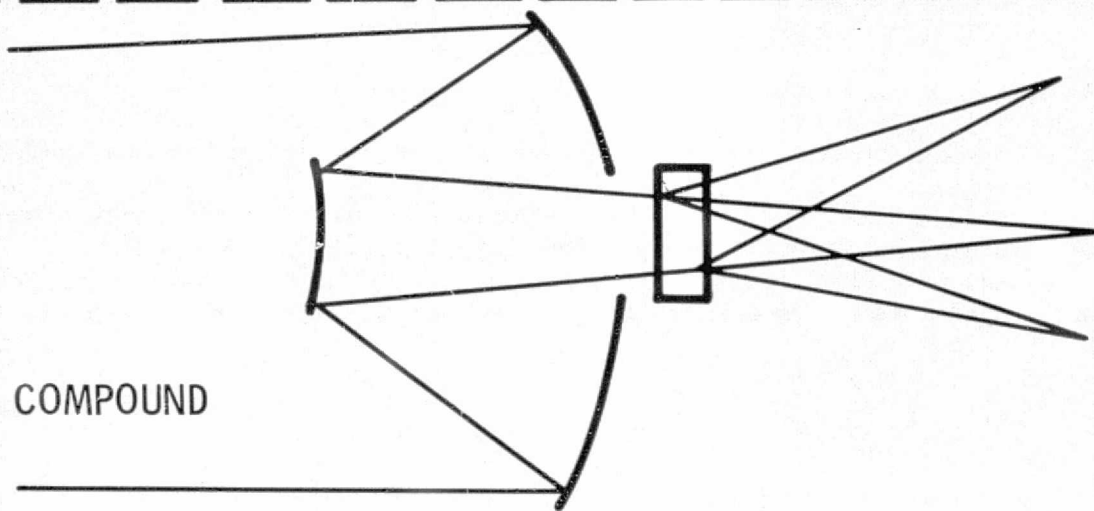
For the purposes of this design study, the on-axis design was chosen although it is not at all clear that this is the optimum choice.

# Optical Alternatives

ORIGINAL PAGE IS  
OF POOR QUALITY



OFF-AXIS SIMPLE



ON-AXIS COMPOUND



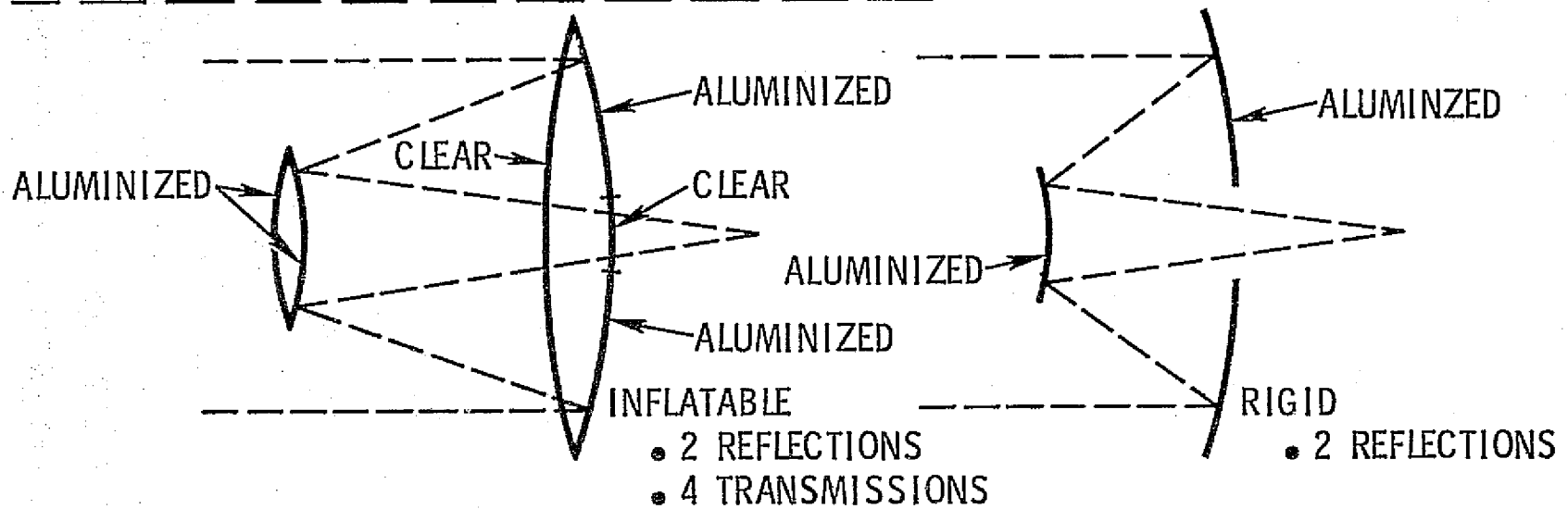
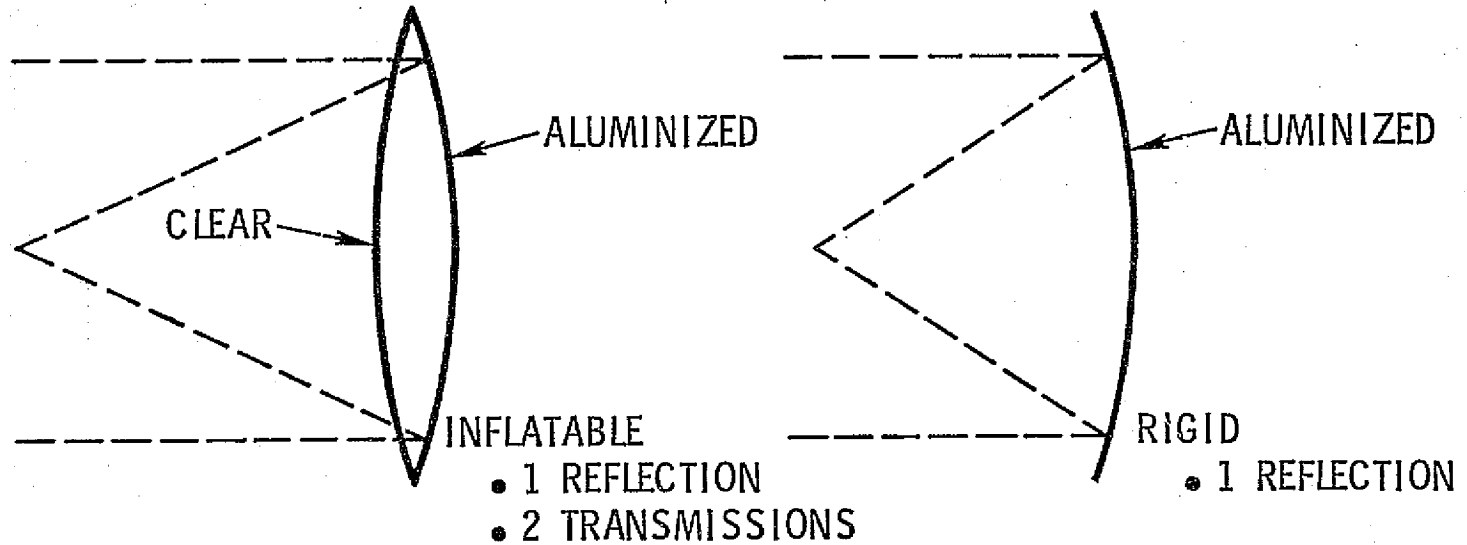
## OPTIONS FOR PRIMARY AND SECONDARY OPTICS - H-1507

The major optical elements could be constructed of rigid structural materials which hold their figure, or from thin-film structures whose figure depends either on inflation pressure, rigidization after deployment, or both. The reason for considering these two options is the likely large weight of a rigid set of optics, based on analogy with radio and radar antennas which must hold about the same surface tolerances as will be shown to be required here. It is in principle possible to make inflatable or thin-film optics with a non-spherical figure by constraining the figure with tension wires of given lengths tied against a mast or other supporting structure. These techniques have been explored considerably in large space antenna studies but have not been utilized here due to the complexity of the design, and the likelihood that spherical surfaces will suffice.

One of the major differences between optical systems using rigid and inflatable optics is the efficiency obtained after the required number of reflections and transmissions through the devices. The facing page shows simple and compound systems of both types in which the lightweight optics are assumed constructed from clear films, aluminized in the proper regions for reflection, inflated to attain a spherical figure, and rigidized to resist micro-meteorites. The primary differences between the rigid and film-type optics is shown to be the number of transmissions required through clear material. Since each transmission involves reflection losses at each surface which is crossed, compound inflatable systems will have lower efficiency than simple rigid systems.

A preliminary design of a power module was generated during the early phases of this study, which utilized rigid compound optics sized for collecting about three times the energy required in electrical output (thus allowing for 30 percent overall system efficiency including the effects of optical reflections, spectrum splitter efficiencies, and the use of 50 percent efficient solar cells). The optics and support structures in that design weighed close to 300 lb, and the entire module close to 1000 lb. Since the SEPS array at 12.5 kW weighs about 400 lb, such a design would have been non-competitive. Thus, a second design using inflatable optics was forced, resulting in the inclusion of film optics in this section.

# Options for Primary and Secondary Optics



AEROSPACE FORM NO. 1550-2



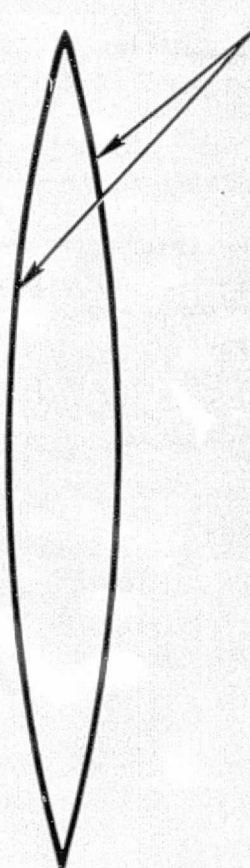
## INFLATABLE OPTICS - H-1508

One possible concept for constructing lightweight film optics is illustrated on the facing page. It is recognized that two factors will affect the construction material and technique: One being the requirement that surfaces which are to be transparent must not darken under exposure to sunlight, and second that the device not lose its figure under bombardment by micrometeorites. The first requirement rules out practically all plastics and results in the choice of thin quartz film for the basic structural material; while the second consideration regarding micrometeorite damage leads to consideration of a material which is rigidized after inflation so that it does not depend on gas pressure alone to maintain the figure. For the purposes of this study, thin quartz film was used. It satisfies the first requirement and perhaps with some innovative combination of localized stretching of an adjacent film (in the reflector areas) to obtain elastic deformation, could satisfy the second requirement and maintain its shape in the presence of micrometeorite damage.

Quartz film has been manufactured in thicknesses of about 0.003 in. with film widths of 2 ft and very large lengths. These films could be welded at the edges for producing bigger films or a larger format film produced. The film is flexible enough to be rolled around a 32-in. drum with no permanent set. In use, two circular films of the required diameter would be welded at their circumferential edges and pressurized in between. The gas pressure operating against a peripheral compression ring would form a doubly convex spherical lens. The surfaces which were to act as mirrors would be aluminized and anti-reflection coated, attaining an efficiency probably exceeding 95 percent over the wavelength interval required, i. e., 0.4-2.0  $\mu$ m. The clear surfaces through which the light paths must pass would also be anti-reflection coated on both sides but not aluminized, the efficiency of the entire lens then being primarily a function of the number of times the light paths crossed such surfaces.

The table on the facing page indicates the potential attainable efficiency from such a lens system as a function of the number of surfaces involved. The calculated efficiency is weighted for the likely spectral energy distribution, and is seen to be as high as 98.4 percent for a single surface and as low as 87 percent for 8 surfaces which imply 4 transits through film. It is clear that some form of lightweight inflatable and/or rigidized package of this type could be made practical - however, the exact details will have to be worked out in subsequent design studies. The resultant weight of the inflatable optics will be about 0.09 lb/ft<sup>2</sup> of aperture area, which is about 1 order of magnitude less than typical for high-quality radar antennas, and about 2 orders of magnitude less than that achievable with high-quality imaging optical components.

# Inflatable Optics



QUARTZ FILM, THICKNESS = 0.0076 cm (0.003 in.)

- REFLECTIVE SURFACE ALUMINIZED, ANTI-REFLECTION COATED
  - EFFICIENCY > 0.95
- CLEAR SURFACES ANTI-REFLECTION COATED

No. SURFACES	EFFICIENCY*
1	98.4
2	96.8
4	93.5
8	87.0

\* Efficiency is weighted for spectral energy distribution

- FILM CAN BE ROLLED AROUND 0.8m (32 in.) DRUM
- FILM PRODUCED IN 1-2 ft STRIPS, MELT-JOINED
- FILM DENSITY  $\approx 2.8 \text{ gm/cm}^3$  ( $0.1 \text{ lb/in.}^3$ )

## SPECTRUM SPLITTER OPTIONS - H-1509

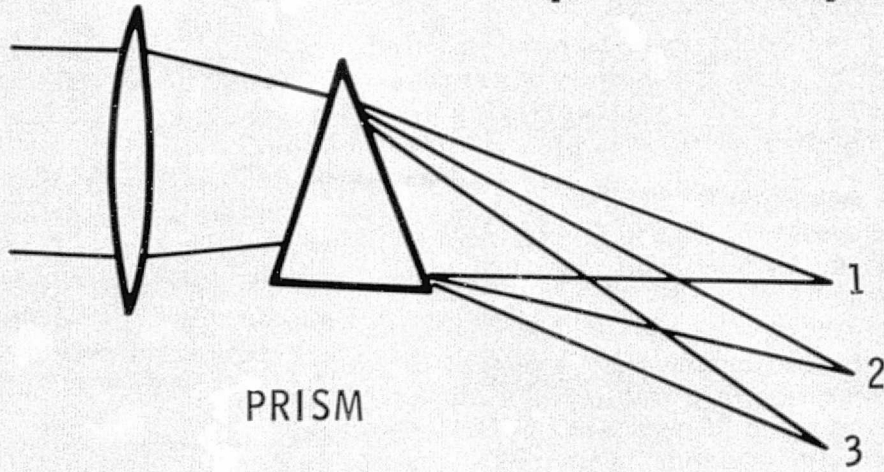
Once the light has been collected with the concentrating optics it must be split into a number of spectral regions, each to be focused on the particular area of solar cells whose bandgap is tailored to best respond to that spectral region. The major options for spectral splitting components are prisms, interference gratings, and dichroic mirrors (otherwise known as beamsplitters). These three options are illustrated on the facing page.

Prisms would probably be placed after the concentrating mirror in an optical system, with a single prism in theory giving rise to as many spectral region areas as desired. Gratings could be either of the transmission or reflection type. In either case, the first order lobe of the diffraction pattern would be focused on the spectral region areas. The gratings could follow or precede the optics, in principle being equivalent. In principle, a single grating would also suffice for an arbitrarily large number of spectral regions. Dichroic mirrors would be placed after the optics, and the number of mirrors required would be one less than the number of spectral regions to be generated. The mirrors would consist of films or glass coated to pass desired wavelengths while reflecting all undesired wavelengths.

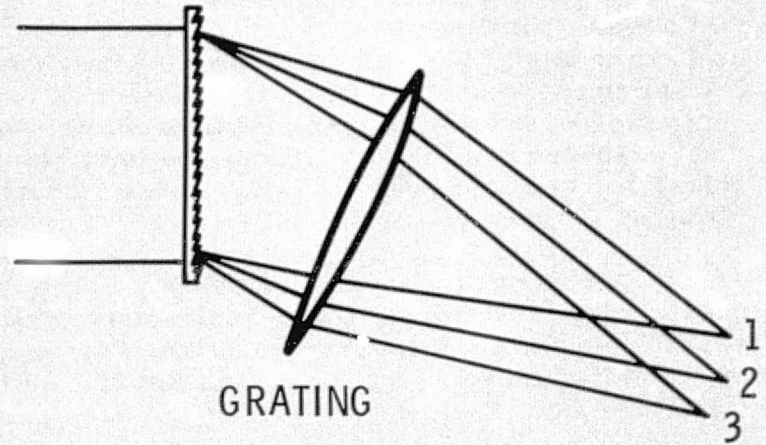
Each of these major options is examined in more detail in the following pages to determine their likely operating efficiency and design features.



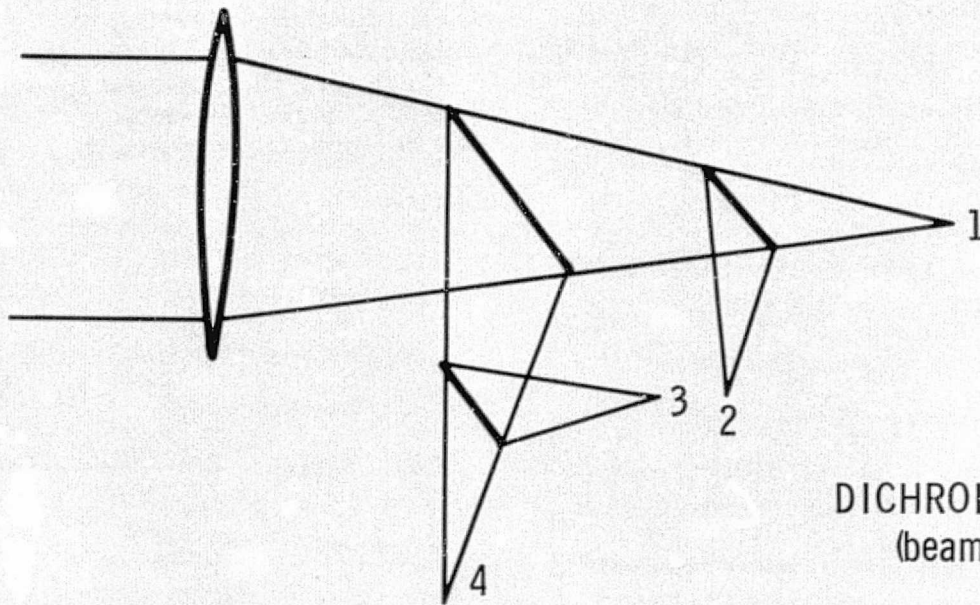
# Spectrum Splitter Options



PRISM



GRATING



DICHROIC MIRROR  
(beamsplitter)



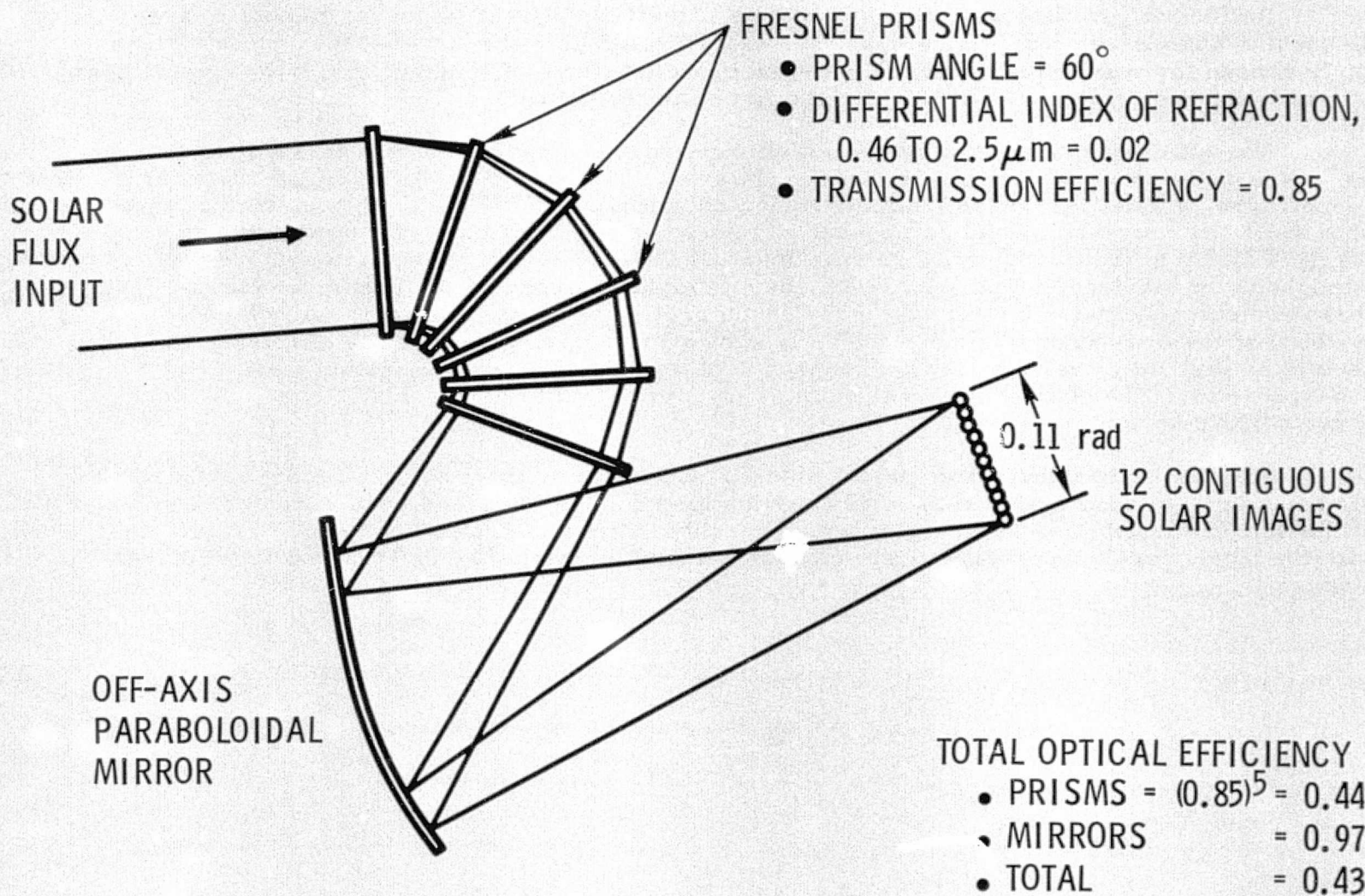
## SPECTRUM SPLITTING BY PRISMS - H-0481

An analysis of the use of prisms for splitting the spectrum has been carried out. The requirement was the generation of 12 solar images to be focused on 12 separate solar cell areas, since the baseline concept chosen consists of 1000/1 concentration and 12 solar cell types at 400°K. Inasmuch as the sun subtends about 8 mrad, the entire spread of the images must be about 0.10 rad. The result is a requirement that the differential index of refraction of the prism material between the lowest and highest wavelengths under consideration (0.46-2.5  $\mu\text{m}$ ) be 0.1. Since the best glasses known today have a differential index of refraction of about 0.02, it follows that 5 prisms in series would be required to obtain the required dispersion.

A concept incorporating these prisms is illustrated on the facing page. It could be constructed from semi-flat fresnel prisms with a prism angle of 60 deg. Each would be expected to have a total transmission efficiency approaching 85 percent. Thus, the total optical efficiency expected of a system of this type would be about 43 percent -- a not very attractive figure.

If the number of spectral images required is reduced by changing the baseline to consist of only two or three spectral intervals, a single prism might suffice, thus raising the expected transmission efficiency to upwards of 80 percent. However, there would be some sacrifice of solar cell efficiency due to the smaller number of spectral intervals. Such a combination was not analyzed in this report, but deserves serious thought due to its inherent simplicity.

# Spectrum Splitting by Prisms



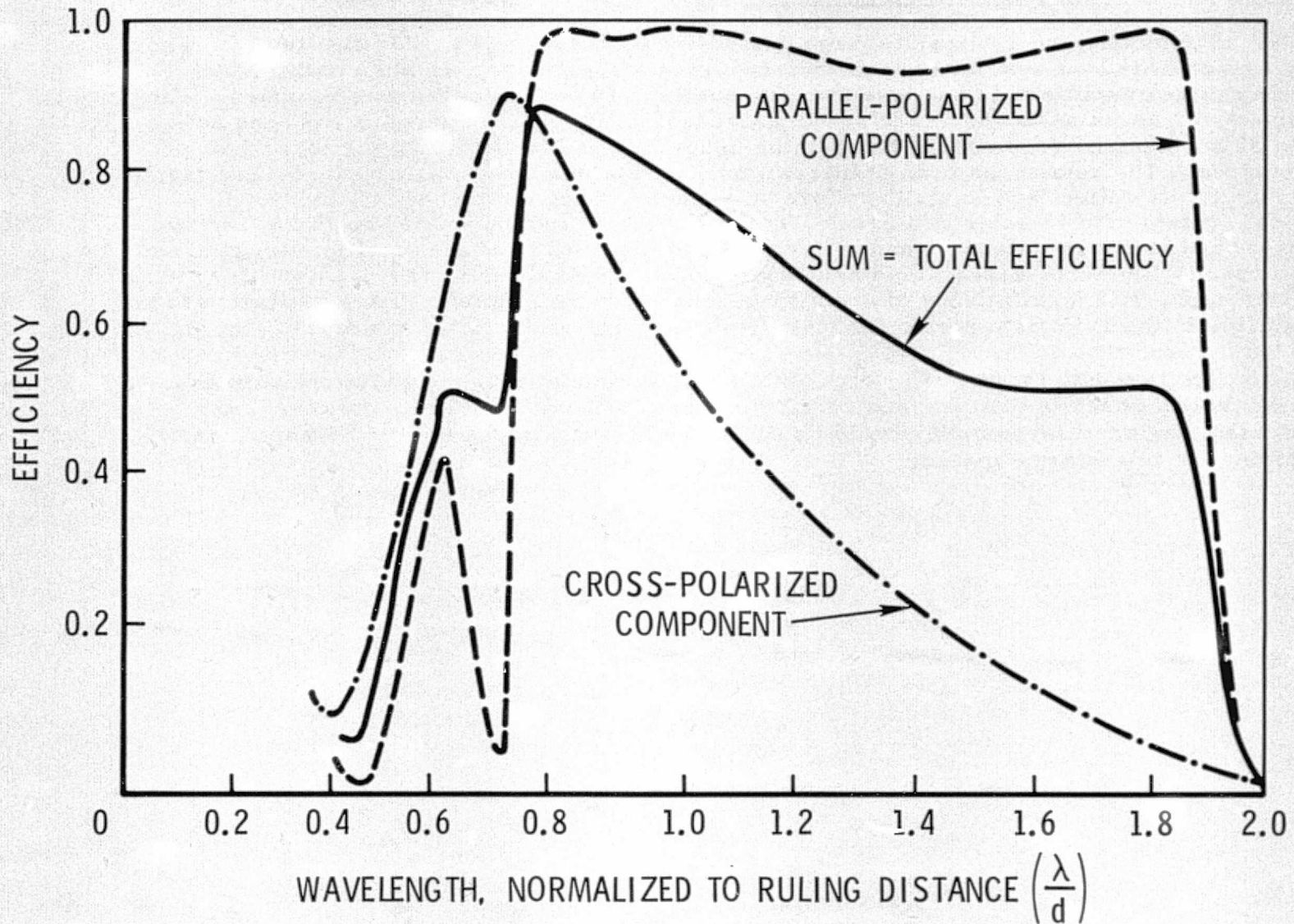
#### EFFICIENCY OF GRATINGS - H-1510

Reflection gratings were investigated as potentially attractive means to obtain large dispersion angles with a single component. Blazed gratings were considered, with the blaze angle chosen for maximum efficiency over the broadest range of wavelengths. The typical best efficiency of such reflection gratings is shown on the facing page.

The efficiency is seen to be quite high, exceeding 90 percent for a range of wavelengths of 0.9-1.8 normalized to the ruling distance. This would probably be adequate for a 10-cell type system. However, this efficiency only applies to the parallel-polarized component while the cross-polarized component is seen to have a very poor efficiency over any except a fairly narrow range of wavelengths, from 0.8-0.9 of the ruling distance. Since sunlight is unpolarized, 50 percent of its energy would be expected to appear in each of these two components, the total efficiency of the grating being the sum of the efficiencies for both of the components. Such a curve is shown on the facing page. The efficiency is seen to be high only over a fairly narrow range of wavelength to ruling distance ratios of 0.8-1.2 or so. The efficiency of a transmission grating would be expected to be equivalent if not slightly lower.

Thus, it is concluded that gratings do not appear to be the most promising candidates for the spectrum splitter function. This conclusion could be reversed upon consideration of the energy distribution in sunlight, which roughly matches the sum efficiency curve, with the likely result that total system efficiency could be fairly high. This requires further study.

# Efficiency of a Blazed Reflection Grating



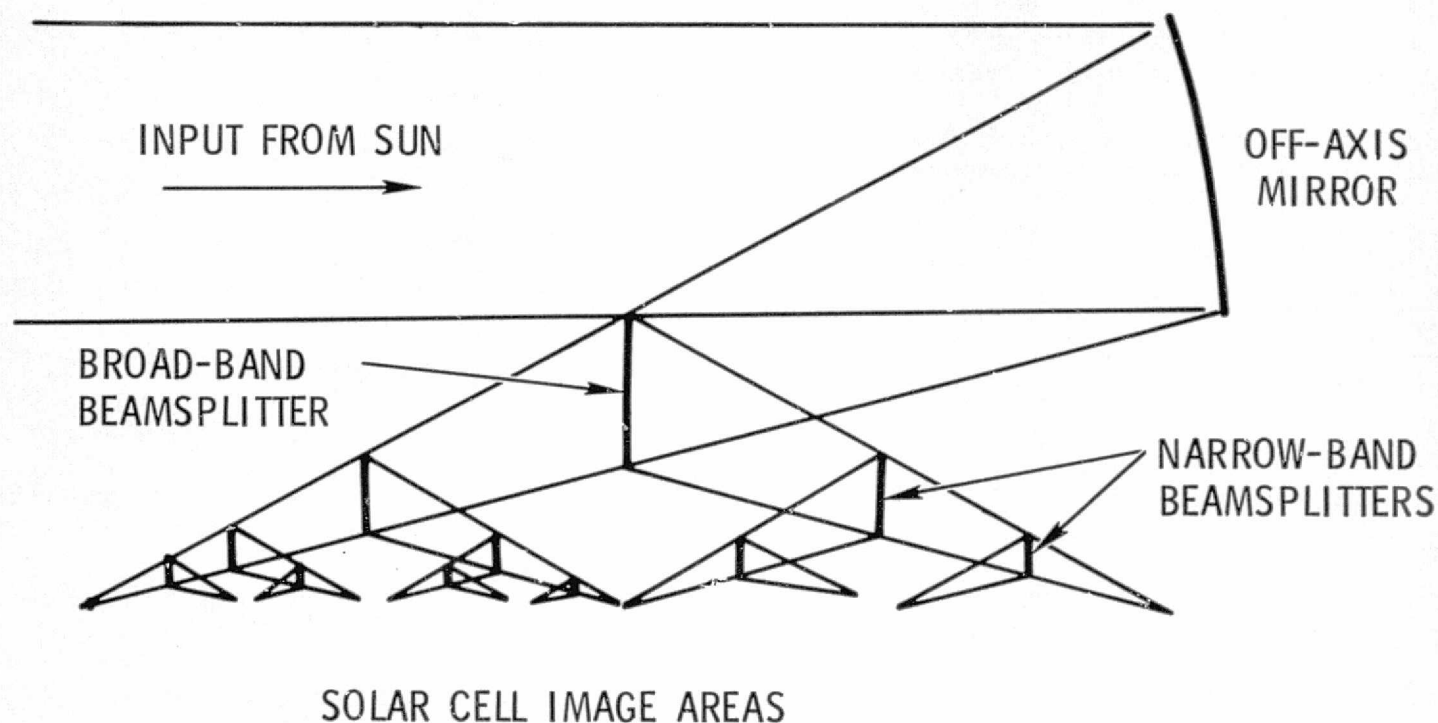
DICHROIC MIRROR BEAMSPLITTERS - H-0482

In principle, an arbitrarily large number of spectrally split solar cell image areas could be created by a system such as pictured on the facing page. In this concept, the number of beamsplitters is one less than the number of spectral cell areas required. They could be so chosen as to require only one broadband beamsplitter operating over the entire band of wavelengths required, reflecting the upper half and transmitting the lower half or vice versa. The rest of the beamsplitters would have a much narrower band of wavelengths to transmit or reflect and would therefore be expected to have a higher efficiency. In a typical system with 12 solar cell areas, four cell areas would have one broadband and two narrowband splitters in tandem each, and would be expected to attain an efficiency of about 80 percent. Eight cell areas would have one broadband and three narrowband splitters in tandem each, with an efficiency of about 77 percent. These efficiencies are estimated to be attainable in the 1985 time period for multilayer coatings on thin film substrate.

Note that with the use of a long focal length system at  $f/4$ , the geometry of such a system becomes fairly long and subject to vibration or heavy structure. However, the equivalent beamsplitter complex could be utilized with a compound optical concentrator, reducing the image area spread.

ORIGINAL PAGE IS  
OF POOR QUALITY

# Dichroic Mirror Beamsplitters



## EFFICIENCY

- BROADBAND BEAMSPLITTER  $\approx 0.87$
- NARROWBAND BEAMSPLITTERS  $\approx 0.96$  EACH
- 4 CELL AREAS HAVE 1 BB AND 2 NB SPLITTERS = 0.80
- 8 CELL AREAS HAVE 1 BB AND 3 NB SPLITTERS = 0.77

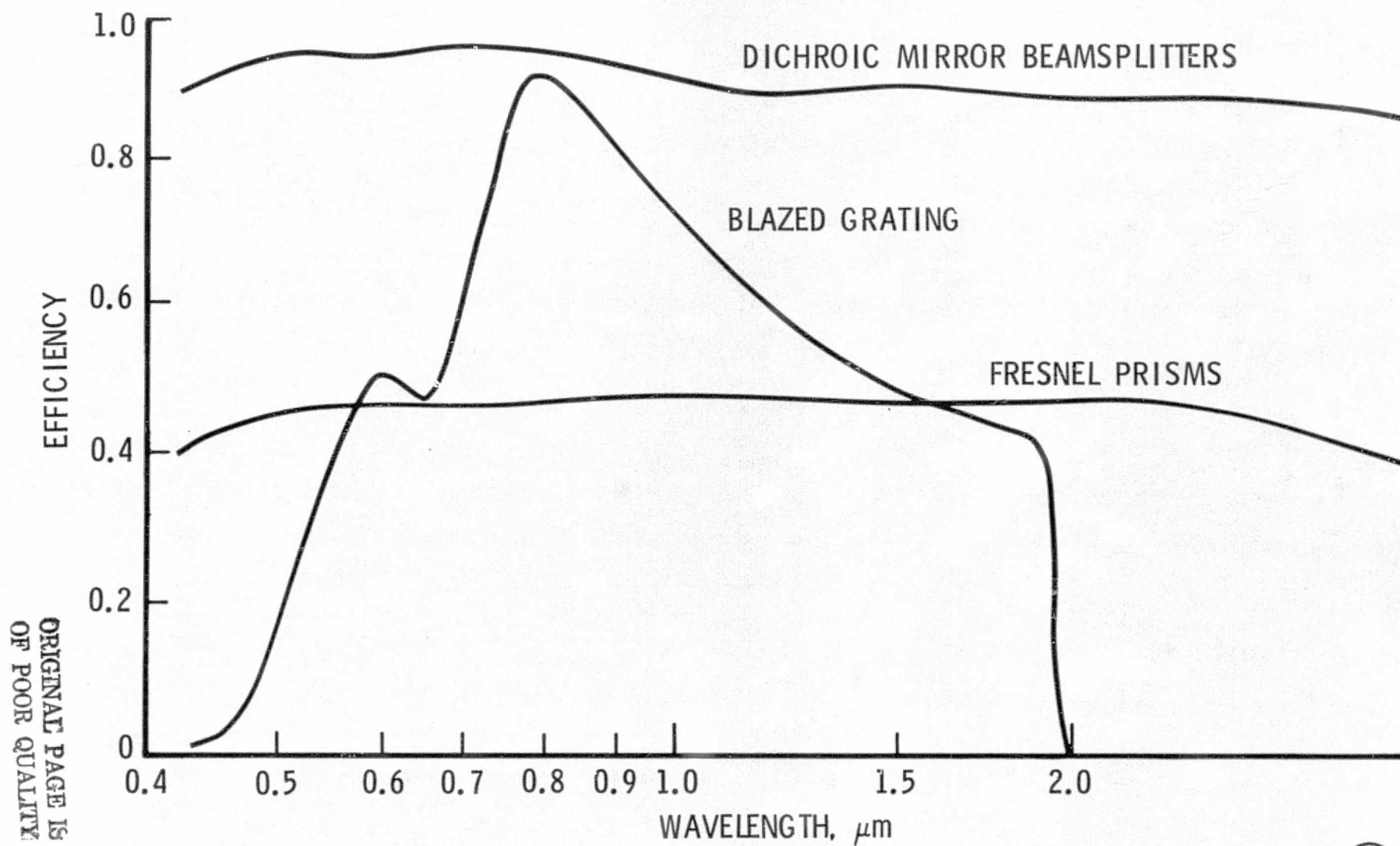


COMPARATIVE EFFICIENCY OF SPECTRUM SPLITTING TECHNIQUES - H-0483

The three major options considered for spectrum splitting are compared on the graph on the facing page. The efficiency of the dichroic mirror beamsplitters is seen to be greatly superior to that of the gratings or Fresnel prisms over the broad wavelength range of interest, and of the three techniques, appears to be the only one that might be acceptable for this application. Upon further study, this conclusion could be changed, but is probably adequate for the purposes of this preliminary investigation.



# Comparative Efficiency of Spectrum Splitting Techniques



AEROSPACE FORM NO. 4650-2

ORIGINAL PAGE IS  
OF POOR QUALITY

PRECEDING PAGE BLANK NOT FILMED

SECTION 3.3

THERMAL CONTROL

All solar cell systems require a means for radiating away the waste heat represented by that fraction of incident energy not reflected or converted to electricity by the solar cells. In a conventional planar array, the mounting plate itself provides that function, since the cells and the substrate are maintained roughly at room temperature in thermal equilibrium by radiation from the cells and the mounting plate, the temperature being determined by the emissivities, absorptivities, and reflectivities of the surfaces.

When a concentrated solar cell system is used, the same backing plate area could be utilized as a radiator, with the thermal flux being spread over the same area by conduction from the smaller cell areas, providing the same weight can be tolerated. However, in order to be competitive the concentrated system must have a smaller radiator area in order to weigh less, thus allowing for optics and other structural components not present in a planar array. A smaller weight radiator can probably result if a surface is optically coated, shaped, oriented, and made smaller than the area required for a conventional solar cell array. The heat generated in the concentrated solar cell areas must be conducted or otherwise transported to this smaller sized radiator to maintain them at their design temperature. One attractive method for doing this is to transport the heat via heat pipes, gaining flexibility in shape and orientation while minimizing the required radiator area due to the very small thermal drop in the heat pipes themselves. An alternative is to use a lighter weight radiator than possible with a flat plate. Though none currently exist, one highly promising advanced concept utilizing transport of small spheres will be discussed later.

The following several pages discuss design aspects of thermal control.

PRECEDING PAGE BLANK NOT FILLED

## RADIATOR AREA REQUIRED - H-0484

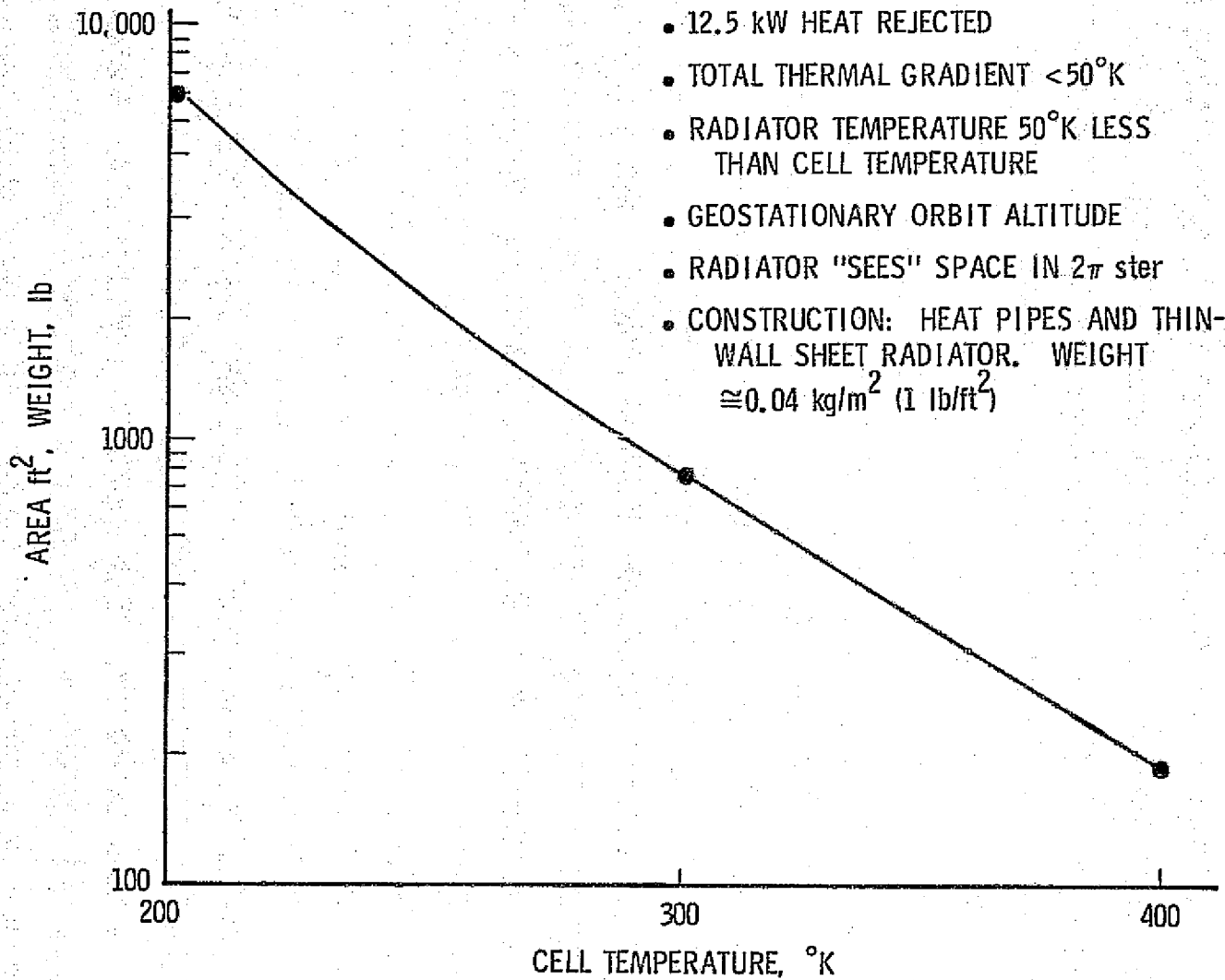
A calculation was performed to determine the required radiator area for a baseline design as a function of the solar cell temperature to be maintained. The baseline conditions were assumed to be 50 percent efficient solar cells and a 12.5 kW electrical output, thus requiring 12.5 kW of heat to be rejected. It was calculated that a total thermal gradient of at most 50°K would result between the cells and the extreme radiator components, based on design features to be discussed in the next chart. A further constraint was the assumption of operation in geostationary orbit, thus effectively removing radiation from the earth as a significant factor in radiator design,

For the above conditions, the radiator area shown on the curve of the facing page is seen to be 200 sq ft to maintain the cells at 400°K, 800 sq ft for 300°K, and 6000 sq ft for 200°K. Some of the important assumptions are indicated. In addition, no radiation was assumed from the cell covers, a radiator surface emissivity of 1 was assumed, and a fin effectiveness of 0.8. Since the typical construction of a sheet radiator fed by heat pipes results in a weight in the order of 1 lb/ft<sup>2</sup>, the above numbers also represent the approximate weight in pounds to be expected. It is seen that the radiator weight becomes very large for temperatures much below 400°K, and in order for the entire power system to weigh less than the SEPS array (400 lb), the radiator weight should probably not exceed half that, or less than 200 lb. Thus, it is seen that the cells will probably have to be operated at 400°K. This represents the baseline design.

It is clear that should the radiator cost or weight be lowered, that the cell temperature could drop, increasing efficiency. Such a trade study should be performed.

ORIGINAL PAGE IS  
OF POOR QUALITY

# Radiator Area Required



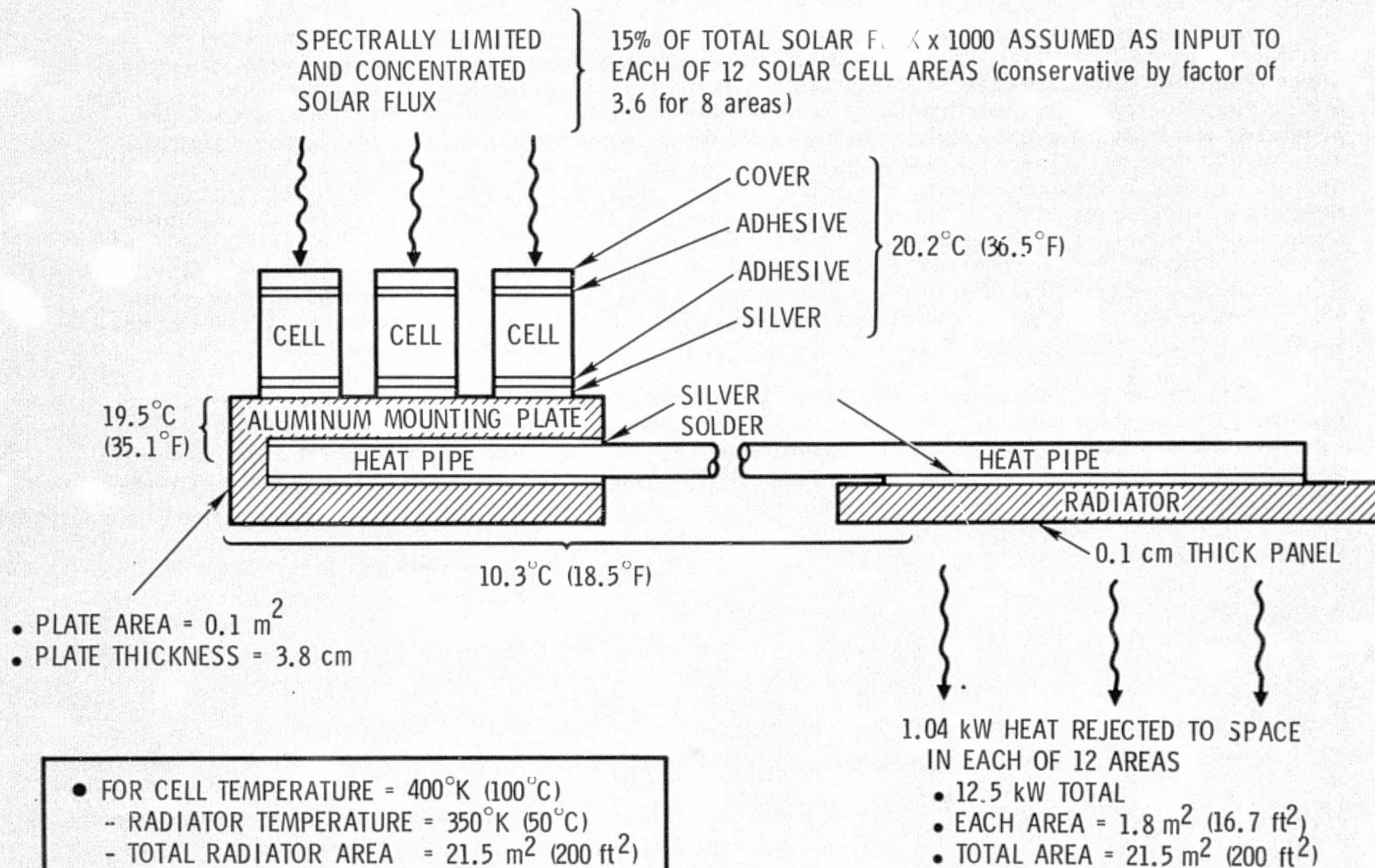
## DESIGN OF THERMAL CONTROL SYSTEM - H-0485

A design was performed for the thermal control system and modeled as the diagram on the facing page. The cells were assumed to contain cover glass for radiation shielding and to be directly bonded or soldered to an aluminum mounting plate. The plate itself would transfer its heat to the hot end of the heat pipes which would conduct it to the radiator surface, assumed to be a 1 mm thick panel of coated stainless steel. The baseline concept assumed 12 solar cell areas, each of which received 15 percent of the total solar flux concentrated by a factor of 1000. This is conservative by a factor of 3.6 for 8 of the 12 solar cell areas and by a factor of 1.8 overall.

The total temperature drop calculated for the solar cells was about 20°C with another 20 deg being allocated for the gradient between the bottom of the cells and the hot end of the heat pipe. Another 10°C was calculated to be the total thermal drop from the hot end of the heat pipes to the furthestmost corner of the radiator panel. The radiator itself was taken to be the 200-sq ft radiator resulting in a cell temperature of 400°K (and a radiator temperature of 350°K) under a flux of 12.5 thermal kW.

This is a fairly conventional design for a thermal control system. It may well be possible to reduce the weight by less conservative sizing and by more careful matching of radiator portions to solar cell areas, taking into account actual spectral energy distribution and cell efficiencies. Such studies should be performed.

# Thermal Control System



ORIGINAL PAGE IS  
OF POOR QUALITY

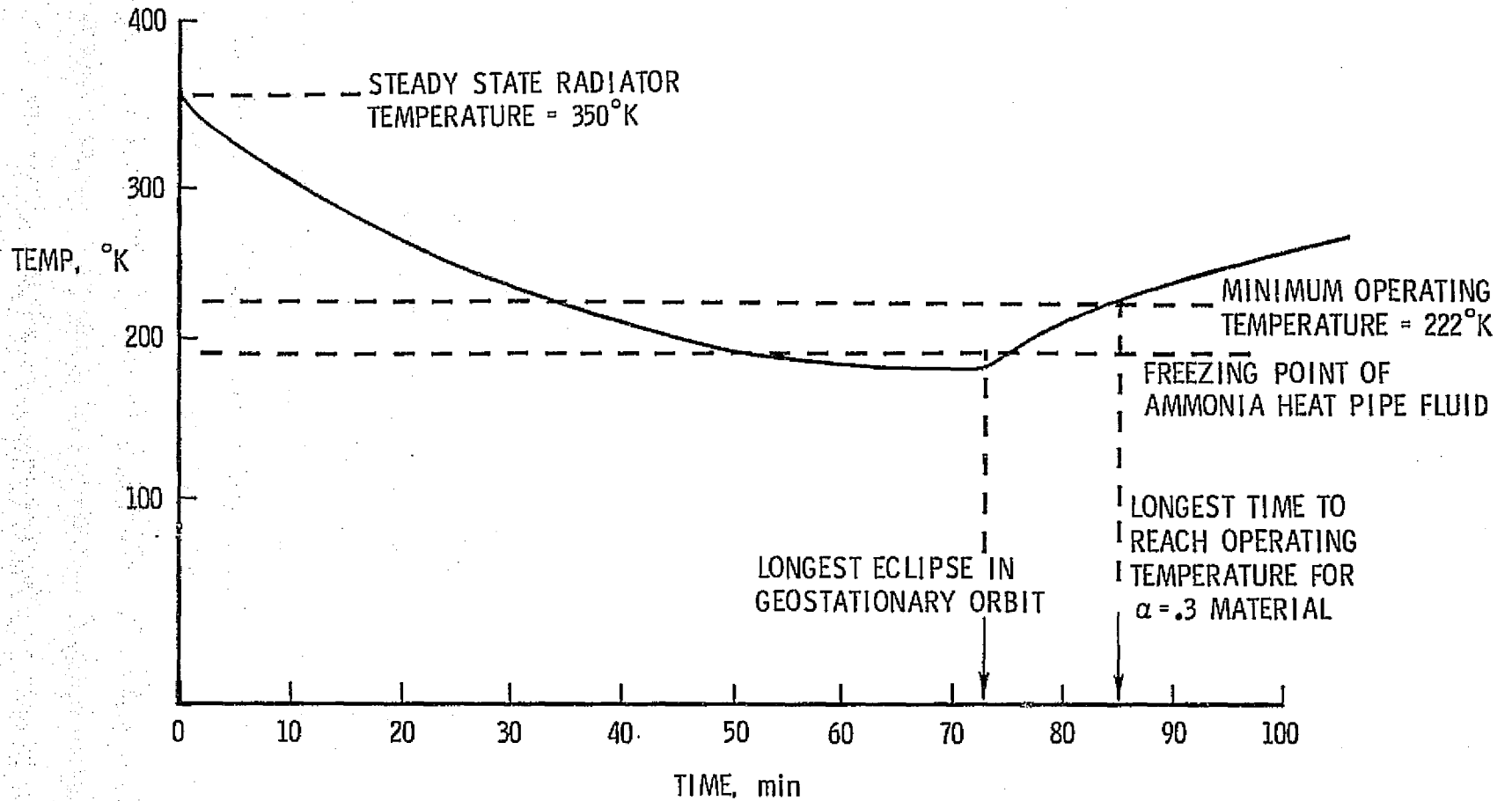
## RADIATOR TEMPERATURE IN ECLIPSE - H-0486

The thermal control system discussed is straightforward and would be expected to operate with no difficulties while sun-illuminated. When the system enters eclipse, however, there could be freezing of the heat-pipe working fluid. As seen from the curve on the facing page, eclipses in geostationary orbit do not exceed 72-min duration. During that time however, the heat pipe fluid temperature would drop below the freezing point of the ammonia assumed for the baseline design heat pipes. When the satellite comes out of eclipse, the normal heat input from the sun to the solar cells would warm up the fluid to the operating temperature of about 220°K in about 11 min, assuming an absorptivity of 0.3 for the radiator material. Thus, the time spent in eclipse would have to be followed by a reorientation of the power system so that the thermal input from the sun is absorbed uniformly in the heat pipes, and the fluid is warmed to the required operating temperature. A second reorientation would then resume the sun tracking of the optics after the fluid had reached operating temperature.

Electrical output would be available 85 min following the beginning of the eclipse, thus resulting in a requirement for only about 13 lb of battery, assuming nickel-hydrogen batteries. An alternative would be to use other heat-pipe working fluids, and other options which should be explored further. It is concluded that the operation of a radiator/heat pipe system of this type appears thoroughly practical.



# Radiator Temperature in Eclipse



## DUST RADIATOR CONCEPT - H-1352

A novel radiator concept was disclosed to the author late in the study by Mr. John Hedgepeth of the Astro- Research Corporation. In their concept, the weight of the radiator per unit watt of heat radiated would be dramatically reduced compared to heat pipe and sheet metal radiators by taking advantage of the fact that spherical particles have a surface-area-to-mass ratio increasing in inverse proportion to the decrease of their diameter. Thus, if a stream of very small spherical particles were to be ejected into space after being heated by the solar cells, they would radiate away their heat to space much more efficiently per unit mass than would an equivalent heat pipe/plate radiator. Upon reaching the desired particle temperature, the stream would be caught, its direction reversed, and pitched back to be caught again and passed over the solar cell back plates, where they would be heated again. A number of different configurations of such a concept are possible. One of the more obvious ones is shown on the facing page together with estimates on its key parameters.

The analysis performed by Astro-Research to date predicts the behavior of the dust particles themselves (in this case small particles of steel) but no work has been done in sizing or designing the catching, turnaround, and pitching equipment. Its size is being estimated by Astro-Research at 300 kg/m<sup>2</sup> of equipment, which appears conservative, it being typical of heavy machinery. Likewise, no design work has proceeded on the mechanism for transfer of heat from the solar cells to the dust stream itself. In principle, a number of apparently simple techniques could probably be made to operate. The solar cells could be bonded to a long hollow honeycomb plate through which the dust stream could be blown, multiple bounces of the spherical particles against the walls serving to heat them up. Pitching could be mechanical with some form of a centrifugal fan. Radial velocities of the dust particles could be removed by linearizing the flow through a series of exit pipes, the catcher and pitcher equipments similarly mechanized. The catcher tube diameter could be larger than the exit diameter of the pitcher tube to allow for some stream dispersion and avoid significant loss of material.

Parameters estimated from scaling relationships in the Astro-Research document<sup>(11)</sup> predict a total radiator weight including heat transfer, pitcher and catcher equipment, and the mass of the dust at 14 kg for a 12.5 kW power module, scaling linearly with power.

ORIGINAL PAGE IS  
OF POOR QUALITY

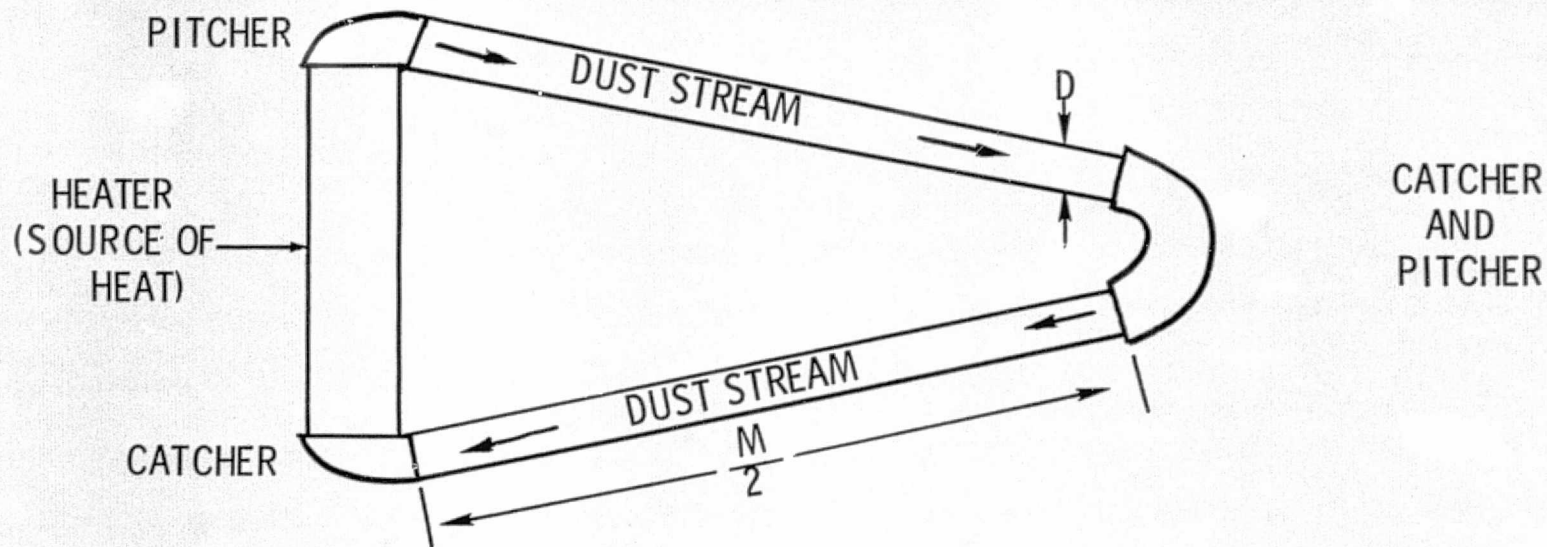
PRECEDING PAGE BLANK NOT FILMED

This is a factor of 6.5 less than the 200 lb for a heat pipe and sheet metal radiator as incorporated in the baseline design, and could make an enormous difference to the advantage of the high efficiency concept. However, due to the very early state of understanding of such a radiator concept, it was not incorporated in the baseline design. It is incorporated as an option in the evaluation portion of this study.

Advanced concepts for radiators, including the transported dust concept, should be studied in depth to determine their potential, as it makes little sense to burden a new and lighter weight collector/solar cell system of great efficiency with a conventional radiator, which severely limits its potential.

## DUST RADIATOR CONCEPT

DISCLOSED BY ASTRO-RESEARCH CORPORATION



ESTIMATED PARAMETERS\*

POWER	STREAM LENGTH, M	STREAM DIAMETER, D	PARTICLE DIAMETER, d	TOTAL WEIGHT, kg
12.5 kW	10	0.03	$2.5 \times 10^{-5}$	14
125.0 kW	40	0.13	$4 \times 10^{-5}$	140
1.25 MW	100	0.33	$1.2 \times 10^{-4}$	1400

\* HEAT SOURCE AT  $350^{\circ}\text{k}$

SECTION 3.4

BASELINE CONCEPT

PRECEDING PAGE BLANK NOT EXAMED

In order to evaluate the performance potential of this new concept, a baseline design was made for a system to supply 12.5 kW of electrical power. This was in order to allow ready comparison with an advanced solar array produced for NASA by Lockheed as an advanced development item intended for the Solar Electric Propulsion Stage.

The definition of the baseline concept was made without benefit of any rigorous optimization process due to the severe funding limits of this contract. Rather an intuitive definition process was followed based on the subsystem parametric characteristics data presented, in the hope that the design point would not be too far off the optimum while still comparing well with the conventional array. The baseline concept selected utilizes 12 spectral intervals, a concentration ratio of 1000/1, lightweight thin-film optics, solar cell temperature of 400°K, and a heat pipe/sheet metal radiator. Considerations on more optimum design points will be discussed presently.

The characteristics and performance of this baseline concept are evaluated and compared with the advanced conventional array in this section.

PRECEDING PAGE BLANK NOT FILMED

ORIGINAL PAGE IS  
OF POOR QUALITY

## SYSTEM EFFICIENCY - H-0505

The overall system efficiency is derived on the facing page in order to define the optical sizes and perform a point design of the baseline. It is seen that even though the baseline solar cell system obtains an efficiency of 48 percent, the optical components in the baseline system probably only attain an efficiency of 48 percent in themselves, thus reducing the overall system efficiency to 23 percent.

The low efficiency of the optics is due in part to the selection of the compound optical system to make a shorter package, with its implications of multiple surface reflections and obscuration; and the selection of a 12-cell type system which results in beam splitting efficiency of 78 percent. However, the implications of the low efficiency of the optical components are not as severe as would appear on first inspection inasmuch as this efficiency does not contribute to the required capacity of the heat radiator, nor does it significantly contribute to the weight of the system inasmuch as the optics are very lightweight. Thus, a factor of 1.44 increase in the diameter of the optics would compensate for the optical system inefficiencies compared to lossless optics, resulting in a weight increase of only 18 lb in the optics -- a good trade-off.

UNCLASSIFIED  
SYSTEM EFFICIENCY

OPTICAL COMPONENTS

●	<u>PRIMARY OPTICS</u>		
-	REFLECTIVE COATING.....	0.97	
-	SURFACE REFLECTIONS .....	0.87	
●	<u>SECONDARY OPTICS</u>		
-	REFLECTIVE COATING.....	0.97	
●	<u>OBSCURATION FACTOR</u> .....	0.75	
●	<u>BROAD BAND BEAM SPLITTER</u> .....	0.87	
●	<u>NARROW BAND BEAM SPLITTER</u>		
-	4 GROUPS OF 2 SPLITTERS, EACH @ 0.96, 0.4-1.2 $\mu$ m, CARRYING 50% OF ENERGY .....	0.92	} 0.9 AVG
-	8 GROUPS OF 3 SPLITTERS, EACH @ 0.96 1.2-2.5 $\mu$ m, CARRYING 50% OF ENERGY .....	0.88	
		<hr/>	
		0.48	

SOLAR CELLS

●	TWELVE CELL SYSTEMS, 1000/1 CONCENTRATION, CELLS @ 400 <sup>0</sup> K .....	0.48
---	--	------

OVERALL EFFICIENCY = 

---

 0.23

ORIGINAL PAGE IS  
OF POOR QUALITY





#### DETERMINATION OF REQUIRED COLLECTOR DIAMETER - H-0504

The sizing of the optical system is performed as illustrated in the table on the facing page. Given a 12.5 kW desired electrical output, the input to the solar cells must be 26 kW due to their 48 percent calculated efficiency. Further, the input to the optics and beamsplitters must be 54.2 kW due to their calculated 48 percent efficiency. Thus, the area of primary collector must be 46 m<sup>2</sup>, and its diameter 7.7 m.

The 7.7-m diameter does not fit into the Space Shuttle in a deployed configuration and thus some means of folding and deploying the mirror system is required -- such means is discussed in the forthcoming pages.

UNCLASSIFIED

DETERMINATION OF REQUIRED COLLECTOR DIAMETER

OUTPUT	=	12.5 kW <sub>e</sub>
INPUT TO CELLS (@ 48 PERCENT EFFICIENCY)	=	26 kW
INPUT TO OPTICS AND BEAM SPLITTERS (@ 48 PERCENT EFFICIENCY)	=	54.2 kW
AREA OF PRIMARY (SOLAR CONSTANT = 126 W/ft <sup>2</sup> )	=	46 m <sup>2</sup> (430 ft <sup>2</sup> )
PRIMARY DIAMETER	=	7.7 m (23.4 ft)

UNCLASSIFIED

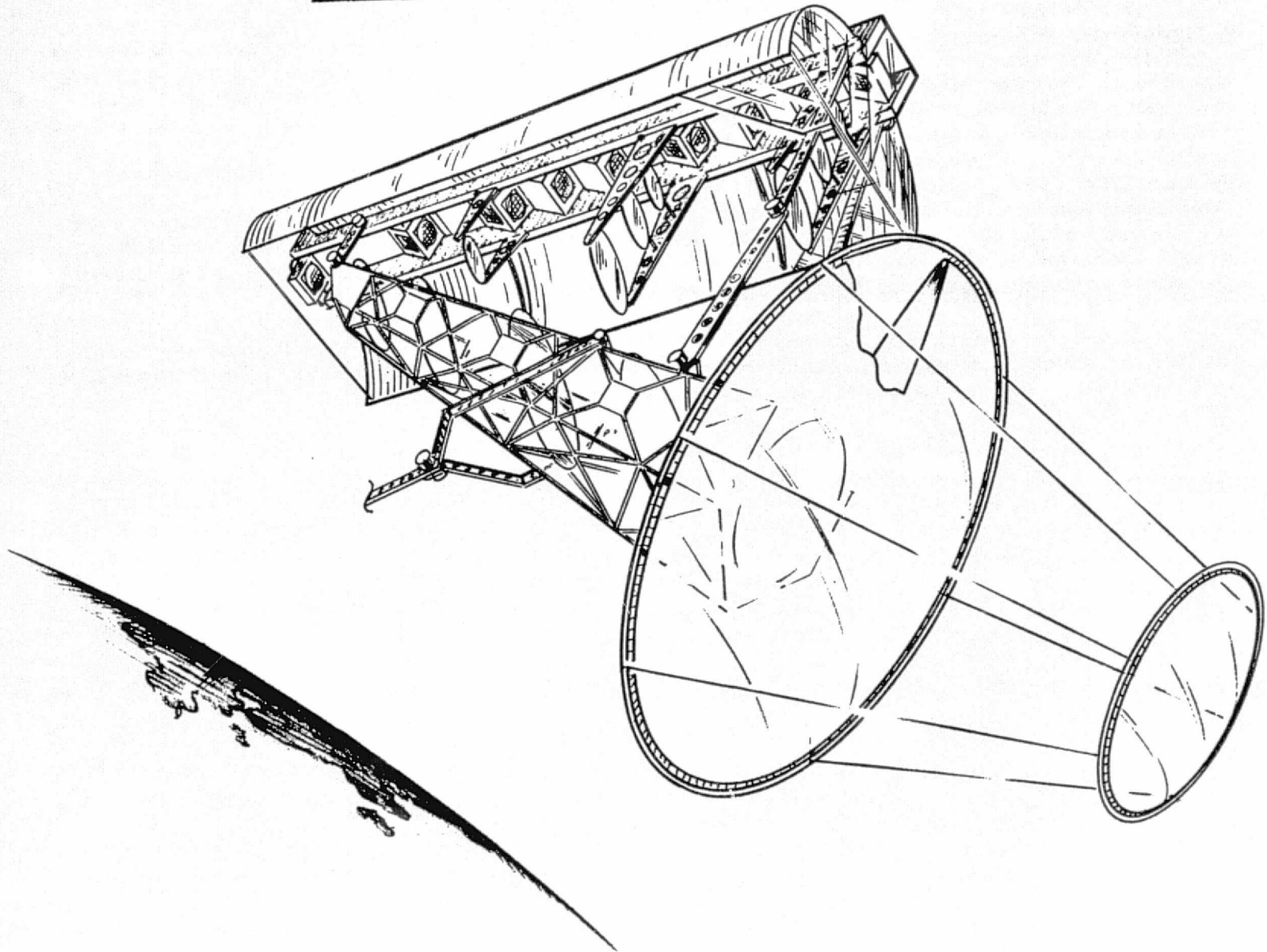


CONCEPTUAL DESIGN - H-2224

Many designs are feasible. One possible conceptual design for the high efficiency solar power system was made with the results illustrated on the facing page. The system is seen to consist of a compound collector system, followed by a series of flat beam-splitters, focusing the light on 12 areas of solar cells on a strongback structure, and a semi-circular radiator for rejecting the waste heat. The entire assembly might have to be gimbaled for decoupling from the spacecraft which would use its output power. Such a gimbal is shown on the main truss. Should the spacecraft itself be sun-pointing such a gimbal will be unnecessary.

Details of the design and some discussion follow.

CONCEPTUAL DESIGN - HIGH EFFICIENCY  
SOLAR POWER SYSTEM

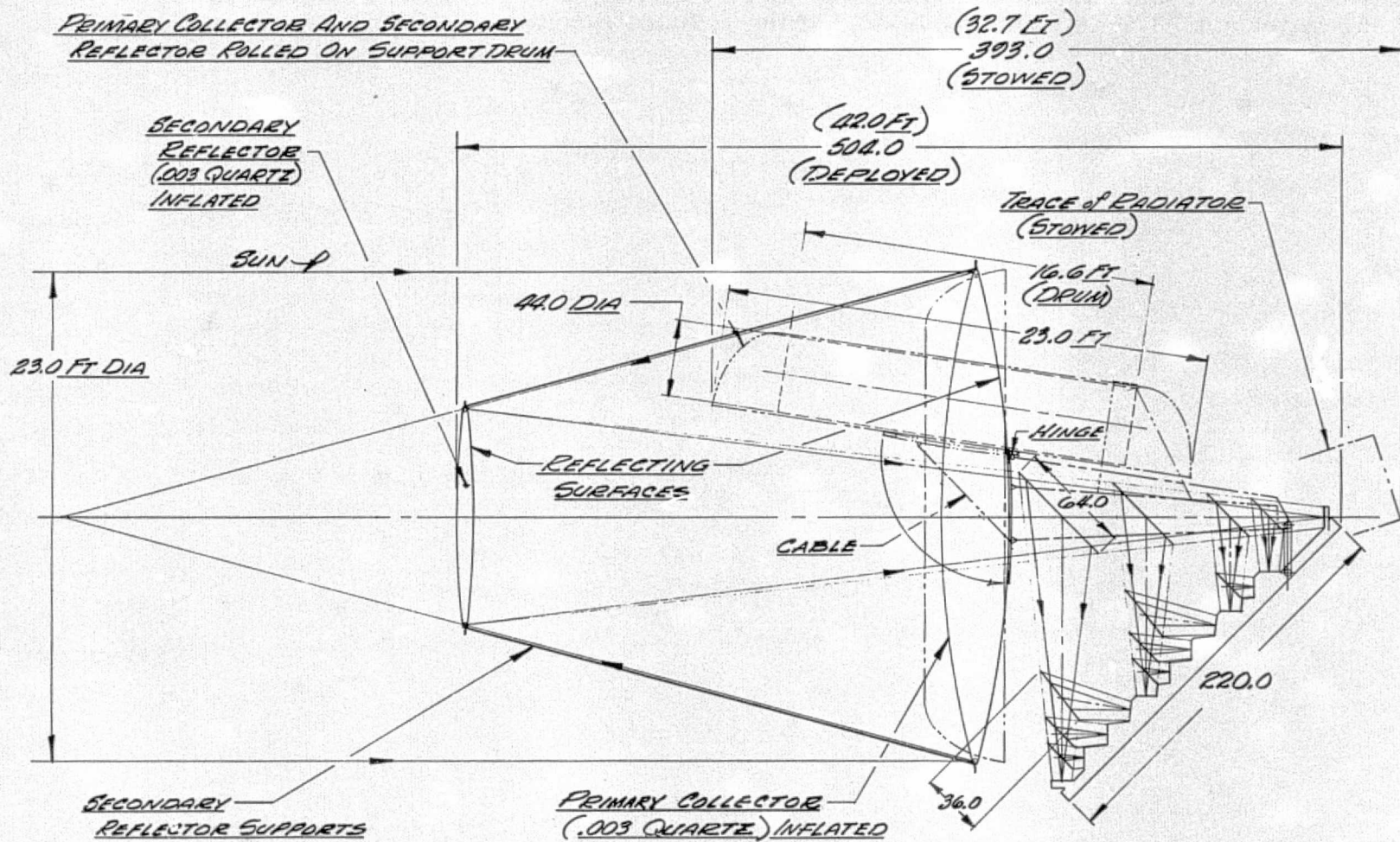


#### LIGHT-PATH DIAGRAM - H-2222

A side view of the system concept is shown with the light path diagram superimposed. A deployment scheme was evolved where the radiator would fold close to the center truss supporting the mirrors, the secondary mirror would be twisted and collapsed onto the primary mirror, and the combination of primary and secondary mirrors rolled onto a support drum, the center of the primary mirror being supported on a hinged ring attached to the central truss. The entire package would then fit readily within the Space Shuttle envelope in a stowed configuration, and would be deployed by releasing the overlapping edges of the rolled up primary mirror. This would allow unrolling of the mirror under its own tension. The free support drum would float away, and drawing on the circular support ring would then rotate the mirrors into position and allow the secondary to deploy using the stored spring tension of the supporting wires. Inflation of the thin-film mirror surfaces would then follow, along with a rigidization operation to prevent micrometeorite damage.

This is certainly not a unique design solution nor is it claimed that it is by any means the best. However, it would probably work, it would fit into the Space Shuttle, and represents a reasonable first cut at a lightweight design solution.

LIGHT PATH DIAGRAM

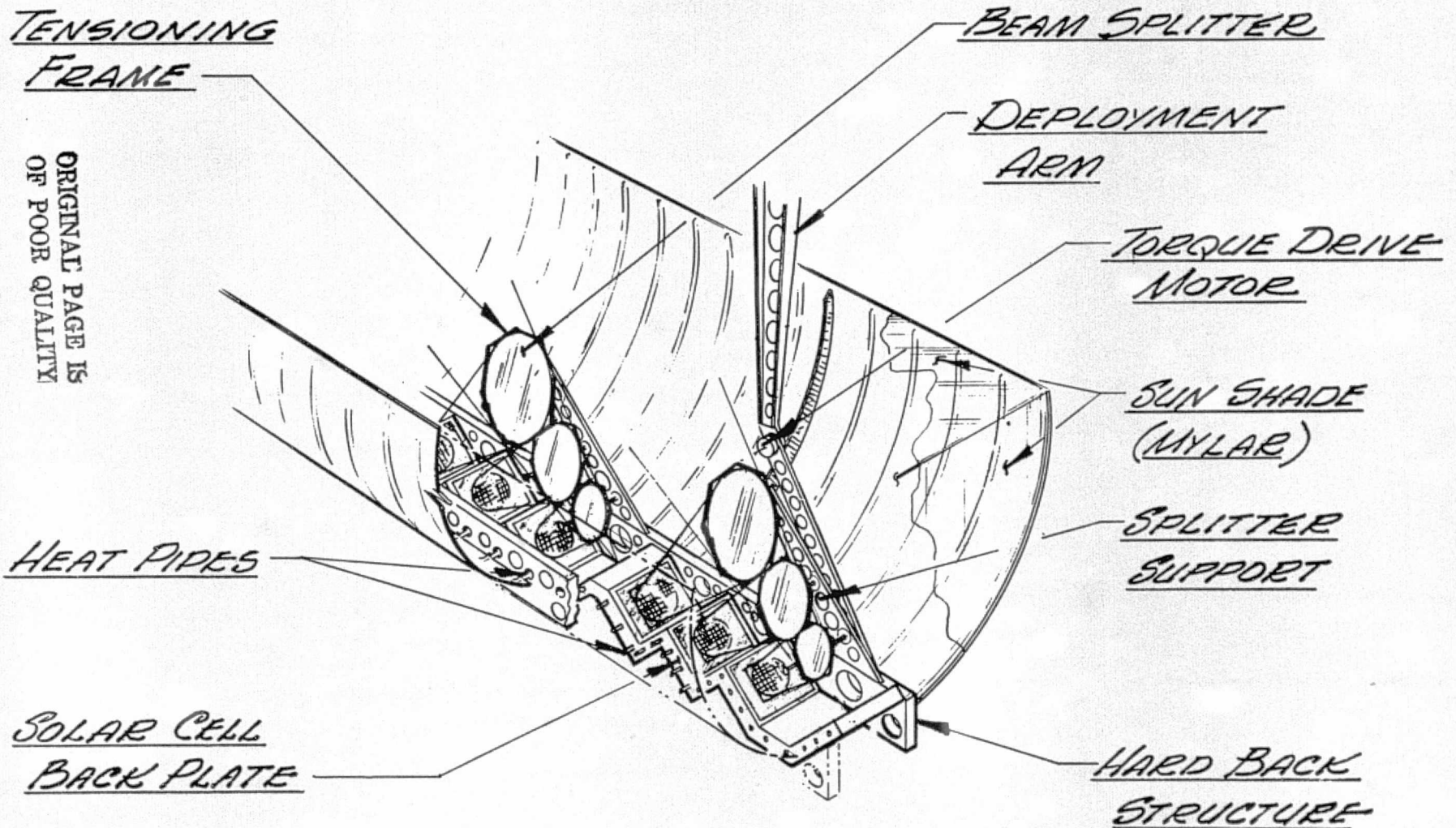


ORIGINAL PAGE IS  
OF POOR QUALITY

DESIGN DETAILS - H-2223

The figure on the facing page shows some of the details of the solar cells, their mounting plate, the deployment and support mechanisms for the beamsplitters, the heat pipe network, and the radiator. The sun shade shown probably will not be required (it was needed when the optical diameter was 15 ft in a previous design iteration. Since the optics are 23-ft diameter, shielding of the radiator is automatic.)

TYPICAL SOLAR CELL, BACK PLATE,  
AND RADIATOR STRUCTURE

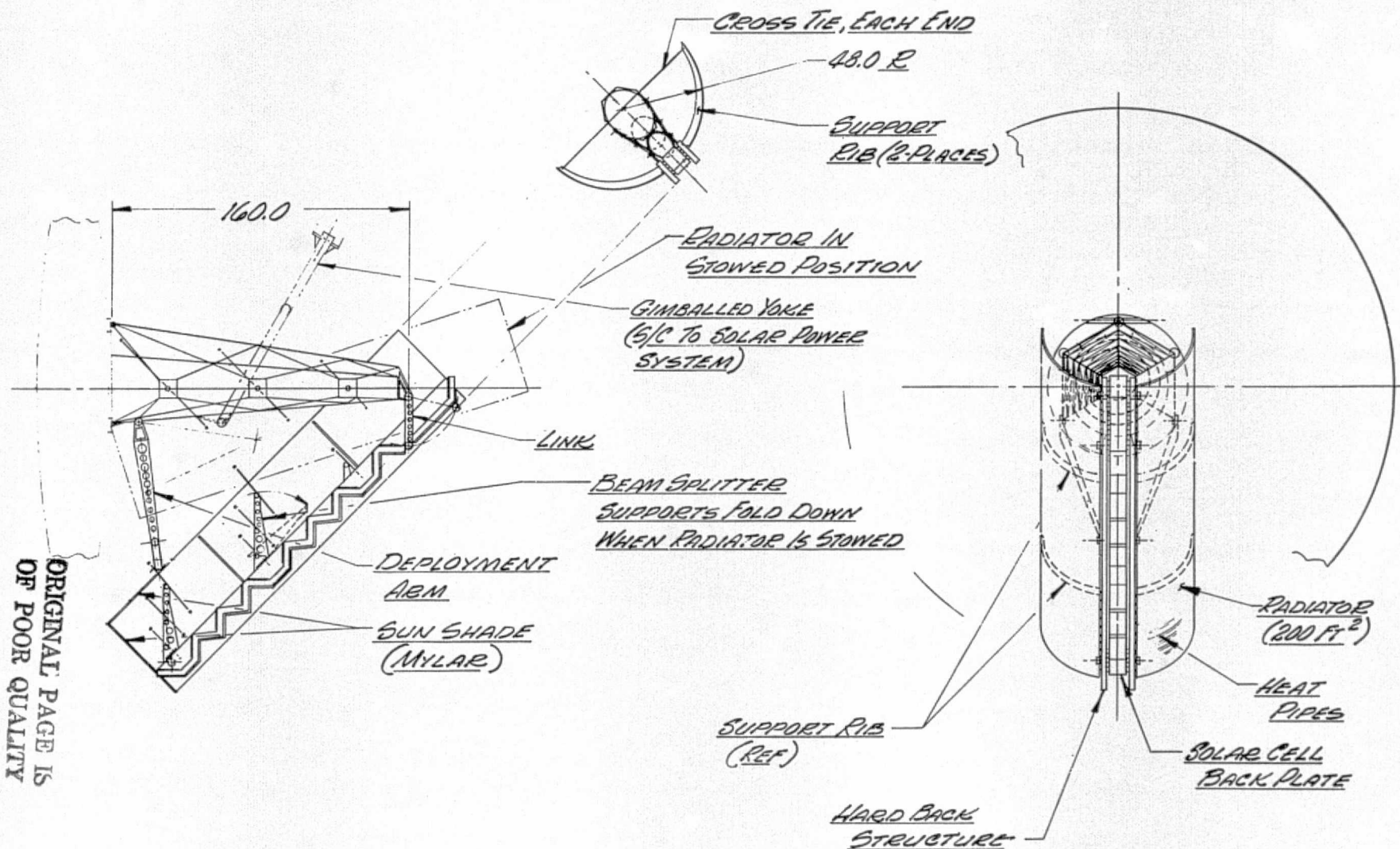




STRUCTURAL DETAILS - H-2225

The diagram on the facing page shows details of the radiator, truss, and deployment mechanisms with a back view, a side view, and an elevation view. The stowed position of the radiator is also indicated. As mentioned previously, this is not a unique design but is rather representative of one that can probably be made to work.

*STRUCTURAL ARRANGEMENT FOR SPLITTER  
AND RADIATOR SUPPORT*

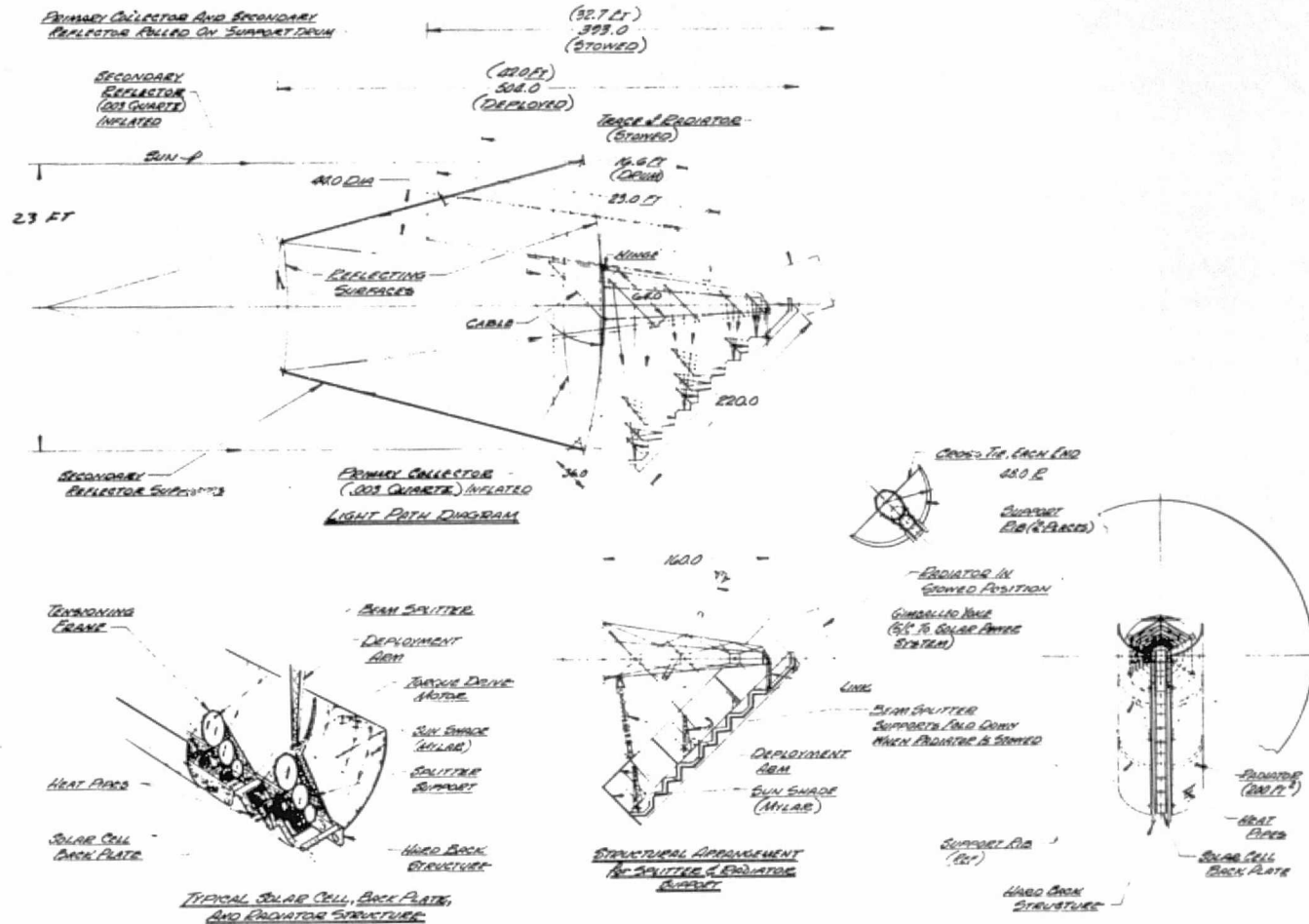


ORIGINAL PAGE IS  
OF POOR QUALITY

COMPOSITE DRAWINGS - H-2226

The figure on the facing page is a composite of the previous design details.

CONCEPTUAL DESIGN - HIGH EFFICIENCY SOLAR POWER SYSTEM



ORIGINAL PAGE IS  
OF POOR QUALITY



## WEIGHT BREAKDOWN - H-1512

The baseline design shown in the last several figures was analyzed for the expected weight breakdown of the individual pieces so that a reasonably confident weight estimate for the system could be generated, and the weights used for a comparative cost estimation.

As shown on the table on the facing page, the concept as designed is expected to weigh approximately 500 lb. Note that almost one half of this is due to the heat radiator, heat pipes, and supporting structure. The total weight of the optical system itself is about 75 lb, and the rest of the weight is in miscellaneous structural, mechanical, gas, gimbal, drive, and solar cell items.

This large weight is somewhat of a disappointment, since the Solar Electric Propulsion Stage power module weighs only about 400 lb for the same electrical output. Therefore, it is unlikely that great cost savings can accrue from this design, inasmuch as costs are very much weight dependent.

WEIGHT BREAKDOWN

<u>ITEM</u>	<u>WEIGHT - LB</u>
PRIMARY REFLECTOR	37
SECONDARY REFLECTOR	9
STOWAGE CYLINDER	16
SECONDARY REFLECTOR POSITIONING ARMS	12
BEAM SPLITTERS AND FRAMES	6
RADIATOR AND HEAT PIPES	200
SOLAR CELL COLD PLATES	40
SOLAR CELLS	11
WIRING	15
TRUSS	15
STRONGBACK STRUCTURE	20
SPLITTER SUPPORTS	5
DEPLOYMENT ARMS AND MECHANISM (RADIATOR SECTION)	18
GAS, GAS BOTTLE AND PLUMBING	8
GIMBAL	25
DRIVE	25
	<hr/>
TOTAL WEIGHT LESS CONTINGENCY	462
CONTINGENCY (10 PERCENT)	46
	<hr/>
TOTAL SUBSYSTEM WEIGHT	508

## AREAS OF POSSIBLE WEIGHT IMPROVEMENT - H-1511

After the design shown on the last several pages was completed, it was recognized that a number of areas represented design choices considerably off optimum. Redesign could therefore be expected to considerably reduce the system weight, which would increase the power per unit weight, and likely decrease the cost. The areas affected and the estimated weight savings are shown in the table on the facing page.

The use of simple rather than compound optics would probably save a total of about 25 lb. The use of a hologram for spectrum splitting rather than separate spectral splitting dichroic mirrors might be feasible, probably saving another 10 lb. A more weight-efficient design attempting to maximize the utility of the structural elements of the radiator and heat pipe to do double duty as the strongback structure could probably save another 30 lb. Less conservative thermal design in the cold plates backing the solar cell areas and use of a probably more realistic smaller thermal drop in the total thermal path would reduce the weight by another estimated 55 lb. The total estimated weight savings would therefore be 120 lb out of 508, resulting in a total system weight of 388 lb.

These weight improvement areas represent low risk design changes, and were utilized in the costing and comparison analyses to follow. A very large additional potential weight saving is possible, but it is much more speculative, involving the replacement of the heat pipes and sheet metal radiator with a radiator utilizing a directed stream of very small dust-like steel particles whose area-to-weight ratio is much greater than that of a sheet metal planar surface. This concept was described earlier (page 71). It is estimated that 180 lb in addition to the 120 identified above can be saved by use of such a radiator, but this number is highly speculative since the radiator concept has not been submitted to even preliminary design at this point. However, with its incorporation in the design, the total system concept weight would be reduced to 208 lb, or about half of the SEPS array.

AREAS OF POSSIBLE IMPROVEMENT

AREA	ESTIMATED WEIGHT SAVINGS
<u>REASONABLE CONFIDENCE</u>	
● USE SIMPLE OPTICS	25 LB
● USE HOLOGRAM SPECTRUM SPLITTER	10 LB
● MORE WEIGHT-EFFICIENT DESIGN	30 LB
● LESS CONSERVATIVE THERMAL GRADIENT BETWEEN CELLS AND RADIATOR (USE 25 <sup>0</sup> K)	55 LB
SUM	120 LB
<u>SPECULATIVE</u>	
● DUST RADIATOR	180 LB
SUM TOTAL	300 LB



### BASELINE CHARACTERISTICS - H-503

The characteristics of the baseline design for the 12.5 kW system concept depicted in the previous pages is summarized on the facing page. The main features of the design are 48 percent solar cell efficiency, use of 12 tailored bandgaps with cells at 400°K, use of 1000/1 concentration ratio, and compound inflatable optics followed by 11 beamsplitters.

Costs were estimated for this system baseline design at \$4.3 M for each recurring unit, \$10.9 M of RDT&E, and an additional \$15-30 M one-time investment in research and technology to bring the industry to the equivalent state of GaAs in 8 other cell materials.

The performance parameters of the system concept as defined are 55 W/kg and \$340 per electrical watt.

## BASELINE CHARACTERISTICS - 12.5 kW<sub>e</sub> SYSTEM

- SOLAR CELL EFFICIENCY = 48 PERCENT
  - 1000/1 CONCENTRATION RATIO
  - 12 BANDGAPS
  - CELLS MAINTAINED  $\leq 400^{\circ}\text{K}$
  - TOTAL CELL AREA =  $0.7 \text{ m}^2$  ( $6.7 \text{ ft}^2$ )
- OPTICS
  - PRIMARY = 7.7 m (23 ft)
  - SECONDARY = 3.8 m (11.5 ft)
  - INFLATABLE QUARTZ FILMS
  - 11 BEAM SPLITTERS, QUARTZ FILM
  - DEPLOYABLE STRUCTURE
- OVERALL TOTAL EFFICIENCY = 23 PERCENT
- GIMBALED AND SUN TRACKING TO  $\pm 0.1$  DEG
- PASSIVE COOLING WITH HEAT PIPES AND RADIATOR
  - $22 \text{ m}^2$  ( $200 \text{ ft}^2$ ) RADIATOR @  $350^{\circ}\text{K}$
- TOTAL WEIGHT = 230 kg (508 lb)
- ESTIMATED COSTS
  - 15-30 M (CELL TECHNOLOGY)
  - R&D = 10.9 M
  - RECURRING = 4.3 M
- PERFORMANCE PARAMETERS
  - 55 W/kg
  - 340 \$/W

PRECEDING PAGE BLANK NOT FILMED

SECTION 4

EVALUATION

The baseline design described in the previous sheets, as well as its modification to include the more speculative dust radiator concept, were compared against the conventional SEPS array. The comparison measures utilized were the W/kg and \$/W of each of the designs being compared. Comparisons were made at 12.5 kW power module size, and also at an order of magnitude larger power to investigate the effects of power scaling. Costs were also compared for two classes of systems: Those designed to operate outside the radiation belts, and those designed to operate for long periods inside the radiation belts.

The study conclusions were then drawn from those comparisons.

PRECEDING PAGE BLANK NOT FILLED

#### NON-RECURRING COSTS - H-1515

The non-recurring costs, exclusive of the special cell R&D required to produce the high efficiency system concept at 12.5 kW, are shown in the table on the facing page together with numbers generated by the same computer program and using the same cost estimating relationships for the Solar Electric Propulsion System power module. As expected, the cell array design and engineering effort for the high efficiency system is very small due to the small cell area, however, the effort for the optics, radiator, and structure is large. The net effect is that of almost equal RDT&E costs for the SEPS-type array and high efficiency concept.

This result was not unexpected since the weight of the SEPS array is 400 lb, and the weight of the high efficiency system is estimated at 388 lb. Note that those costs are for the high confidence design, and do not include the dust radiator. All dollars are in fiscal 78 values. Costs were generated for the SEPS array even though actual numbers exist from the hardware produced by Lockheed, in order to allow a more fair comparison with the predicted costs of the high efficiency array. The numbers predicted for SEPS check reasonably well with actual expenditures, modified for a production contract.

NON-RECURRING COSTS

(FY 78 \$ in Thousands)

	SEPS	HIGH EFFICIENCY
● CELL ARRAY		
- Design/Engineering	2644	200
- Test	442	400
● RADIATOR AND STRUCTURE		
- Design/Engineering	----	1538
- Test	----	733
● OPTICS		
- Design/Engineering	----	375
- Test	----	150
● DRIVE		
- Design/Engineering	714	714
- Test	368	368
HARDWARE SUBTOTAL	4168	4478
● SYSTEM ENGINEERING AND PROGRAM MANAGEMENT		
- Design/Engineering	2351	2431
- Test	308	739
TOTAL	6827	7648
● CONVERT TO 1977 \$	9093	10,186
● FEE	637	713
TOTAL WITH FEE	9730	10,899

RECURRING COSTS - H-1514

The recurring costs for producing a flight unit of either the SEPS-type or high-efficiency type power modules at 12.5 kW power output are shown in the table on the facing page. As expected, the total costs are very comparable. In fact, their difference is probably smaller than the uncertainty in the model used for determining costs and the accuracy of the weight data which comprises its input.

RECURRING COSTS  
(FY 78 \$ in Thousands)

	SEPS	HIGH EFFICIENCY
● CELL ARRAY	883	390
● RADIATOR AND STRUCTURE	---	475
● OPTICS	---	56
● DRIVE	368	368
HARDWARE SUBTOTAL	1251	1289
● SYSTEM ENGINEERING AND PROGRAM MANAGEMENT	525	541
● SUSTAINING ENGINEERING	1351	1220
TOTAL	3127	3050
● CONVERT TO 1977 \$	4158	4056
● FEE	300	290
TOTAL WITH FEE	4458	4346



## POTENTIAL OF CONCEPT - H-1035

The characteristics and performance of the concept were evaluated for applications away from the earth's radiation belts (low altitudes, geostationary orbits, or higher trajectories). The evaluation was made at 12.5 kW and 125 kW in order to take advantage of any efficiencies obtained in scaling with power. The previously identified improvements were used, including simple optics, weight-efficient structure, lower thermal drop, replacing of the cold plates with shaped ends of the heat pipes, use of 3-5 types of new cells, and smaller F/D.

With these improvements, the expected weight is 388 lb, the recurring costs drop to \$3.3 M, the RDT&E costs to \$8.3 M, and the cell technology investment to somewhere between \$6-15M. The resultant performance parameters are therefore likely to be 72 W/kg and 264 \$/W.

The design was scaled to 10 times the power level, and improved cost and performance parameters resulted due to the less than linear scaling of the cost of structural elements as compared to the costs of solar cells (which are roughly linear with cell area), while the weight parameter was essentially unchanged. The cost was predicted to be 173 \$/W, a considerable advantage compared to the 12.5 kW design.

POTENTIAL OF CONCEPT  
HIGH EARTH ORBIT AND PLANETARY APPLICATIONS

@ 12.5 kW

● WITH IMPROVEMENTS IDENTIFIED (SIMPLE OPTICS, WEIGHT-EFFICIENT STRUCTURE, LOWER THERMAL DROP, REPLACING COLD PLATES WITH SHAPED HEAT-PIPE ENDS, 3-5 TYPES OF CELLS, 1000 CONCENTRATION, SMALLER F/D

- WEIGHT  $\approx$  174 kg (388 lb)
- RECURRING COSTS  $\approx$  \$3.3 M
- RDT&E COSTS  $\approx$  \$8.3 M
- CELL TECHNOLOGY INVESTMENT  $\approx$  \$6-15 M
- PERFORMANCE PARAMETERS LIKELY:

72 W/kg  
264 \$/W

@ 125.0 kW

● WITH IMPROVEMENTS ABOVE, ALLOWING FOR LESS STEEP SCALING OF STRUCTURAL ELEMENTS COMPARED TO SOLAR CELLS

- WEIGHT  $\approx$  1770 kg (3900 lb)
- RECURRING COSTS  $\approx$  \$21.7 M
- RDT&E  $\approx$  \$46.9 M
- CELL TECHNOLOGY INVESTMENT  $\approx$  \$10-15 M
- PERFORMANCE PARAMETERS LIKELY:

71 W/kg  
173 \$/W

IMPACT OF USE OF SYSTEM IN THE RADIATION BELTS - H-1036

8-9  
A simplified analysis was performed to evaluate the comparative performance of the SEPS-type array and a high-efficiency concept design in a mission involving long-term immersion in the earth's radiation belts. Such immersion could result from deployment in medium altitude orbits or from use of the power module in conjunction with ion thrusters to perform as an upper stage to transfer satellites from low to geostationary orbit. The model mission used for the comparison utilized a 190-day transfer from 250 nmi altitude, 28-deg orbit to geostationary orbit.

It was determined from previous analyses that the deterioration in SEPS-type solar cells, which use 6 mil cover glass, would exceed 30 percent during such a 190-day mission. The thickness of shield cover glass would have to be increased to almost 1/4 in. to reduce the deterioration to less than 5 percent and would impose a weight penalty of about 3 lb/ft<sup>2</sup> of area, for a total penalty of 3900 lb for a 12.5 kW design nominally weighing only 400 lb. An alternative way of surviving in the presence of the radiation is simply to oversize the array by 25 percent, the amount required to assure that the degradation does not exceed 5 percent upon reaching geostationary orbit. This increase produces a penalty of only 100 lb. Thus, the area increase is the most weight-efficient action for the SEPS-type planar array as compared to shielding with 1/4 in. glass.

A similar analysis was performed for the high-efficiency system concept. Due to the very small area of solar cells compared to the area of the SEPS array for the same power, the solar cells can be shielded, resulting in a negligible weight increase amounting to less than 8 lb out of a 388-lb design at 12.5 kW, or 80 lb out of 3900 lb for the 125.0 kW scaled power system. These results are summarized on the facing page. This is probably one of the most significant differences between the high-efficiency concept and the planar array.

## IMPACT OF USE OF SYSTEM IN RADIATION BELTS

- MISSION: PERFORM AS POWER SOURCE FOR ION THRUSTERS (SEPS-TYPE)
  - 190-DAY TRANSFER FROM 250 NMI, 28-DEG ORBIT TO GEOSTATIONARY ORBIT.
  
- POWER LOSS EXPECTED AS A RESULT OF THE RADIATION EXPOSURE
  - SEPS-TYPE CELLS (0.006 IN. COVER GLASS)  $\geq$  30 PERCENT
  - SHIELDED CELLS (0.24 IN. COVER GLASS)  $<$  5 PERCENT
  - WEIGHT OF SHIELD GLASS  $\approx$  3 LB/FT<sup>2</sup>
  
- WEIGHT INCREASE EXPECTED:
  - SEPS @ 12.5 kW - IF INCREASE AREA BY 25 PERCENT = 100 lb
  - IF SHIELD = 3,900 lb
  
  - SEPS @ 125.0 kW - IF INCREASE AREA BY 25 PERCENT = 1000 lb
  - IF SHIELD = 39,000 lb
  
  - HIGH EFFICIENCY @ 12.5 kW - SHIELD GLASS AND STRUCTURE INCREASE = 8 lb
  
  - HIGH EFFICIENCY @ 125.0 kW - SHIELD GLASS AND STRUCTURE INCREASE = 80 lb

## CONCEPT POTENTIAL IN RADIATION BELTS - H-1037

The potential performance parameters of the high-efficiency concept for long-term operation in the radiation belts are compared in the tables on the facing page with that of a SEPS-type design at 12.5 and 125.0 kW. There is seen to be a considerable advantage in the performance parameters of the high-efficiency concept as compared to a SEPS-type planar array at 12.5 kW - resulting in a performance of 71 W/kg as opposed to 55 W/kg for the SEPS, and 252 \$/W as opposed to 445 \$/W for the SEPS-type design.

Scaling of both of the concepts to 125.0 kW results in about the same ratio of advantage to the high-efficiency concept over that of the SEPS-type array, with lower cost parameters for both owing to the efficiencies of scale. The cost savings represent a 75 percent cost differential in favor of the high-efficiency concept.

The high-efficiency concept parameters apply to a concept using a conventional heat pipe/sheet metal radiator.

POTENTIAL OF CONCEPTLONG-TERM OPERATION IN RADIATION BELTS

(&lt; 5 Percent Power Loss After 190-Day Transfer From 28 Deg, 250 nmi Orbit to GEO)

@ 12.5 kW

● WITH IMPROVEMENTS PREVIOUSLY IDENTIFIED

	HIGH EFFICIENCY	SEPS
- Weight	177 kg	225 kg
- Recurring Costs	\$3.25 M	\$5.6 M
- Performance Parameters	71 W/kg 252 \$/W	55 W/kg 445 \$/W

@ 125.0 kW

● WITH IMPROVEMENTS PREVIOUSLY IDENTIFIED

	HIGH EFFICIENCY	SEPS-TYPE
- Weight	1790 kg	2250 kg
- Recurring Costs	\$21.8 M	\$37.5 M
- Performance Parameters	70 W/kg 177 \$/W	56 W/kg 300 \$/W

## PERFORMANCE COMPARISON - H-1038

An overall performance comparison table is shown on the facing page. The high-efficiency concept is shown both with and without the more speculative dust radiator concept. The performance comparisons are made at 12.5 and 125.0 kW, and for designs intended to operate only outside the radiation belts as well as for long-term transfer vehicle operations inside the radiation belts.

The potential performance of the concept incorporating spectral splitting, high concentration, and a dust radiator is shown to be at least a factor of 3 and as much as a factor of 6 less expensive per watt than a planar array of the SEPS type. The corresponding weight parameters show an increase in the W/kg by a factor of 3 1/2 in favor of the new concept. The advantages appear to increase with increasing power level.

The potential weight and cost savings are so large that the concept certainly deserves immediate further attention.

PERFORMANCE COMPARISON

POWER	APPLICATION	HIGH-EFFICIENCY/ DUST-RADIATOR CONCEPT	HIGH-EFFICIENCY CONVENTIONAL RADIATOR CONCEPT	SEPS-TYPE CONCEPT
12.5 kW	HIGH EARTH ORBIT AND PLANETARY	60 kg 208 W/kg 100 \$/W	174 kg 72 W/kg 264 \$/W	180 kg 70 W/kg 356 \$/W
	LONG-TERM OPERATION IN RADIATION BELTS*	65 kg 192 W/kg 100 \$/W	177 kg 71 W/kg 252 \$/W	225 kg 55 W/kg 445 \$/W
125.0 kW	HIGH EARTH ORBIT AND PLANETARY	600 kg 208 W/kg 51 \$/W	1770 kg 71 W/kg 173 \$/W	1800 kg 70 W/kg 240 \$/W
	LONG-TERM OPERATION IN RADIATION BELTS*	650 kg 192 W/kg 52 \$/W	1790 kg 70 W/kg 177 \$/W	2250 kg 56 W/kg 300 \$/W

\* 190-DAY TRANSFER FROM 28 DEG, 250-NMI ORBIT TO GEOSTATIONARY,  
WHILE OPERATING

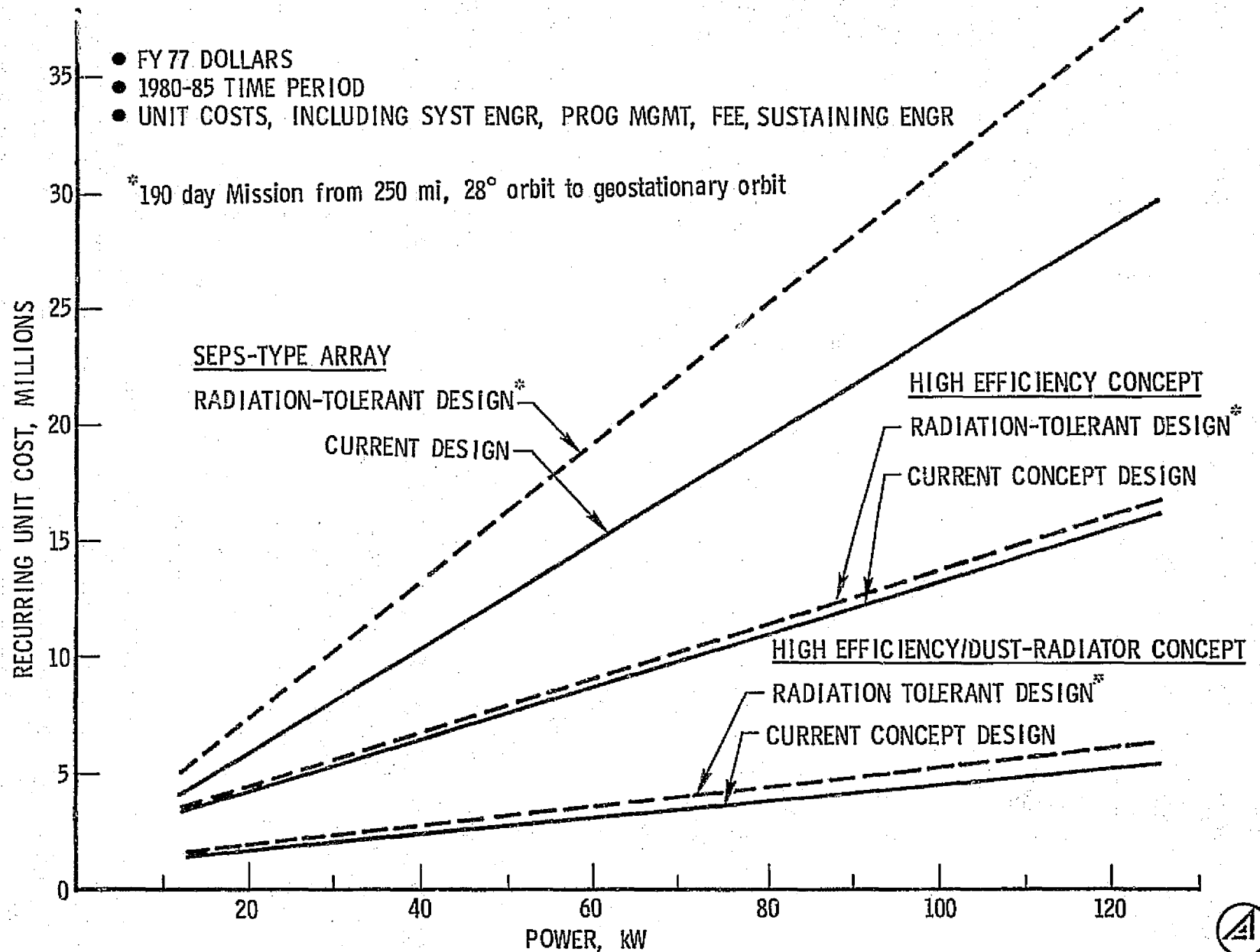


#### COMPARATIVE PROJECTED COSTS - H-1034

The tabular data incorporated in the previous chart was plotted as a function of power level to compare the projected recurring costs of the various design concepts evaluated. The resulting curves show dramatically the advantages of the high-efficiency concept even without resorting to the dust radiator. Even more dramatic are the effects of incorporating the dust radiator concept, which can probably result in a savings sufficient to pay for all of the R&D required for the tailored bandgap solar cells and the radiator in the production of a single power unit at 70 kW of power.

These curves also show the insensitivity to radiation of the concentrated/split concept compared to a planar array. It is to be noted that these curves are shown as continuous straight lines, while only 2 points were calculated for each -- at 12.5 and 125.0 kW. The scaling laws predict the curves to be linear, but this should be verified by several point designs. For that matter, the 125.0 kW points were established by scaling the 12.5 kW design, and should be verified by a separate design study.

# Comparative Projected Costs



SECTION 5

CONCLUSIONS

PRECEDING PAGE BLANK NOT FILLED

A number of significant conclusions may be drawn from the design study and the comparative tables presented in the previous sections. It should be borne in mind that these conclusions and observations are based on numbers obtained from a non-optimum design, and scaled an order of magnitude. Thus, they must be viewed as very preliminary, pending further analysis and design studies.

PRECEDING PAGE BLANK NOT REPRODUCED

## OBSERVATIONS - H-1349

A number of generalized observations were made based on trade-offs that became apparent during the course of the investigation. It appears that the optics weight can be made essentially negligible by the use of thin-film designs. If that is substantiated by further design effort, then all designs will be driven to high concentration to maximize the efficiency and minimize the radiator weight. The use of a few large bandgap, high energy cells would be favored, operated at moderate (350-400°K) temperatures and would both contribute to minimizing radiator weight.

If the radiator weight can be made negligible by incorporation of new concepts such as the dust radiator, the design will be driven to very low temperature cells of a single bandgap, -- such as silicon or GaAs operated at high concentration. This is because high efficiency could be attained without resorting to splitting of the spectrum due to the availability of lightweight radiators. A combination of lightweight optics and lightweight radiator would therefore probably result in a design optimization in which at most a few cell types are used in a highly concentrated system, kept at a low temperature.

All concepts which utilize high concentration will demonstrate very significant weight and cost advantages in missions which must operate for long periods of time in the earth's radiation belts, because of their small solar cell area to be shielded. It is clear that configurations other than the one explored in this short study need to be investigated and a number of parameters and variations studied. Among them is the use of multiple small concentrators rather than one large concentrator; the choice of the optimum concentration ratio; the optimum number of different cell types; the use of concentration in combination with stacked multi-bandgap solar cells which do not need spectral splitting; and design of lightweight rigidized film optics to maintain their optical figure in the presence of micrometeorite damage. It is not clear what shape the optimum concept will take following such design studies. It is clear, however, that such concepts will have very significant advantages over planar arrays.

OBSERVATIONS

- IF OPTICS WEIGHT IS NEGLIGIBLE - DESIGN DRIVEN TO HIGH CONCENTRATION, HIGH EFFICIENCY, LARGE BANDGAP CELLS ONLY AT MODERATE TEMPERATURES, TO MINIMIZE RADIATOR WEIGHT
- IF RADIATOR WEIGHT IS NEGLIGIBLE - DESIGN DRIVEN TO HIGHLY CONCENTRATED SILICON OR Ga As CELL SYSTEM OPERATED AT LOW TEMPERATURE
- ALL LARGE CONCENTRATION RATIOS RESULT IN VERY SIGNIFICANT WEIGHT AND COST ADVANTAGES FOR RADIATION-TOLERANT DESIGNS
- OTHER CONFIGURATIONS NEED TO BE TRADED OFF, INCLUDING
  - MULTIPLE SMALL CONCENTRATORS
  - OPTIMUM CONCENTRATION RATIO
  - OPTIMUM NUMBER OF CELL TYPES
  - ADVANTAGES TO SEPARATE VS. STACKED CELLS
  - LIGHT-WEIGHT RIGIDIZED FILM OPTICS (TO CIRCUMVENT MICROMETEORITE PROBLEM)

## CONCLUSIONS - H-1351

This study resulted in a number of significant conclusions. Practical solar cell efficiencies exceeding 50 percent and probably 60 percent are achievable in a solar photovoltaic system in space, using an innovative combination of inflatable and rigidized thin-film optics, spectrum splitting, tailored bandgap cells, and a dust radiator or other lightweight radiator type. The potential advantages over a SEPS-type planar array are very dramatic, particularly so at higher power levels and for operation inside the radiation belts for extended periods of time. The potential performance parameter comparison, indicated in the table on the facing page, shows a 3-1/2 fold increase in the power output per unit weight and a 6-fold reduction in the cost per unit power as compared to a SEPS-type planar array.

A \$6-15M research and technology program would be required to bring 2-3 other solar cell types to the same state of the art as GaAs. Research and development of the dust radiator is expected to be about \$10M more, requiring an estimated \$15-25M investment. However, the expected savings in a single power module at 70 kW could be enough to pay for all this special R&D. It is clear that more detailed trade-offs and design studies will be required to verify the performance projections due to the very limited depth of this design study.

This technique should be compared with that of stacked multi-bandgap solar cells in a planar array without concentration. The performance of such a system is uncertain at this time. It may well be that a combination of such stacked cells with the innovative concepts of concentration and lightweight radiation will result in the most attractive power module concept, achieving high efficiency without resorting to spectrum splitters and separate solar cell type areas. Assuming that the performance parameters predicted are verified in further studies, it is quite likely that the cross-over point between the economic application of solar photovoltaic versus nuclear space power would be raised to power modules of at least many megawatts. Perhaps there might not be a crossover at all.

Application of techniques such as this to the Satellite Solar Power System concept could result in a very significant savings in weight and cost, and might make the SSPS at least more competitive with terrestrial power sources, and at most clearly the most economically attractive option.

CONCLUSIONS

- PRACTICAL SOLAR CELL EFFICIENCY EXCEEDING 50 PERCENT IS ACHIEVABLE
- INNOVATIVE COMBINATION OF INFLATABLE THIN-FILM OPTICS, SPECTRUM SPLITTING, TAILORED BANDGAP CELLS, AND ADVANCED RADIATOR SUCH AS THE DUST TYPE IS DESIRABLE FOR A SYSTEM
- POTENTIAL ADVANTAGES OVER SEPS ARE DRAMATIC, PARTICULARLY AT HIGHER POWER LEVELS AND FOR OPERATION IN RADIATION BELTS
- POTENTIAL PERFORMANCE PARAMETERS @ 125 kW, FOR 190-DAY LEO-GEO TRANSFER MISSION:

NEW CONCEPT	SEPS TYPE
192 W/kg 52 \$/W	56 W/kg 300 \$/W

ORIGINAL PAGE IS  
OF POOR QUALITY

AEROSPACE FORM NO. 40

- TECHNOLOGY/RESEARCH PROGRAM REQUIRED FOR 2-3 OTHER SOLAR CELL TYPES TO REACH STATUS OF Ga As AND FOR DUST RADIATOR - BUT COST RECOUPED IN SAVINGS ON ONE UNIT AT 70 kW
- MORE DETAILED TRADE-OFFS AND DESIGN STUDIES REQUIRED TO VERIFY PERFORMANCE PROJECTIONS
- CLOSEST RIVAL TECHNIQUE: STACKED MULTI-BANDGAP CELLS. COMBINATION WITH CONCENTRATOR AND ADVANCED RADIATOR MAY BE A WINNER





## RECOMMENDATIONS - H-1350

Inasmuch as the performance projections are based on very preliminary design analyses, it is recommended that more detailed trade-off and design studies be performed. Such studies would treat all elements of the concept, including dust radiators. It is estimated that about \$250K would be required for such studies.

It would also be desirable to conduct at least two laboratory experiments to verify the attainable efficiency in a spectrally split multi-bandgap system utilizing say 2-3 types of cells, illuminated by an actual solar spectrum through dichroic mirrors. This experiment might be performed for about \$300K. In addition, verification of some of the critical design parameters for a dust radiator, such as the heat transfer to the particles in a hollow honeycomb structure and the basic mechanical devices required to propel and catch them, might also be performed for about \$400K.

It is expected that expenditures of this size would be well worth the effort in terms of identifying and narrowing the uncertainties associated with the performance projections of this report.

RECOMMENDATIONS

- PERFORM MORE DETAILED TRADE-OFF AND DESIGN STUDIES,  
INCLUDING DUST RADIATOR
  - ≈\$250 K REQUIRED
  
- PERFORM LABORATORY EXPERIMENTS TO VERIFY
  - ATTAINABLE EFFICIENCY ≈ \$300 K
  - DUST RADIATOR PERFORMANCE ≈ \$400 K

---

\$700 K REQUIRED



SECTION 6

REFERENCES

PENDING PAGE BLANK NOT ERASED

## REFERENCES

1. W. Blocker, Projections for Spacecraft Power Supplies in the Post-1985 Time Period, Report No. TOR-0076(6020-01)-2, The Aerospace Corporation, El Segundo, CA (February 1976).
2. W. Blocker, "High Efficiency Solar Energy Conversion Through Flux Concentration and Spectrum Splitting," Proceedings of IEEE, Vol. 66, No. 1, p 104-105 (January 1978).
3. F. Sterzer, "The Conversion Efficiency of Ideal Shockley P-N Junction Photovoltaic Converters in Concentrated Sunlight," RCA Rev., Vol 36, pp. 316-323 (June 1975).
4. Ad Hoc Panel on Solar Cell Efficiency, Space Science Board, National Academy of Sciences, Washington, D. C., "Solar Cells, Outlook for Improved Efficiency," (1972).
5. M. Wolf, "Limitations and Possibilities for Improvement of Photovoltaic Solar Energy Converters, Part I: Consideration of Earth's Surface Operation," Proceedings of IRE, Vol 48, pp. 1246-1263, (1960).
6. E. D. Jackson, "Areas for Improvements of the Semiconductor Solar Energy Converter," in Trans. Conf. Use of Solar Energy (Univ. Arizona Press, Tucson), Vol. 5, pp. 122-126 (1955).
7. P. Rappaport, "The Photovoltaic Effect and Its Utilization," RCA Rev., Vol. 20, pp. 373-397 (September 1959).
8. K. H. Spring, "Direct Generation of Electricity," in The Solar Cell, K. H. Spring, Ed. New York Academic Press, pp. 333-360 (1965).
9. R. H. Dean, L. S. Napoli, and S. G. Liu, "Silicon Solar Cells for Highly Concentrated Sunlight," RCA Rev., Vol 36, pp. 324-335, (June 1975).

RECORDING PAGE BLANK NOT FILMED

ORIGINAL PAGE IS  
OF POOR QUALITY

10. L. S. Napoli, G. A. Swartz, S. G. Liu, N. Klein, D. Fairbanks, and D. Tamutus, "High-Level Concentration of Sunlight on Silicon Solar Cells," RCA Rev., Vol. 38 pp. 76-108, (March 1977).
11. John M. Hedgepeth, and Karl Knapp, Preliminary Investigation of a Dust Radiator for Space Power Systems, " Report No. ARC-TN-1054, Astro Research Corporation, Santa Barbara, CA. (1 March 1978).

APPENDIX

APPENDIX

CALCULATIONS OF ATTAINABLE EFFICIENCIES OF SOLAR CELLS

Part 1 - Cells Dominated by Diffusion Current

Part 2 - Cells Dominated by Recombination Current;  
Effect of Real Materials

PRECEDING PAGE BLANK NOT FILMED

## PART 1: CELLS DOMINATED BY DIFFUSION CURRENT

### 1. INTRODUCTION

The maximum solar energy conversion efficiency of a single p-n junction solar cell is around 25%. A very important loss mode is the loss that is inherent when the photon energy exceeds the bandgap energy. This excess photon energy ( $h\nu - E_g$ ) is converted into heat. A promising approach to achieve high efficiency is to use several solar cells of different bandgaps so that the excess photon energy loss is minimized. The present study examines the efficiencies that can be achieved using such a scheme for space applications.

The use of a multi-color solar cell system was proposed by E. D. Jackson.<sup>(1)</sup> He suggested arranging the solar cells in tandem in the order of decreasing bandgap energy, i. e.  $E_{g1} > E_{g2} > E_{g3} \dots$ . In this way, the first cell will convert the solar spectral interval from  $E_{g1}$  to  $\infty$ , the second one from  $E_{g2}$  to  $E_{g1}$ , and so on. This type of solar cell stack has been recently analyzed by Loferski<sup>(2)</sup> who found a theoretical efficiency as high as 40% using 6 cells in tandem. It is evident that conceptually it is not mandatory to arrange the solar cells in tandem. The same sort of efficiency would apply if the solar spectrum is first dispersed and properly divided and each cell receives the appropriate portion of the spectrum. From the standpoint of efficiency calculations, the two schemes may be considered equivalent. Hardware design and losses due to practical considerations obviously would be very different.

The present study examines how the efficiency of such a multi-color solar cell array depends on (1) the number of cells, (2) solar concentration, and (3) temperature. The objectives are to define the general characteristics of a multi-color array and to provide numerical results for design and trade-off studies. The three chosen parameters are the basic ones, they have to be known to provide a basis for the selection of materials and the formulation of design concepts. Solar concentration is considered inherent because of the expected high cost of multi-color arrays and the increased efficiency that comes with concentration. Temperature is considered an independent parameter; it is assumed that thermal design will fix the array at some desired temperature independent of solar concentration.



In this first phase of the study, emphasis is placed on obtaining numerical results over a wide range of conditions. The simplest model of the solar cell is used. It is taken to be a p-n junction with the junction current attributed to the diffusion of carriers, the so-called ideal diodes. This approach is similar to that reported by Loferski<sup>(2)</sup>. Other possible models for the junction and their effect on the calculated efficiency will be the subject of future communications.

## 2. MODEL OF THE SOLAR CELL ARRAY

The solar cell is assumed to be of the conventional p-n junction type with an equivalent circuit as shown in Fig. 1. It will be assumed that the series resistance  $R_s = 0$  and the shunt resistance  $R_{SH} = \infty$ . These assumptions will tend to overestimate the calculated efficiency but it is unlikely that for cells comparable to current typical high quality cells, the assumptions will affect the major conclusions on the optimum distribution of bandgaps, the dependence of system efficiency on the number of cells, and the effect of temperature.  $R_s$  may play a significant role at high solar concentrations; this problem will be considered in the future. For the parametric study, the idealized model will be used.

In Fig. (1), the short-circuit current  $I_{sc}$  is the current produced by the light-generated electron-hole pairs in the vicinity of the p-n junction.  $I_j$  is the junction dark current and is obtained from the (usually) known I-V characteristics, it subtracts from the photocurrent. From Fig. (1)

$$I = I_{sc} - I_j(V) \quad (1)$$

Since the output power is  $P = IV$ , maximum power is delivered to the load when

$$-\frac{dI}{dV} = \frac{I}{V}$$

or

$$-\left(\frac{dI}{dV}\right)_{I_{mp}} V_{mp} = \frac{I_{mp}}{V_{mp}} \quad (2)$$

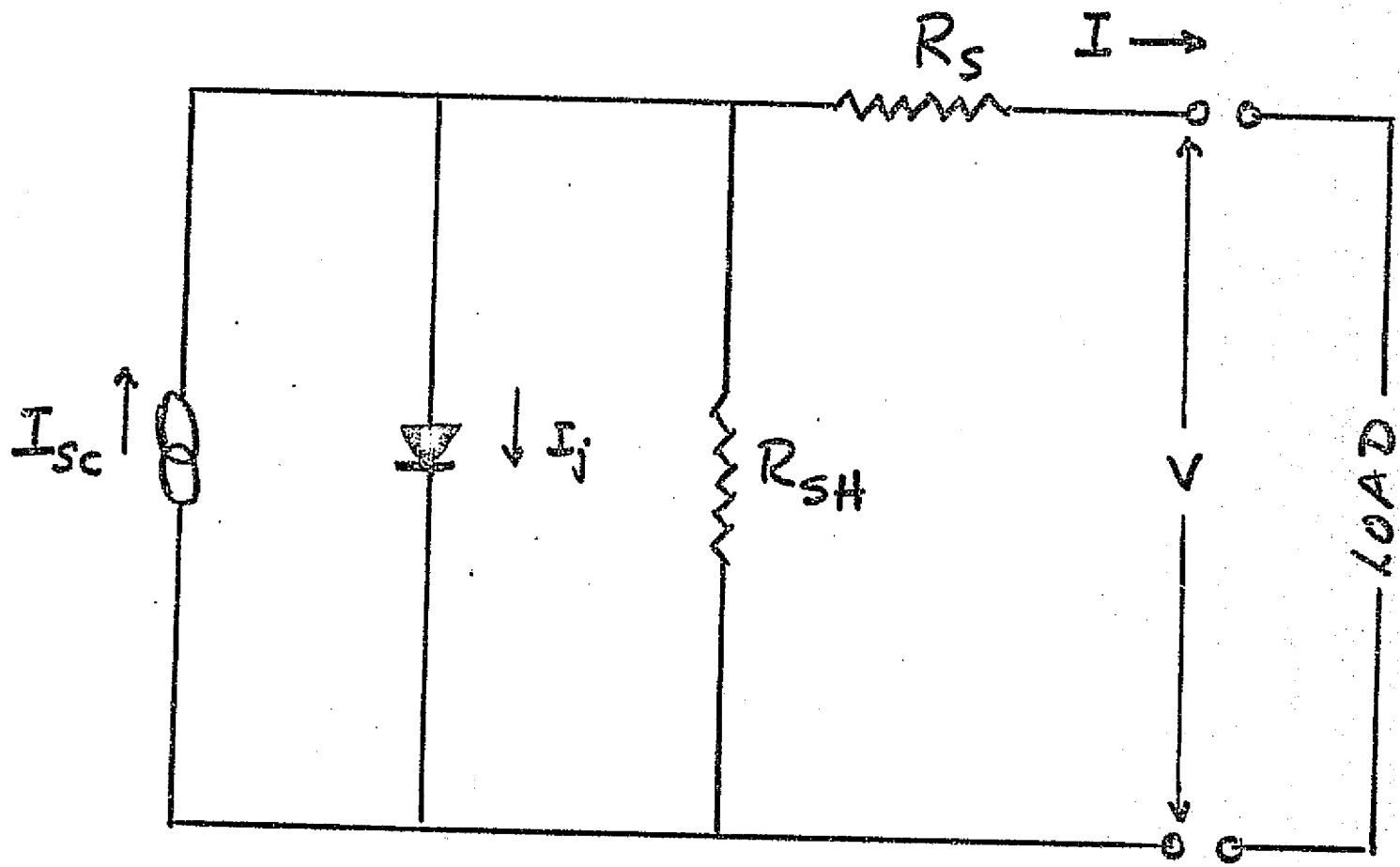


Fig. 1. Equivalent Circuit of a Solar Cell

where  $I_{mp}$  and  $V_{mp}$  are the current and voltage at maximum power.

The short-circuit current,  $I_{sc}$ , is determined by the light intensity, the spectral bandwidth, the absorption coefficient, the collection efficiency, and reflectivity, etc. In this discussion, unity collection efficiency will be assumed to be a step function at the bandgap energy. In other-words, every incident photon of energy greater than the bandgap will create one electron-hole pair which will be separated by the field of the p-n junction and contributes one electronic charge to the short-circuit current.  $I_{sc}$  can then be expressed as an integral of the solar spectral intensity curve.

$$I_{sc}(E_c, E_g) = C q \int_{E_g}^{E_c} n_{ph}(E) dE \quad (3)$$

where  $C$  is the solar concentration factor,  $n_{ph}(E)$  the number of incident photons-cm<sup>-2</sup>-sec<sup>-1</sup> between  $E$  and  $E + dE$ ,  $E_g$  is the energy gap and  $E_c$  is the short-wavelength cutoff, or the bandgap of the next higher energy gap solar cell in the case of tandem operation and  $q$  is the electronic charge.  $n_{ph}(E)$  is available in the literature for various types of solar spectrum. For this study we will use the 1971 NASA air mass zero spectrum (NASA SP-800 T, May 1971) as given in Ref. 3. The NASA power spectrum has been converted to photon flux spectra as shown in Table 1, which can be used directly to compute  $I_{sc}$  from Eq. (3).

For some computation, it is convenient to describe the solar spectrum in a closed-form. The NASA spectrum was found to fit the following empirical equation to within 7% between  $E$  0.6 eV and  $E$  4. eV.

$$I_{sc}(\infty, E) = C C_1 \exp \left[ - (C_2 E + C_3 E^2) \right] \text{mA-cm}^{-2} \quad (4)$$

where

$C$	=	solar concentration factor
$C_1$	=	115.9
$C_2$	=	0.4485
$C_3$	=	0.2192

Table 1. Air mass zero, AMO, solar radiation. Number of photons per  $\text{cm}^2$  per second,  $N_{\text{ph}}$ , is taken to be zero at  $E = h\nu = 7 \text{ eV}$ , where  $h$  is Planck's constant,  $\nu$ , frequency per second, and  $\text{eV}$ , electron Volts. Wavelength,  $\lambda$ , in micrometers is related to  $E$  by  $h\nu = 1.23984/\lambda$ . Short circuit current  $I_{\text{sc}}(E)$  is in  $\text{mA per cm}^2$ ; it is equal to  $N_{\text{ph}}$  times electronic charge,  $1.6021 \times 10^{-16} \text{ mCoul. per photon or electron}$ .  $N_{\text{ph}}(E)$ ,  $I_{\text{sc}}(E)$  and Solar Energy ( $E$ ) are values integrated from  $7 \text{ eV}$  to  $E$ .

$E = h\nu$	$\lambda$	$10^{-14} N_{\text{ph}}$	$I_{\text{sc}}(E)$	Solar Energy <sub>2</sub> $\text{mW/cm}^2$	$E = h\nu$	$\lambda$	$10^{-14} N_{\text{ph}}$	$I_{\text{sc}}(E)$	Solar Energy <sub>2</sub> $\text{mW/cm}^2$
7.000	0.1772	0	0	0	1.900	0.6526	1382.7	22.152	56.61
5.000	0.2480	2.9	0.046	0.25	1.800	0.6888	1568.8	25.134	61.87
4.000	0.3100	31.8	0.510	2.24	1.700	0.7293	1757.3	28.154	67.32
3.900	0.3179	41.1	0.569	2.84	1.600	0.7757	1966.9	31.512	72.94
3.800	0.3263	53.4	0.856	3.59	1.500	0.8273	2198.8	35.227	78.65
3.700	0.3351	68.9	1.104	4.51	1.400	0.8862	2445.0	39.171	84.43
3.600	0.3444	85.9	1.377	5.51	1.300	0.9539	2715.9	43.512	90.34
3.500	0.3542	104.7	1.678	6.57	1.200	1.0353	3020.5	48.391	96.35
3.400	0.3647	125.2	2.006	7.71	1.100	1.1289	3335.6	53.439	102.23
3.300	0.3757	149.3	2.392	8.99	1.000	1.2418	3674.9	58.875	107.89
3.200	0.3875	174.8	2.800	10.30	0.900	1.3789	4011.4	64.267	113.34
3.100	0.3999	203.9	3.267	11.79	0.800	1.5514	4413.5	70.709	118.60
3.000	0.4133	249.2	3.993	14.00	0.700	1.7724	4817.7	77.184	123.42
2.900	0.4275	301.7	4.833	16.46	0.600	2.0675	5175.4	82.915	127.14
2.800	0.4428	358.5	5.743	19.09	0.500	2.4803	5513.2	88.327	130.17
2.700	0.4592	433.5	6.945	21.37	0.400	3.0996	5854.2	93.790	132.64
2.600	0.4769	518.6	8.309	25.99	0.300	4.1333	6122.0	98.080	134.14
2.500	0.4959	611.7	9.800	29.78	0.200	6.2249	6325.6	101.343	134.95
2.400	0.5166	711.8	11.404	33.71	0.100	12.4177	6426.9	102.966	135.25
2.300	0.5391	818.9	13.120	37.84	0.000	00	6476.6	103.762	135.30
2.000	0.5636	935.5	14.987	42.08					
2.100	0.5904	1068.3	17.116	46.66					
2.000	0.6199	1223.8	19.606	51.53					

The particular form of solar spectrum that was used will be specified with the discussion of the results.

The model of the junction is largely determined by what is assumed for the junction current  $I_j$  of Eq. (1). In the so-called ideal diode approximation,  $I_j$  is due to the diffusion of carriers across the junction, its dependence on voltage  $V$  and temperature  $T$  is given by:

$$I_j(V) = I_o(E_g) \left[ e^{\frac{qV}{AkT}} - 1 \right] \quad (5)$$

where  $A$  is a parameter, and  $A = 1$  applies to the ideal diode case and  $kT$  has its usual meaning.  $I_o$ , the saturation current has the form:

$$I_o(E_g) = 6.03 \times 10^9 \left[ \frac{-E_g}{BkT} \right] \text{mA-cm}^{-2} \quad (6)$$

where the numerical constant has been chosen to be representative of Si solar cells.  $B$  is a parameter equal to unity for the ideal diode approximation.

The procedure to calculate the maximum efficiency of a solar cell with bandgap  $E_g$ , and a high-energy cutoff  $E_c$  is as follows:

- (1) Given  $(E_c, E_g)$  and  $C$ ,  $I_{sc}(E_c, E_g)$  is obtained by Eq. (3).
- (2) Given  $E_g$  and  $T$ ,  $I_o(E_g)$  is calculated by Eq. (6).
- (3) Eqs (1), (2), and (5) can be combined into:

$$I_{mp} = \left[ \frac{V_{mp}/(AkT)}{1 + (V_{mp}/AkT)} \right] I_{sc}(E_c, E_g) \quad (7)$$

and

$$V_{mp} = AkT \left[ \ln \left( \frac{I_{sc}(E_c, E_g)}{I_o(E_g)} \right) - \ln \left( 1 + \frac{V_{mp}}{AkT} \right) \right] \quad (8)$$

for  $qV/kT \gg 1$

Eqs. (7) and (8) are then solved for  $I_{mp}$  and  $V_{mp}$  by successive approximation with  $A = B = 1$ .

- (4) The maximum efficiency for the cell between  $E_g$  and  $E_c$  is  $\eta = (I_{mp} \cdot V_{mp}) / 135.3 \text{ mW-cm}^{-2}$ .

The array efficiency is obtained by adding the individual efficiency from each spectral increment. To obtain the optimum value for the array efficiency, however, it is necessary to go through a selection of the  $E_g$  values of the individual cells in order to have an optimum combination. The optimization method are discussed with the results below.

### 3. RESULTS

As discussed in Section 2, the results presented here have been obtained in the ideal diode approximation. Mathematically, it corresponds to setting  $A=B=1$  in Eqs. (5) through (8). Physically, it assumes the junction current consists only of the diffusion current.

From the design standpoint, it may be an issue on power conditioning whether each spectral segment should have the same current output. For this reason, the optimization of the multi-color array was studied in both cases: (1)  $I_{mp}$  values not necessarily equal and (2)  $I_{mp}$  values required to be the same for each spectral division.

#### A. Efficiency with No Constraint on $I_{mp}$

The approach was to calculate the efficiency of a solar cell between the spectral region ( $E_g, E_c$ ) using the procedure described in Section 2. The NASA-AMO spectrum was used directly. To calculate the array efficiency, it is necessary to assume a certain range of values for  $E_g$ . After some preliminary calculation, it was decided to restrict the bandgap values to  $0.6 \text{ eV} \leq E_g \leq 2.40 \text{ eV}$ . Any solar cell with  $E_g < 0.6 \text{ eV}$  has negligible output because of the low solar power in the long wavelength region (~6% at less than 0.6 eV) and more importantly because of the low open-circuit voltage of the cells. The upper limit for  $E_g$  is somewhat

arbitrary but the conclusions are not sensitive to small changes in the choice of the limit. In the actual calculation, the smallest  $E_g$  determines the long wavelength limit of the solar spectrum that is used. The entire short wavelength region (to  $h\nu = 7$  eV) is however used regardless of choice of the maximum value for  $E_g$ .

A typical computer output of the calculation is shown in Table 2. It shows the maximum solar cell efficiency ( $I_{mp} \cdot V_{mp} / 0.1353$ ) in a matrix form for different  $E_g$  and  $E_c$ . As an example of its use, suppose we have a 2-color array with the first solar cell at  $E_g = 2.30$  eV which absorbs all the higher energy photons. Its efficiency, reading down on the  $E_g = 2.30$  column to  $E_c = 6.90$  eV, is 16.01% (relative to  $135.3 \text{ mW-cm}^{-2}$ ). If the second cell has  $E_g = 1.60$  eV, it absorbs between 1.60 eV and 2.30 eV and its output efficiency is 13.22%. The array efficiency of this 2-color array is therefore 29.23%.

Tables comparable to Table 2 were constructed for different conditions:  $T = 200\text{K}, 300\text{K}, 400\text{K}, 500\text{K}$  and solar concentration  $C = 1, 100, 500, 1000$ . From these tables, the array efficiency was determined as a function of the number of cells operating at different temperatures and solar concentrations. The calculated efficiencies are optimum; they were deduced to be optimum by trial and error using various combinations of  $E_g$  -values following the procedure outlined in the above example.

The multi-color array efficiency is plotted vs.  $N$ , the number of cells or spectral divisions in Figs. 2-4. The following observations are evident from these curves.

- (1) For all the different operating conditions in  $T = 200 - 500\text{K}$ , and  $C = 1 - 1,000$ , the limiting maximum efficiency is nearly reached with 10-12 cells. Thus there is relatively little to gain by increasing the spectral division beyond 10-12.
- (2) Elevated temperature decreases array efficiency. Typically for  $C = 100$ , and  $N = 12$ , array output drops by about 0.17 of its value per 100K increase. Thus it is important to maintain a low operating temperature.





Figure 2. Attainable Solar Cell Efficiency  
Concentration Ratio = 1

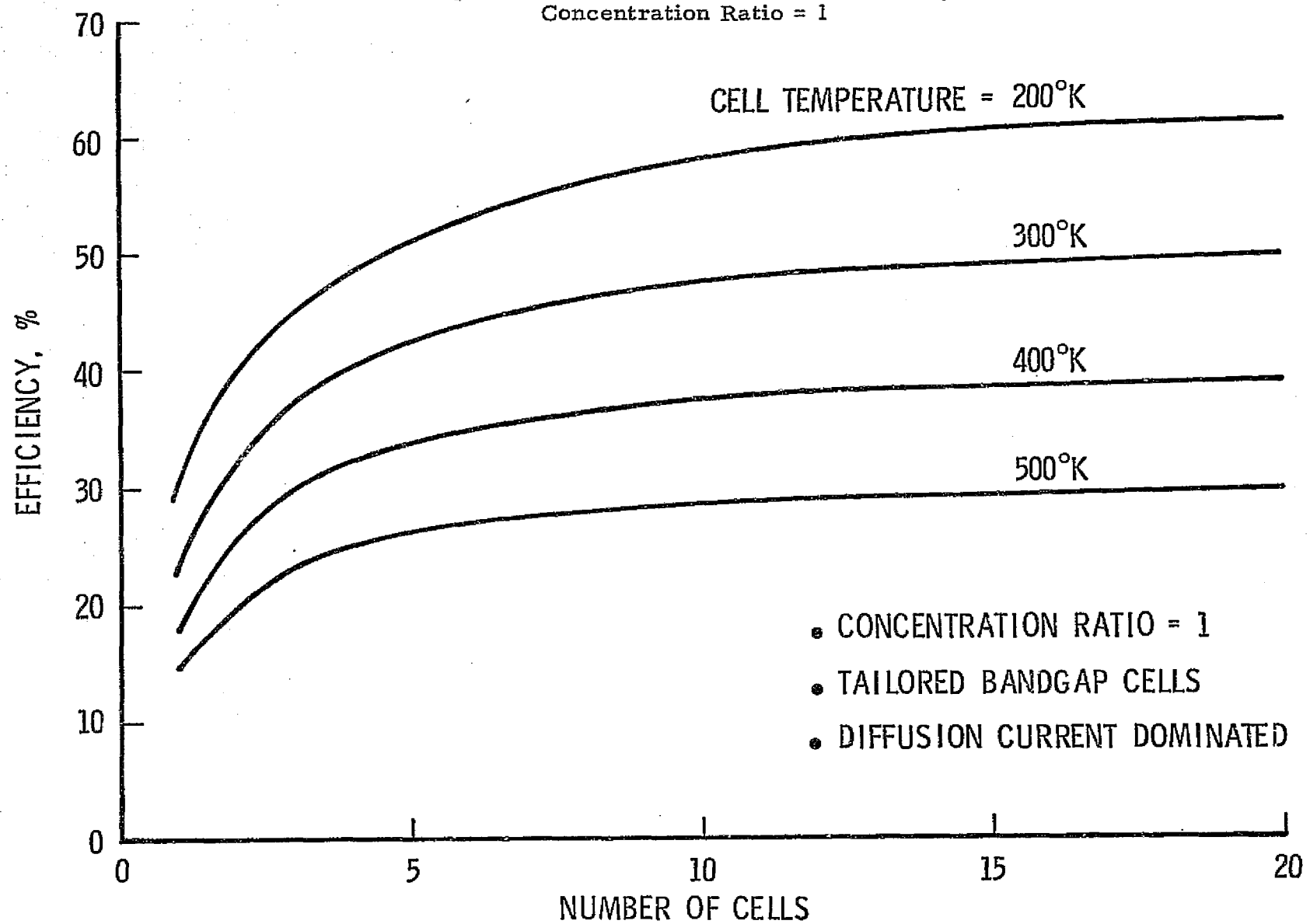


Figure 3. Attainable Solar Cell Efficiency  
Concentration Ratio = 100

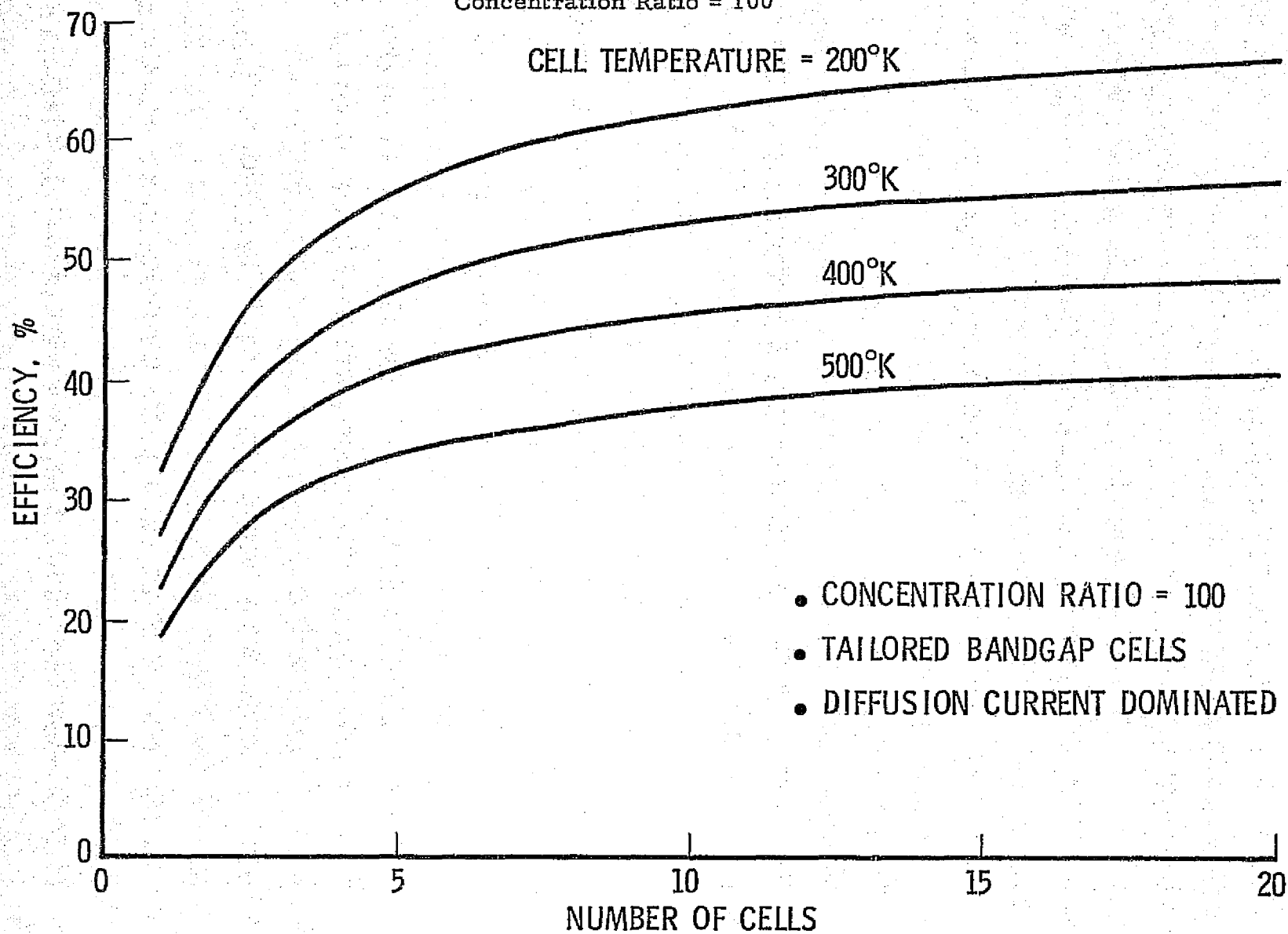
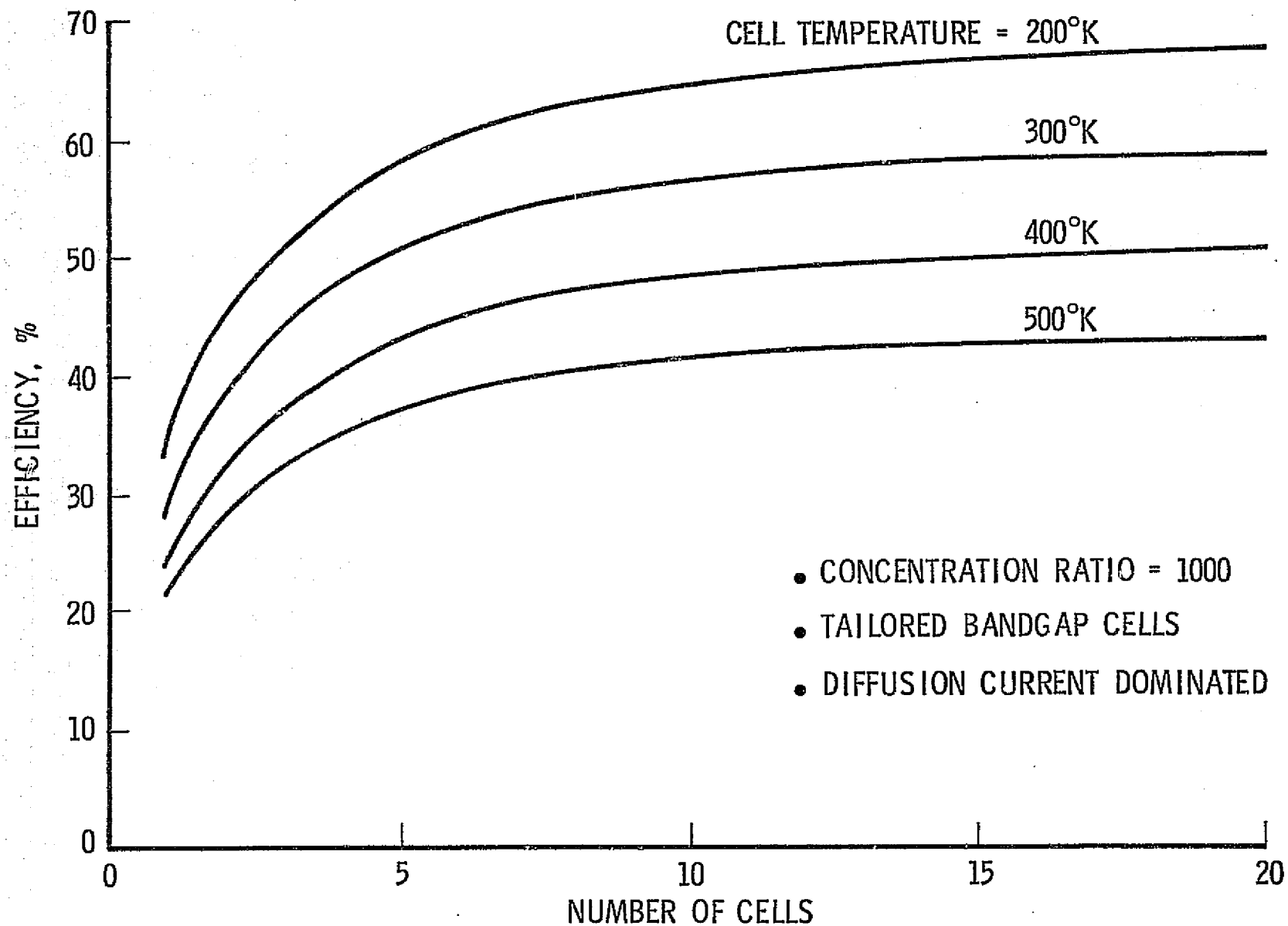


Figure 4. Attainable Solar Cell Efficiency  
Concentration Ratio = 1000



- (3) The optimum efficiency increases significantly with concentration. A conversion efficiency of over 55% is possible at  $C \geq 100$  and  $N = 12$  at 300K.
- (4) Efficiency increases rapidly between  $C = 1$  and 200, and continues to rise but only gradually. The model used is probably not valid at  $C \geq 10,000$ , but may be confidently used at  $C = 1000$ .
- (5) A good range of conditions for preliminary design considerations for high efficiencies appear to be is  $C = 100 - 500$ ,  $N = 6 - 12$ , and  $T \leq 300K$ .

#### B. Efficiency at Equal $I_{mp}$

To treat this case where all the cells must have the same  $I_{mp}$ , it was found convenient to use a different computer program. The solar spectrum was approximated by Eq. (4). Using this closed form, the  $I_{sc}$ , and therefore  $I_{mp}$ , can be calculated readily between any two energies  $E_g$  and  $E_c$ . An example of typical results is shown in Fig. 5 where  $I_{mp}(E_g, E_c)$  is plotted against  $E_g$  with  $E_c$  as a parameter. The high-energy cutoff is set at 4 eV since there is negligible solar energy above 4 eV. To see how this figure is used, suppose  $I_{mp} = 500$  mA is the desired current. Following the  $E_c = 4$  eV curve, we find the intersection with 500 mA at  $E_g = 2.8$  eV. Thus a cell with  $E_g = 2.8$  eV will give  $I_{mp} = 500$  mA. To determine the next cell, we drop down to the  $E_c = 2.8$  eV curve, and following it to 500 mA. We find for the next cell  $E_g = 2.4$  eV. This process can be repeated to determine the positions of all the  $E_g$  values for a given  $I_{mp}$ . Knowing the  $E_g$  values and the given  $I_{mp}$ , the array efficiency can then be calculated. It is evident, however, that as the low energy cutoff is approached, usually there will be an end portion of the spectrum which cannot be used because it does not contribute the required 500 mA. The array efficiency would then be lower than optimum. To obtain the optimum efficiency for equal rather than fixed  $I_{mp}$ ,  $I_{mp}$  can be adjusted up and down in this case about 500 mA until the

ORIGINAL PAGE IS  
OF POOR QUALITY

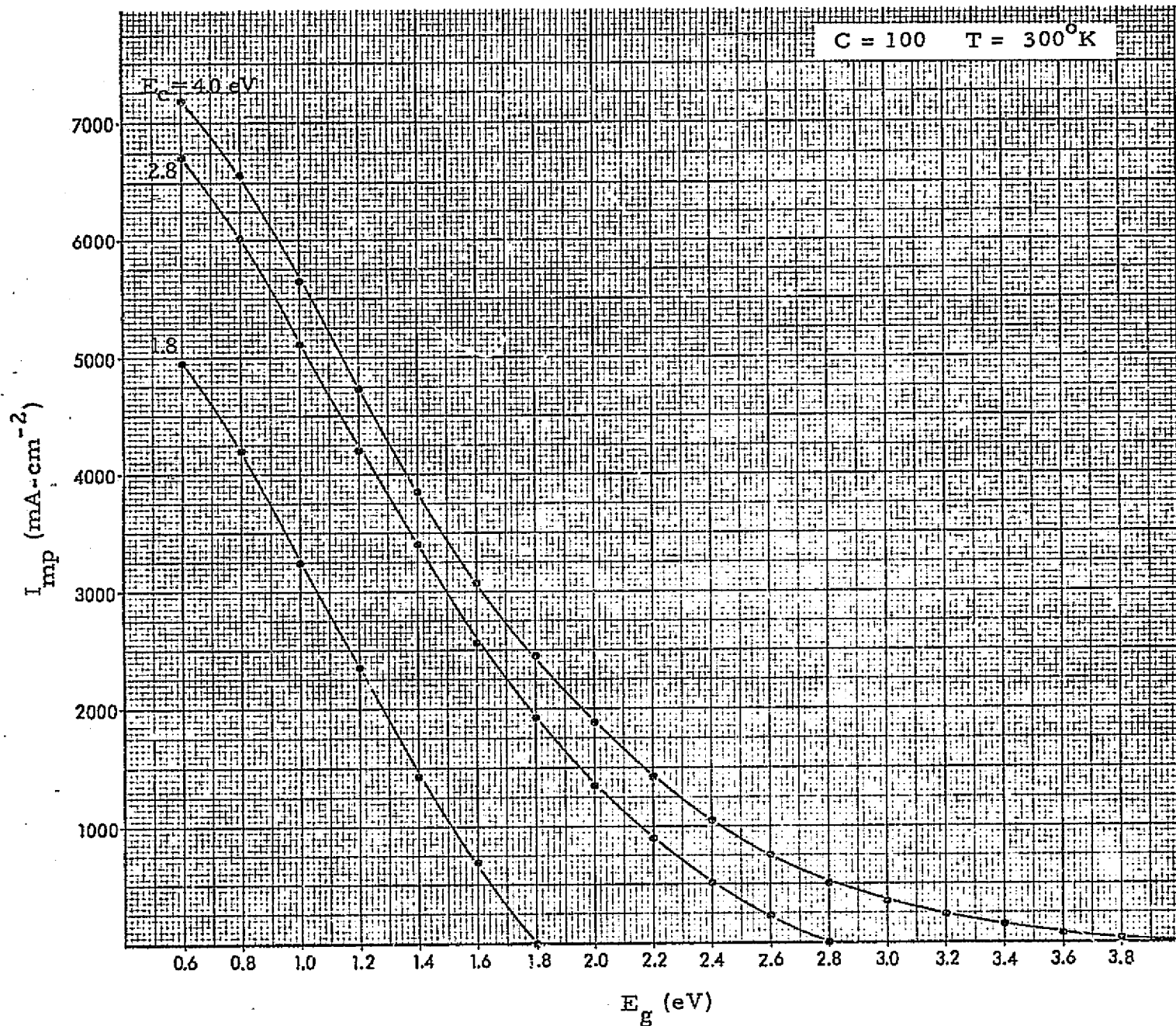


Fig. 5.  $I_{mp}$  Output as a Function of  $E_c$  and  $E_g$ .  $E_c$  is shown as a parameter.

total array efficiency is a maximum consistent with  $N$  being an integer. This procedure was actually used to determine the efficiency, current, and bandgap positions under a variety of conditions. The results are shown in Tables 3-6. These tables can be used to select the required materials to make up an efficient array.

Additional results are shown in Fig. 6 for a 12-cell array operating at 300K and  $C = 100$ . It shows the  $E_g$  positions of an optimum array and their contributions to the array efficiency. It is evident that Cell No. 1 with a wide bandgap of 2.74 eV contributes nearly 10% efficiency out of a total efficiency of 54%. On the other hand, Cells No. 11-12, with bandgap at 0.72 and 0.6 eV contribute less than 2%. This trend of favoring wide bandgap cells is common in all the operating conditions studied and points out that it is important to develop wide bandgap solar cell materials if multi-color arrays are to be considered.

The calculated array efficiency curves are nearly the same as those shown on Figs. 2-4, where equal  $I_{mp}$  was not imposed as a condition. Thus, equal  $I_{mp}$  apparently is not a severe restriction in determining the functional dependence of the ultimate theoretical efficiency although the absolute values are in some cases slightly slower.

#### 4. DISCUSSION

The general conclusion of this study is that a good starting point for a design study is on an array with about 10 cells operating at 100-500 solar concentrations and at as a low temperature as possible.

Favorable efficiency values in the 50-55% region have been obtained from this study of ideal diodes. The calculated values can be considered theoretical limits since most real cells have additional junction current and other losses not included in the idealized model. In a future communication, the efficiency of solar cells with junction current dominated by generation - recombination will be treated. The efficiency is expected to be lower than those presented here. It is reasonable to expect the efficiency of a real multi-color array to fall within the two limits since

Table 3. Characteristics of Multi-Color Solar Cell Arrays at Equal Current from Each Cell

EG TABLE

C= 1; T= 300

N	EFF	I	EG	EG	EG	EG	EG	EG	EG	EG	EG	EG	EG	EG	EG	EG	EG
1	23.8	35.5	1.48														
2	32.3	24.5	1.80	1.16													
3	37.2	19.5	1.98	1.40	.98												
4	40.0	16.0	2.12	1.58	1.20	.86											
5	41.6	13.5	2.24	1.72	1.36	1.06	.78										
6	42.9	11.2	2.36	1.86	1.52	1.26	1.02	.78									
7	44.2	9.7	2.44	1.98	1.66	1.40	1.18	.98	.78								
8	45.0	9.0	2.50	2.04	1.72	1.48	1.26	1.06	.88	.68							
9	46.1	8.0	2.56	2.12	1.82	1.58	1.38	1.20	1.04	.88	.72						
10	46.1	7.0	2.64	2.20	1.92	1.70	1.50	1.32	1.16	1.02	.88	.74					
12	46.6	6.0	2.72	2.30	2.02	1.80	1.62	1.46	1.32	1.16	1.06	.94	.82	.70			

C= 10; T= 300

N	EFF	I	EG	EG	EG	EG	EG	EG	EG	EG	EG	EG	EG	EG	EG	EG	EG
1	25.1	370.0	1.44														
2	34.4	250.0	1.78	1.14													
3	39.6	200.0	1.96	1.38	.94												
5	44.6	130.0	2.26	1.76	1.40	1.10	.84										
7	46.7	100.0	2.42	1.94	1.62	1.36	1.14	.94	.74								
10	48.6	75.0	2.60	2.16	1.86	1.62	1.42	1.24	1.08	.92	.78	.62					
15	50.6	50.0	2.82	2.42	2.16	1.96	1.78	1.62	1.48	1.36	1.24	1.14	1.04	.94	.84	.74	

C= 100; T= 300

N	EFF	I	EG	EG	EG	EG	EG	EG	EG	EG	EG	EG	EG	EG	EG	EG	EG
1	26.9	3880.0	1.40														
2	36.7	2612.0	1.74	1.10													
3	42.3	2047.0	1.94	1.36	.92												
4	45.5	1654.0	2.10	1.56	1.16	.82											
5	47.0	1336.0	2.24	1.72	1.36	1.06	.80										
6	49.5	1200.0	2.32	1.82	1.48	1.20	.96	.72									
8	50.3	1000.0	2.42	1.94	1.62	1.36	1.14	.94	.74	.52							
10	52.7	800.0	2.56	2.12	1.82	1.58	1.38	1.20	1.04	.88	.72	.54					
13	54.3	600.0	2.74	2.32	2.04	1.82	1.64	1.48	1.34	1.20	1.08	.96	.84	.72	.60		

Table 4. Characteristics of Multi-Color Solar Cell Arrays at Equal Current from Each Cell

EG TABLE

C = 1; T = 350

ORIGINAL PAGE IS  
OF POOR QUALITY

N	EFF	I	EG	EG	EG	EG	EG	EG	EG	EG	EG	EG	EG	EG	EG	EG	EG
1	21.1	33.0	1.54														
2	23.3	22.0	1.33	1.26													
3	22.5	17.0	2.06	1.50	1.10												
4	35.4	14.0	2.20	1.68	1.32	1.00											
5	37.0	12.0	2.30	1.80	1.46	1.18	.92										
6	37.8	11.0	2.36	1.88	1.54	1.26	1.02	.76									
7	39.3	9.0	2.50	2.04	1.72	1.46	1.24	1.04	.84								
8	40.5	8.0	2.56	2.12	1.82	1.58	1.38	1.20	1.02	.84							
9	40.0	7.0	2.64	2.20	1.90	1.68	1.48	1.30	1.14	.98	.82						
11	41.4	6.0	2.72	2.30	2.02	1.80	1.62	1.46	1.32	1.18	1.06	.84	.80				
15	42.0	4.5	2.88	2.48	2.22	2.02	1.86	1.72	1.58	1.46	1.34	1.24	1.14	1.04	.94	.84	.84

C = 10; T = 350

N	EFF	I	EG	EG	EG	EG	EG	EG	EG	EG	EG	EG	EG	EG	EG	EG	EG
1	22.6	348.0	1.48														
2	31.1	240.0	1.60	1.18													
3	35.7	178.0	2.04	1.48	1.06												
4	38.8	143.0	2.20	1.68	1.30	.98											
5	39.9	120.0	2.30	1.80	1.46	1.18	.92										
6	41.9	103.0	2.40	1.92	1.60	1.34	1.10	.88									
9	44.9	80.0	2.56	2.12	1.82	1.58	1.38	1.20	1.02	.86	.68						
10	43.9	70.0	2.64	2.20	1.90	1.68	1.48	1.30	1.14	1.00	.86	.70					
12	45.1	60.0	2.72	2.30	2.02	1.80	1.62	1.46	1.32	1.18	1.06	.94	.82	.68			
13	44.8	55.0	2.78	2.36	2.08	1.86	1.68	1.52	1.38	1.26	1.14	1.02	.90	.78	.64		
14	45.7	50.0	2.82	2.42	2.16	1.96	1.78	1.62	1.48	1.36	1.24	1.14	1.04	.94	.84	.74	.74

C = 100; T = 350

N	EFF	I	EG	EG	EG	EG	EG	EG	EG	EG	EG	EG	EG	EG	EG	EG	EG
1	24.4	3570.0	1.46														
2	31.2	3300.0	1.54	.78													
3	38.4	1875.0	2.00	1.42	1.00												
4	41.2	1500.0	2.16	1.62	1.24	.92											
6	44.9	1250.0	2.28	1.78	1.44	1.16	.90	.62									
7	45.8	1000.0	2.42	1.94	1.62	1.36	1.14	.94	.74								
9	48.1	800.0	2.56	2.12	1.82	1.58	1.38	1.20	1.04	.88	.72						
12	48.6	600.0	2.72	2.30	2.02	1.80	1.62	1.46	1.32	1.18	1.06	.94	.82	.70			



Table 5. Characteristics of Multi-Color Solar Cell Arrays at Equal Current from Each Cell

ES TABLE

C= 1; T= 400

N	EFF	I	ES	ES	I	ES	I	ES	I	ES	I	ES
1	18.3	37.0	1.42	1.30	1.24	1.28	1.00	1.02	1.14	.98	1.04	.90
2	25.6	21.0	1.90	1.62	1.58	1.48	1.22	1.30	1.32	1.18	1.24	1.12
4	31.0	15.0	2.16	1.74	1.54	1.44	1.48	1.46	1.48	1.36	1.24	1.00
4	31.7	13.0	2.26	1.88	1.70	1.58	1.48	1.46	1.48	1.36	1.24	1.00
5	33.1	11.0	2.36	2.02	1.90	1.68	1.48	1.46	1.48	1.36	1.24	1.00
6	33.7	9.0	2.48	2.20	2.02	1.80	1.62	1.62	1.48	1.36	1.24	1.00
8	35.3	7.0	2.64	2.30	2.02	1.80	1.62	1.62	1.48	1.36	1.24	1.00
10	36.5	6.0	2.72	2.42	2.16	1.96	1.78	1.62	1.48	1.36	1.24	1.00
12	37.0	5.0	2.82	2.42	2.16	1.96	1.78	1.62	1.48	1.36	1.24	1.00

C= 10; T= 400

N	EFF	I	ES	ES	I	ES	I	ES	I	ES	I	ES
1	20.8	330.0	1.54	1.26	1.14	1.04	1.00	1.20	1.02	.84	1.04	.78
2	28.4	220.0	1.68	1.54	1.54	1.36	1.12	1.20	1.32	1.18	1.24	1.02
3	32.2	165.0	2.06	1.70	1.52	1.58	1.38	1.46	1.32	1.18	1.24	1.02
4	34.4	135.0	2.22	1.86	1.62	1.68	1.62	1.46	1.32	1.18	1.24	1.02
5	36.3	112.0	2.36	1.94	1.62	1.68	1.62	1.46	1.32	1.18	1.24	1.02
6	37.3	100.0	2.42	2.12	1.82	1.80	1.62	1.46	1.32	1.18	1.24	1.02
8	39.7	80.0	2.56	2.42	2.02	1.96	1.78	1.62	1.48	1.36	1.24	1.02
11	40.2	60.0	2.72	2.30	2.02	1.96	1.78	1.62	1.48	1.36	1.24	1.02
13	40.9	50.0	2.82	2.42	2.16	1.96	1.78	1.62	1.48	1.36	1.24	1.02

Table 6. Characteristics of Multi-Color Solar Cell Arrays at Equal Current from Each Cell

EG TABLE

C = 100; T = 400

N	EFF	I	EG														
1	22.4	3400.0	1.56														
2	31.0	2350.0	1.82	1.20													
3	35.2	1800.0	2.02	1.46	1.04												
4	38.1	1450.0	2.18	1.66	1.23	.96											
5	39.7	1200.0	2.30	1.80	1.46	1.16	.92										
7	41.6	1000.0	2.42	1.94	1.62	1.36	1.14	.68									
9	43.8	800.0	2.56	2.12	1.82	1.58	1.38	1.20	1.02	.86	.56						
12	44.6	600.0	2.72	2.30	2.02	1.80	1.62	1.46	1.32	1.18	1.06	.94	.82	.68			
14	44.9	500.0	2.82	2.42	2.16	1.96	1.78	1.62	1.48	1.36	1.24	1.12	1.02	.92	.82	.70	
15	44.9	450.0	2.88	2.48	2.22	2.02	1.86	1.72	1.58	1.46	1.34	1.24	1.14	1.04	.94	.84	

C = 1000; T = 400

ORIGINAL PAGE IS OF POOR QUALITY

N	EFF	I	EG														
1	24.5	35500.0	1.46														
2	32.4	24500.0	1.78	1.14													
3	38.3	19000.0	1.98	1.40	.96												
4	41.3	15000.0	2.16	1.62	1.24	.92											
7	46.0	10000.0	2.42	1.94	1.52	1.36	1.14	.94	.74								
9	47.9	8000.0	2.56	2.12	1.82	1.58	1.38	1.20	1.02	.86	.68						
12	48.7	6000.0	2.72	2.30	2.02	1.80	1.62	1.46	1.32	1.18	1.06	.94	.82	.70			
15	49.5	5000.0	2.82	2.42	2.16	1.96	1.78	1.62	1.48	1.36	1.24	1.14	1.04	.94	.84	.74	

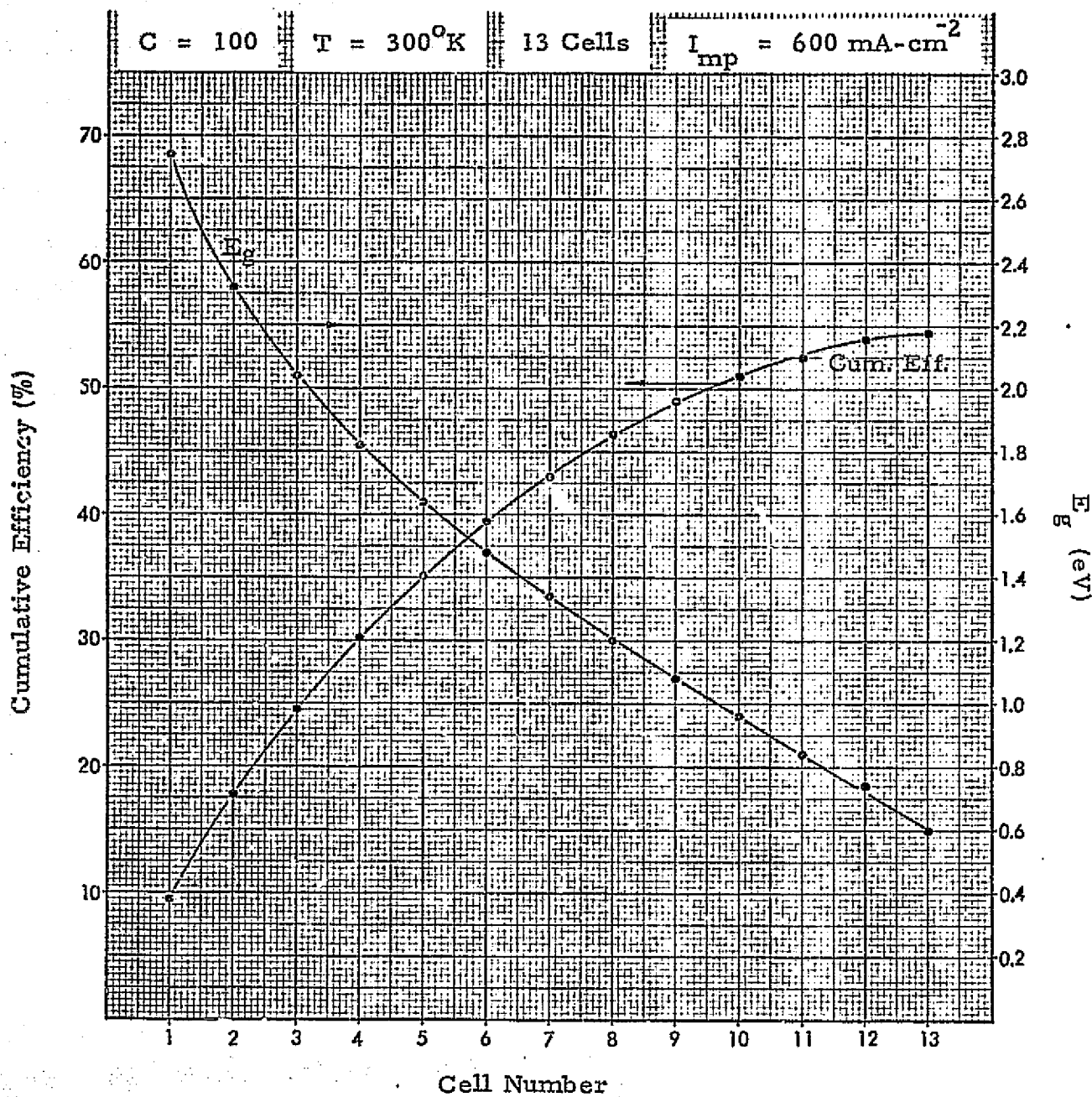


Fig. 6. The Bandgap Positions and Their Cumulative Efficiencies of a 13-Cell Array. Equal  $I_{mp}$ .

state-of-the-art high efficiency Si solar cells do lie between the two limits.

While the results here show a trend of higher efficiency with increasing solar concentration, certain limitations of the model must be noted. The most severe limitation is the neglect of series resistance. At high current densities that are attained at higher concentrations, series resistance will cause a large voltage drop in the cell. The problem becomes one of obtaining close spacing between metallization grids without at the same time covering up a large fraction of the active area. With increasing concentration, at some point, the simple p-n junction model will breakdown as the minority carrier density exceeds that of the majority carrier, but the point at which this occurs can be made to fall at a higher concentration by increasing the number of spectral divisions.

The increase in efficiency at lower temperatures is interesting. It shows a definite need to dissipate the heat generated by concentration. The design should maintain the array at as low a temperature as possible by connecting it to a radiating surface.

Finally, the real need of developing wide bandgap materials in the region of 2-2.7 eV has been identified. The utility of the multi-color concept will be severely limited without wide bandgap solar cells.

ORIGINAL PAGE IS  
OF POOR QUALITY

PART 2: CELLS DOMINATED BY RECOMBINATION CURRENT;  
EFFECT OF REAL MATERIALS

1. INTRODUCTION

Part 1 of this appendix addressed the attainable efficiency of multi-color solar cell arrays. Array efficiency was calculated as a function of the number of cells (spectral division), temperature, and solar concentration. We found that the limiting efficiency would be nearly reached with about 10 cells, and a high conversion efficiency, exceeding 50%, was predicted. All practical losses (reflection, series resistance, etc.) were neglected. Moreover, the array was conceived to be a series of ideal diodes, i. e., the junction current was taken to be due to diffusion current only. Both assumptions tend to overestimate the efficiency. In this study, we repeat the calculation but take the diode to be less ideal; the junction current is now assumed to be dominated by the generation-recombination current. This model will give lower efficiency of a nine-cell array using the bandgaps of real materials chosen to closely simulate the optimum bandgap distribution determined in Part 1 of the study. The results show that the real material array has the same efficiency as that predicted by the hypothetical and optimized case.

2. EFFICIENCY CALCULATION

The procedure to calculate array efficiency is described in Part 1. A brief summary is given below showing the difference between the two studies. The current  $I$  to an external load is given by the difference between the light-generated current  $I_{sc}$ , and the junction current  $I_j$ :

$$I = I_{sc} - I_j \quad (1)$$

PRECEDING PAGE BLANK NOT FILMED

$I_{sc}$  is determined by the specified spectral interval with an assumed unity quantum efficiency. The current-voltage (V) relation and the effect of bandgap ( $E_g$ ) on the saturation current ( $I_o$ ) are given by

$$I_j (V) = I_o (E_g) \left[ \frac{qV}{eAkT} - 1 \right] \quad (2)$$

$$I_o (E_g) = 6.03 \times 10^9 \left[ \frac{-E_g}{eBkT} \right] \text{ mA-cm}^{-2} \quad (3)$$

The chosen numerical constant in (3) is representative of Si and GaAs and is assumed to be applicable to other materials as well. In the earlier study, the ideal diode case,  $A=B=1$  was used. In the present case,  $A=B=2$  is appropriate when generation-recombination current dominates  $I_j$ .

Following the procedure of Part 1, the optimum array efficiency, as determined by the maximum power point, was calculated as a function of the number of cells (N) at 200K, 300K, and 400K, and solar concentrations of 1X, 100X, and 500X. The results are shown in Table 1. The way efficiency depends on the three parameters is very similar in both cases. The major difference is that the overall efficiency is lower in the present case. As an example, at 300K, the efficiency for  $A=B=2$  is reduced to roughly 0.81 of the earlier  $A=B=1$  results at 1 sun, 0.93 at 100 suns, and 0.98 at 500 suns. It is evident that the difference between the two models becomes smaller with higher solar concentration. Table 2 illustrates the decrease in percent efficiency compared to the case of diffusion-dominated junction current.

The results so far have been obtained without an identification of the real materials that may be used for the multi-color arrays. A survey was made of the semiconductor materials that are potentially useful for this application. Specifically we chose a series of materials that closely resemble the calculated bandgaps for a nine-cell array. The materials are shown in Table 3, where we have indicated also the type of optical

Table 1. Efficiency of Multi-Color Solar Cell Array (A=B=2) (%)

<u>No. of Cells</u>	<u>1</u>	<u>2</u>	<u>3</u>	<u>6</u>	<u>10</u>	<u>12</u>
<u>1 SUN</u>						
200 K	25.3	35.4	40.6	47.6		51.4
300 K	19.2	26.7	30.6	35.3	37.1	37.9
400 K	14.4	19.7	22.7	25.7		27.3
<u>100 SUNS</u>						
200 K	30.1	42.0	48.3	56.2		60.0
300 K	25.2	35.1	40.1	46.7	48.9	49.9
400 K	21.1	29.2	33.3	38.3		40.6
<u>500 SUNS</u>						
200 K	32.1	42.5	51.1	59.5		63.2
300 K	27.7	38.5	44.0	51.0		54.2
400 K	24.0	33.2	37.8	43.5		46.2

ORIGINAL PAGE IS  
OF POOR QUALITY

Table 2. Decrease in Percent Attainable Efficiency  
Due to Generation-Recombination Current

CONCENTRATION	CELL TEMPERATURE °K	NUMBER OF CELLS				
		1	2	3	6	12
1	300	4.0	5.8	6.8	8.5	9.9
	400	4.2	6.2	7.2	9.1	10.4
100	300	1.2	2.0	2.4	3.4	4.2
	400	1.3	2.1	2.6	3.5	4.6
500	300	0.4	0.3	0.5	1.3	2.2
	400	<0.1	<0.1	0.4	1.1	2.0



Table 3. Materials for a 9-Cell Array

$E_G$ (eV)	Material	Transition
2.86	Si C	Indirect
2.5	Al P or CdS	Indirect
2.24	Ga P	Indirect
2.0	* (Ga, In) P	Direct
1.8		
1.6		
1.4	Ga As	Direct
1.1	Si	Indirect
0.7	Ge	Indirect

\*This range can also be covered by Ga As P and Ga Al P  
 Ga In P was picked because it is direct to higher energies

transitions in each material. Variable composition alloys are included; they are helpful because their bandgaps can be tailored to specific values within certain limits. The efficiency of the prototype solar cell array was calculated using the bandgaps of these materials. The results are shown in Table 3 and 4 for both cases:  $A=B=1$  and  $A=B=2$ . The efficiency values can be seen to be practically identical to those calculated earlier from a hypothetical and optimized list of bandgaps.

### 3. DISCUSSION

The modeling of the junction current by the generation-recombination process results in a lower efficiency for the multi-color array. Still, at 100 sun concentration and 300K, a nine-cell array will yield 48% compared to 53% in the earlier ideal diode case. In a good practical solar cell, the junction current effect is expected to fall within these two limits as is found in silicon solar cells. Practical losses such as reflection, sheet and shunt resistances, and surface recombination will reduce the achievable efficiency to a lower value.

The use of a prototype using the bandgaps of nine real materials give a predicted efficiency the same as that calculated from theoretical bandgaps. This is not surprising since with enough spectral increment, one would not expect the array efficiency to be sensitive to small bandgap variations. The discrepancy between the real material and the hypothetical case will be more noticeable when a smaller number of solar cells are used.

The only material property that has been used in our studies is the bandgap. Theoretically, the transport properties enter into the pre-exponential factor in Eq. (3). However, that factor has been treated here as an empirical parameter which is found to have about the same value for GaAs and Si, and therefore was taken to be a constant for all materials. It remains to be seen whether this is a good assumption.

Table 5. Efficiency of Prototype 9-Cell Array with Bandgaps Given by Table 2, at Different Temperatures T and Solar Concentrations C. A=B=2

	T = 200 K			T = 300 K			T = 400 K		
	C=1	C=100	C=500	C=1	C=100	C=500	C=1	C=100	C=500
$\eta(2.86)$ :	8.57	9.17	9.38	7.47	8.36	8.68	6.42	7.60	8.01
$\eta(2.5)$ :	6.38	6.91	7.10	5.42	6.21	6.48	4.50	5.53	5.90
$\eta(2.24)$ :	5.28	5.80	5.97	4.37	5.12	5.39	3.49	4.48	4.83
$\eta(2.00)$ :	5.52	6.13	6.35	4.44	5.34	5.67	3.41	4.60	5.02
$\eta(1.8)$ :	4.89	5.52	5.75	3.80	4.72	5.05	2.77	3.97	4.40
$\eta(1.6)$ :	4.75	5.48	5.73	3.52	4.58	4.96	2.38	3.75	4.23
$\eta(1.4)$ :	4.65	5.52	5.82	3.22	4.48	4.93	1.93	3.53	4.10
$\eta(1.1)$ :	5.86	7.45	8.01	3.45	5.72	6.53	1.43	4.15	5.18
$\eta(0.7)$ :	3.59	6.09	6.99	0.65	3.71	4.95	0.00	1.79	3.22
$\eta(\text{Total})$ :	49.49	58.07	61.10	36.34	48.24	52.64	26.33	39.40	44.89 %

ORIGINAL PAGE IS  
OF POOR QUALITY

Table 4. Efficiency of Prototype 9-Cell Array with Bandgaps Given by Table 2, at Different Temperatures T and Solar Concentrations C. A=B=1

	T = 200 K			T = 300 K			T = 400 K		
	C=1	C=100	C=500	C=1	C=100	C=500	C=1	C=100	C=500
$\eta(2.86) =$	6.85	9.50	3.600	8.36	8.81	8.97	7.54	8.13	8.35
$\eta(2.50) =$	6.94	7.20	7.30	6.19	6.59	6.73	5.48	6.01	6.19
$\eta(2.24) =$	5.81	6.06	6.16	5.10	5.49	5.62	4.41	4.92	5.10
$\eta(2.00) =$	6.13	6.44	6.55	5.29	5.75	5.92	4.47	5.08	5.30
$\eta(1.8) =$	5.51	5.83	5.94	4.65	5.13	5.29	3.81	4.44	4.66
$\eta(1.6) =$	5.44	5.81	5.94	4.46	5.01	5.20	3.51	4.23	4.49
$\eta(1.4) =$	5.44	5.88	6.03	4.28	4.94	5.16	3.18	4.03	4.33
$\eta(1.1) =$	7.14	7.95	8.24	5.10	6.30	6.72	3.19	4.73	5.28
$\eta(0.7) =$	5.25	6.58	7.04	2.25	4.10	4.76	0.11	1.91	2.71
$\eta(\text{Total}) =$	56.85	61.25	62.8	45.68	52.12	54.37	35.70	43.48	46.41%

The materials that are listed in Table 3 have well-known semiconductor properties except possibly SiC. However, not all of them have been made into solar cells. In most cases, the technological problems associated with their use are yet to be identified. There are, however, some general statements that can be made based on the characteristics associated with the type of optical transition. The direct transition materials have a much higher absorption coefficient than the indirect materials. As a result, they can be made thinner, will tolerate a shorter diffusion length, but will also require a good control of surface treatment to reduce surface recombinations. The materials problems to be solved are exemplified by those found in the development of Si (direct) and GaAs (indirect) solar cells.

## REFERENCES

1. E. D. Jackson, "Transactions of the Conference in the Use of Solar Energy, Tucson, Arizona, October 31 through November 1, 1955," P. 122.
2. J. J. Loferski, "Tandem Photovoltaic Solar Cells and Increased Solar Energy Conversion Efficiency," 12th IEEE Photovoltaic Specialists Conference - 1976, p. 957. IEEE, New York (1976).
3. "Solar Array Design Handbook," JPL-SP43-38, Vol. 1, NASA, Washington, D. C. (1976).

PRECEDING PAGE BLANK NOT FILMED